Synthesis, Characterization and Structure-Property Relationships of Post-sulfonated Poly(arylene ether sulfone) Membranes for Water Desalination

Shreya Roy Choudhury

Dissertation submitted to the faculty of the Virginia Polytechnic Institute and State University in partial fulfillment of the requirements for the degree of

Doctor of Philosophy
In
Macromolecular Science and Engineering

Judy S. Riffle, Chair
S. Richard Turner
Richey M. Davis
John Matson
Bruce E. Orler

December 11th , 2018

Blacksburg, VA

Keywords: desalination, reverse osmosis, poly(arylene ether sulfone),ionomers, membrane, polycondensation, post-sulfonation

Synthesis, Characterization and Structure-Property Relationships of Post-sulfonated Poly(arylene ether sulfone) Membranes for Water Desalination

Shreya Roy Choudhury

ABSTRACT

Clean water is critical to the safety, security and survivability of humankind. Nearly 41% of the Earth's population lives in water-stressed areas, and water scarcity will be exacerbated by an increasing population. Over 96% of the total water is saline and only 0.8% is accessible fresh water. Thus, saltwater desalination has emerged as the key to tackle the problem of water scarcity. Our current work deals with the membrane process of reverse osmosis. Sulfonated polysulfones are a potential alternative to state-of-the-art thin film polyamides. Synthesized by step growth polymerization, polysulfone membranes have smooth surfaces and they are more chemically resistant relative to polyamides.

Previously studied sulfonated polysulfone membranes were synthesized by direct copolymerization of pre-disulfonated comonomer and the sulfonate ions were placed on adjacent rings of bisphenol moiety. This study focuses on placing the sulfonate ions differently along the polysulfone backbone – on isolated rings of hydroquinone moiety, and on adjacent rings of biphenol moiety- and its effect on the transport and hydrated mechanical properties of the membranes. Selective post sulfonation of poly(arylene ether sulfone) in mild conditions was also found to be an effective way to strategically place the sulfonate ions along the backbone of the polymer chain without the need to synthesize a new monomer.

Hydroquinone based, amine terminated oligomers were synthesized with block molecular weights of 5000 and 10,000 g/mol. They were post-sulfonated and crosslinked at their termini with epoxy reagents. Such crosslinked and linear membranes had sulfonate ions on isolated rings

of hydroquinone moiety. Synthesis and kinetics of controlled post-sulfonation of poly(arylene ether sulfones) that contained biphenol units were also reported. The sulfonation reaction proceeded only on the biphenol rings. The linear membranes had sulfonate ions on adjacent rings of biphenol moieties.

The tensile measurements were performed on the membranes under fully hydrated conditions. All membranes remained glassy at values of water uptake. It was found that elastic moduli and yield strengths in the hydroquinone- based linear and crosslinked membranes increased with decrease in water uptakes in the membranes. The effect of plasticization of water superseded the effect of block length and degree of sulfonation in the membranes. The highest elastic modulus of 1420 MPa at lowest water uptake of 18% was observed in cross linked membrane with 50% repeat units being sulfonated (50% repeat units contain hydroquinone)and target molecular weight of 5000 g/mol. However, the hydroquinone membranes broke at low strains of < 20%. The hydrated mechanical properties could be improved by replacing the hydroquinone with biphenol moieties. The biphenol based post-sulfonated membrane showed high elastic modulus that was comparable to the hydroquinone-based counterparts at similar values of water uptake. The biphenol based membrane broke at higher strains of >80%.

The post-sulfonated membranes- hydroquinone-based linear and crosslinked membranes and biphenol-based linear membranes had better transport properties than the previously studied sulfonated polysulfones that were synthesized by disulfonated comonomers.The post sulfonated hydroquinone-based membranes did not show a compromise in the rejection of monovalent ions in the presence of divalent ions in mixed feed water. The superior properties of the post-sulfonated membranes can potentially be attributed to the kinked backbone that potentially increased the free volume in the membranes and the sulfonate ions were spaced apart to potentially reduce their

chelation with calcium (divalent) ions in mixed feed water. Interestingly, the biphenol based post-sulfonated membranes also did not have any compromise in the rejection of monovalent ions in the presence of divalent ions. This was potentially because the sulfonate ions were spaced far apart on the non-planar biphenol rings.

Synthesis, Characterization and Structure-Property Relationships of Post-sulfonated Poly(arylene ether sulfone) Membranes for Water Desalination

Shreya Roy Choudhury

GENERAL AUDIENCE ABSTRACT

According to the World Economic Forum, the water crisis has remained one of the top five global risks that has had a huge impact on the society. The world population has tripled in the twentieth century. Close to 2 billion people live in water scarce regions, 1.2 billion people lack access to safe drinking water, 2.6 billion have little or no access to sanitation and countless die due to diseases transmitted through unsafe water. Industrialization and climate change have worsened the water crisis. Furthermore, in today's economies food, energy and water are inherently linked. Thus, a water crisis can have a cascading effect on availability of food and energy. To obtain an adequate and sustainable supply of water, it is important to improve already existing methods and develop new and inexpensive technologies for water purification. According to the U.S. geological survey over 96% of the earth's water is saline. Thus, salt water desalination has emerged as the key to tackle the problem of scarcity of potable water.

Reverse osmosis is a membrane-based process for water desalination wherein the membrane allows water to pass through while rejecting salts. The membranes are composed of long chain molecules called polymers. The current state of the art polymeric membrane made of polyamides show high rejection of salts with fast permeation of water. However, these membranes can be degraded by the chlorinated disinfectants added to the feed water.

An alternative polymeric material, sulfonated polysulfone, can potentially be applied for reverse osmosis as these polymers are resistant to the chlorinated species. These membranes are composed of a polysulfone with sulfonate ions present randomly on the chain. This study

investigates the effect of the position of the ions on the polymer chain. It is found that the membranes ability to reject salt from water can be improved by strategically placing the charged species on the polymer chain.

Dedicated to my loving parents, Mrs. Debjani Roy Choudhury and Mr. Prabir Roy Choudhury,

for their constant support and motivation

Acknowledgement

My PhD journey was rich with new experiences and opportunities that helped me grow not only as a researcher but also as a person. I could not have achieved anything without the constant support and encouragement of many people. I would like to extend my gratitude to everyone who have been there by me while I pursued the roller coaster ride of attaining my doctoral degree.

I will forever be indebted to my thesis advisor, Prof. Judy Riffle, for everything she has done for me. Firstly, I would like to thank her for giving me the opportunity to work with her. I have benefitted immensely from her both professionally and personally that enabled me to grow from a student to an independent researcher. Apart from the technicalities of research, I look up to her for her professionalism, dedication and endless curiosity that made me passionate about my work. This dissertation would not have been complete without her guidance, patience and valuable suggestions.

I would like to thank my committee members Prof. Richard Turner, Prof. Richey Davis, Prof. John Matson and Dr. Bruce Orler for their valuable suggestion and feedback towards my research. I am thankful to Prof. Benny Freeman from University of Texas at Austin for his collaboration and countless scientific discussions. I would also like to thank Dr. Sue Mecham for her valuable guidance on SEC.

My earnest thanks to all the Riffle group members especially Amin Daryaei, Matt Joseph and Dana Kazerooni for their helpful scientific discussions, support, friendship and making our lab a fun place to work in. I would also like to thank Dr. Ozma Lane for being available to help me even after graduating. I'd like to thank Virginia Tech NMR staff, Dr. Narsimhamurthy Shanaiah for his insights on NMR.

I am fortunate enough to have a loving family and friends without whom I would have been able to finish my PhD. I am thankful to my friends Aheli, Debarati, Cigdem, Ami, Brittany, Diana, Yifan, Lourdes, Rajani, Shraddha who helped me get through many difficult times personally and professionally. My earnest thanks go to my family members, Drs. Abhishek Roy and Mou Paul who were instrumental in helping me start my graduate school at Virginia Tech and for their constant guidance throughout my PhD.

Finally, I would like to thank my parents, Mrs. Debjani Roy Choudhury and Mr. Prabir Roy Choudhury. They have made many sacrifices to see me earn a PhD and have been patient, kind and understanding all through their life and especially in the last five years. Thank you Maa and Baba for your unconditional love and support. Last but not the least I would like to thank my husband and best friend, Dr. Naveen Prakash, for his selfless love. He has been my biggest supporter and helped me, in every possible way and I couldn't have asked for a better partner in life. This work might not have been complete without him by my side.

ATTRIBUTES

Chapter 2: Synthesis and characterization of post-sulfonated poly(arylene ether sulfone) membranes for water desalination

Ozma Lane, PhD, is currently working at Owens Corning corporation. Ms. Lane performed the kinetic studies of the polymers.

Dana Kazerooni, B.S. is currently a graduate student in the Department of Macromolecular Science and Engineering. This coauthor performed the analysis of the mechanical properties of the membranes. He also assisted in the water uptake measurements.

Gurtej Narang, PhD, is from the Department of Macromolecular Science and Engineering and contributed to the synthesis of some of the oligomers.

Chapter 3: Structure- property relationships of post-sulfonated poly(arylene ether sulfone) membranes for water desalination

Eui Soung Jang, B.S, is currently a graduate student in the Department of Chemical Engineering at the University of Texas at Austin. Mr. Jang contributed to the water purification property testing of the membranes.

Dana Kazerooni, B.S. is currently a graduate student in the Department of Macromolecular Science and Engineering. This coauthor assisted in the water uptake measurements and film casting.

Chapter 4: Synthesis, characterization, reaction kinetics of biphenol containing post-sulfonated poly(arylene ether sulfone) membranes for water desalination.

Eui Soung Jang, B.S, is currently a graduate student in the department of Chemical Engineering at the University of Texas at Austin. Mr. Jang contributed to the water purification property testing of the membranes

Dana Kazerooni, B.S. is currently a graduate student in the Department of Macromolecular Science and Engineering. This coauthor measured the transport properties of the membranes.

TABLE OF CONTENTS

LIST OF FIGURES

LIST OF TABLES

Chapter 1 : Literature review

1.1 Need for water desalination

According to the World Economic Forum, the water supply crisis has remained one of the top five global risks in terms of societal impact since 2012 [1]. The global population has tripled in the twentieth century and is projected to reach 8.6 billion by 2030 [2], leading to a rise in water demand. The water crisis has been further worsened by industrialization and climate change. Close to 2 billion people live in water scarce regions, 1.2 billion people lack access to safe drinking water, 2.6 billion have little or no access to sanitation and countless die due to diseases transmitted through unsafe water [3]. Furthermore, Sanders and Webber have reported that 12.6% of the total national primary energy consumption in 2010 was for water related purposes (i.e. treatment, transportation) [4]. In today's economies, food, energy and water are inherently linked (food-energy-water nexus) [5–7]. Thus, a water crisis can have a cascading effect on availability of food and energy. To obtain an adequate and sustainable supply of water, it is important to improve already existing methods and develop new and inexpensive technologies for water purification.

According to the U.S. Geological Survey, ~96.5 % of the Earth's water is located in seas and oceans with the remaining in surface and ground water, mostly frozen in glaciers and ice caps [8]. This implies that over 96% of the total water is saline and only 0.8% is considered to be accessible fresh water [9]. Solutions such as water conservation and water transfer or dam construction are not sufficient to meet increasing demands. Traditional fresh water resources like lakes and rivers have been misused or over used and consequently are either diminishing or

becoming saline. Thus, saltwater desalination is economically the key to tackle the problem of scarcity of potable water.

Many countries have adopted national standards for drinking water with respect to the total dissolved solids, contaminants etc. However, these standards vary from region to region [10–12]. Water is classified according to its salinity content: Fresh water has a salinity up to 1500 ppm, brackish water has a salinity in the range of 1500-10,000 ppm, and sea water has a salinity in between 10,000-45,000 ppm.

Early research on water desalination was started in the US during World War II to satisfy the need for freshwater in remote locations [13]. As a major effort funded by the U.S government the Saline Water Conversion Act of 1952 was the first step towards research and development in desalination [14]. The Office of Saline Water funded research aimed at developing processes to recover drinking water from the oceans and brackish groundwater resources in collaboration with various institutions, universities and private companies. This initiative opened the door for new concepts and helped develop new strategies for desalination

1.2 Processes of desalination

Membrane and thermal processes are the two major methods for desalination. Table 1.1 lists various thermal and membrane processes for desalination. The choice of desalination technology is a site-specific combination of factors like the form of energy available, source water quality and other local conditions.

Thermal processes	Membrane processes
Multi-Stage Flash Distillation (MSF)	Electrodialysis
Multi-Effect Distillation (MED)	Electrodialysis Reversal
Vapor Compression Distillation (VCD)	Reverse Osmosis

Table 1.1: Various thermal and membrane processes for water desalination

The global desalination capacity is currently 100 million m^3day^{-1} of which 69% is from membrane processes and 31% is from thermal processes (Figure 1.1) [15]. As reported in 2009, over 15,000 desalination plants were operating worldwide and approximately 50% were reverse osmosis plants [9]. The water sources that are being desalinated are sea water (58.9%), brackish groundwater (21.2%), and surface water and saline waste water (19.9%).

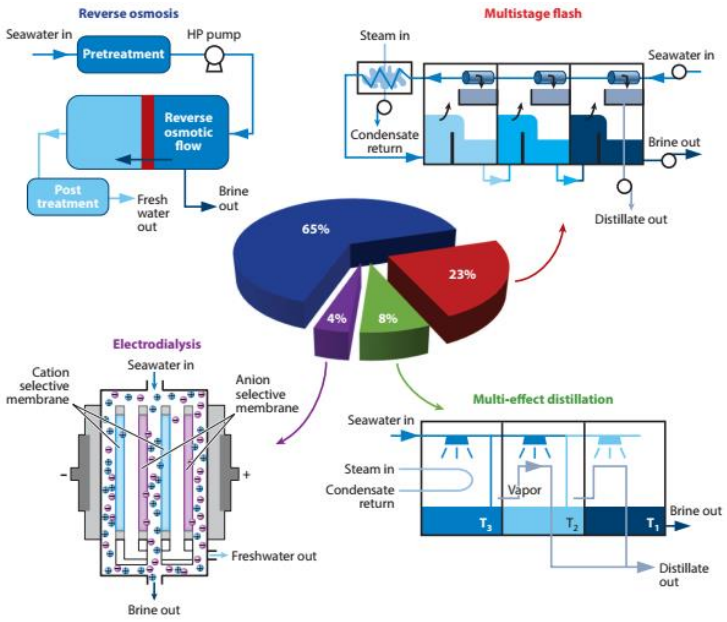

Figure 1.1: Dominant desalination technologies and their contributions to the worldwide desalination capacity of sea water and brackish water

Thermal evaporation or sea water distillation were the earliest commercial methods of sea water desalination, first developed in the 1950s [16]. Thermal methods of distillation dominate

the desalination market in the Gulf States where this process remains competitive due to low energy costs [13,17]. Thermal processes consist primarily of vapor compression and multi-effect flash distillation, although most the world's distillation plants now use multi-stage distillation. Thermal methods employ a phase change that have some advantages over membrane-based processes. High purity water can be obtained without lengthy pretreatment processes or extensive monitoring of feed water components. However, water recovery levels are lower than those obtained by the membrane process.

1.3 Membrane processes for water purification and desalination

Separation of a mixture in a membrane process is due to different transport rates of different compounds through the membrane. Separation occurs because the membrane has the ability to selectively transport one component of the feed mixture. The flux of the component across the membrane can be due to convective bulk flow of matter through defined pores in the membrane or diffusion of individual components through a dense membrane material. The membranes used in various applications differ widely in their function and the way they are operated in a given process. However, all membranes and membrane processes share several features that make them particularly attractive for separation of molecular mixtures. Separation occurs by physical means at ambient temperature without chemically altering the constituents.

1.3.1 Types of membrane processes

Membrane processes used in separations can be grouped according to the applied driving forces as described below:

i) Hydrostatic pressure-driven processes such as reverse osmosis, nano-, ultra-, and microfiltration.

ii) Concentration or chemical potential gradient-driven processes such as dialysis, Donnan dialysis, pervaporation, and the use of membrane contactors and scrubbers.

iii) Electric potential gradient-driven processes such as electrolysis and electrodialysis.

The discussion here is focused on processes used in the production of potable water by removal of ions and particles from water as shown in Figure 1.2. The five common processes used in the treatment of water for human consumption are reverse osmosis (RO), nanofiltration ultrafiltration, microfiltration, and electrodialysis/electrodialysis reversal.

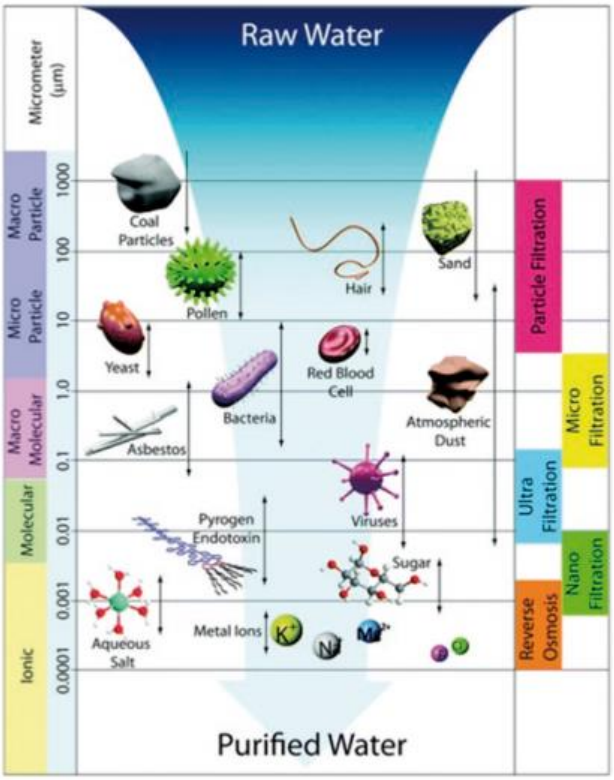

Figure 1.2: Schematic representation of water purification using different membrane processes. Reproduced from [17] with permission from The Royal Society of Chemistry.

Microfiltration and Ultrafiltration

Pressure-driven membrane processes differ from non-pressure-driven methods in the mass transport mechanism and the membranes that are used. Differences in pore diameters leads to vast differences in their applications. Ultrafiltration and microfiltration are similar with increasing fine pores. The mode of separation is molecular sieving and can be described by the pore flow model

of membrane separation. These processes use macro- and mesoporous membranes [18]. Microfiltration membranes have pore diameters of 0.2-10 μm. The applied pressure is in the range of 0.5×10^5 - 2×10^5 Pa. The components separated in ultrafiltration are macromolecules with molecular weights of ~0.5×10^3 - 500×10^3 g/mole. These techniques can be used to remove microorganisms and suspended and colloidal particles from drinking water supplies.

Since the early 1900s, there has been rapid growth in the use of low pressure hollow fiber microfiltration and ultrafiltration membrane processes for production of drinking water. One of the main drivers for the increase in growth of microfiltration and ultrafiltration is the increasingly stringent environmental legislation implemented in the last decade [15]. These techniques are applied as a pretreatment method prior to reverse osmosis in integrated membrane systems where they have replaced lime softening and filtration as the preferred method for pretreatment [19]. These membranes are designed to remove particulate matter. The pretreated water was found to be significantly better in terms of turbidity and silt density index. However, the primary disadvantage is that both systems are prone to fouling. Microfiltration frequently uses hollow fibers or membranes made from cellulose acetate, polypropylene, polysulfone, poly(vinylidene fluoride), poly(ether sulfone), or other materials

Nanofiltration

Nanofiltration membranes lie in the transition region between reverse osmosis and ultrafiltration membranes. Typically, these membranes have sodium chloride rejections between 20 and 80%. They are characterized by pore diameters less than 2 nm, passage of an appreciable amount of monovalent ions, substantially high rejection of divalent ions relative to monovalents, molecular weight cut-offs for neutral species in the 150-2000 Da range and rejection of neutrals

and positive ions relating principally to their size and shape [20]. The separation by solution-diffusion involves dissolution of the permeants in the membrane matrix and diffusion through the concentration gradient.

The success of nanofiltration results from its selective separation of one solute over another. For example, waste streams from textile dying are comprised of dyes and salt. Reverse osmosis would remove both components, however, nanofiltration can be used to retain valuable salts while concentrating dyes into more manageable volumes [21]. Nanofiltration membranes also have an advantage of the ability to operate at low pressures. Interfacial polymerization remains the most common approach to manufacture the barrier layer in commercial nanofiltration membranes. Other approaches for fabricating nanofiltration membranes include phase inversion, layer-by-layer coatings, incorporation of aquaporins, and the use of glassy polymers with high internal porosity.

Reverse Osmosis

The phenomenon of osmosis was first observed by Abbe Nollet [22] in 1748. In osmosis, the diffusion of water across a semipermeable membrane occurs due to a concentration gradient. The water flows from a compartment of lower salt concentration to one with a higher salt concentration due to the osmotic pressure. In reverse osmosis, a hydrostatic pressure is applied that is equal and opposite in direction to the osmotic pressure such that the water flows from high salt concentration (solution side) to a low salt concentration (solvent side) (Figure 1.3).

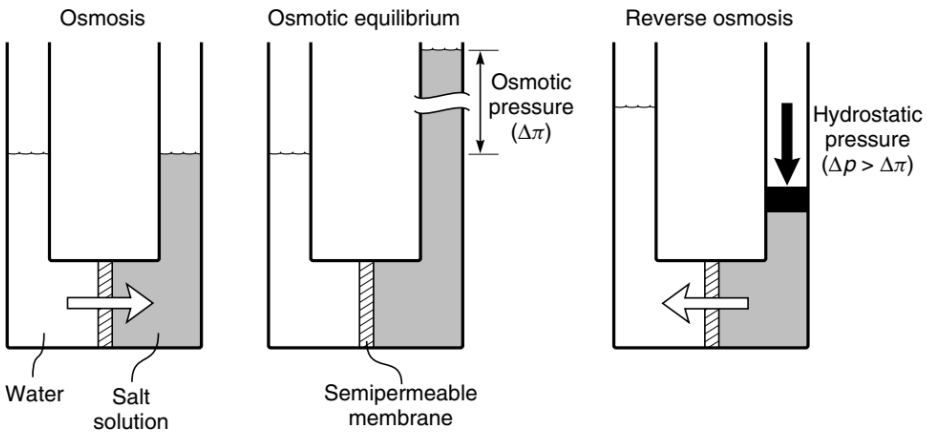

Figure 1.3: Representation of a system in osmosis, osmotic equilibrium and reverse osmosis

The semipermeable membrane is the key component in reverse osmosis. It needs to be selective, allowing water to pass through while rejecting salt. The properties of a good membrane for reverse osmosis are:[2]

i) The membrane must be highly permeable to water, but impermeable to salt/solute.

ii) The membrane should be as thin as possible to achieve a high water flux but mechanically robust enough to withstand the high pressure in reverse osmosis systems.

iii) The membrane should be chemically inert.

iv) The membrane should be capable of being fabricated into configurations with high surface to volume ratio.

Reverse osmosis is widely used because of the low energy demands in the range of 2- 4 $(kW\ h\ m^{-3})^2$ as compared to the processes of MSF and MED that have energy demands that are ten times as much [23]. Although the minimum energy required by reverse osmosis depends on the salinity of the water and operating conditions, the cost of power consumption for sea water reverse osmosis plants has been decreasing drastically and approaching the theoretical minimum as shown in Figure 1.4.

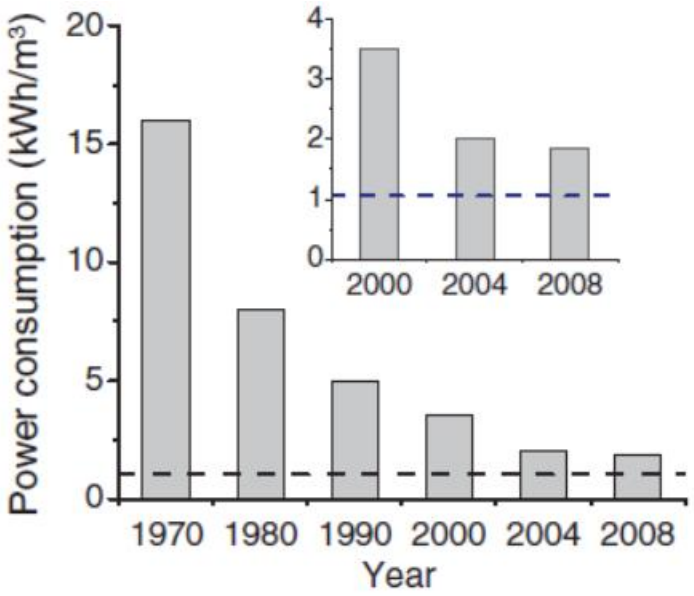

Figure 1.4 Energy consumption in reverse osmosis membranes from 1970-2008. The dashed line stands for the theoretical minimum. From M. Elimelech, W.A. Philip, The future of sea water desalination: energy, technology, and the environment, Science 333 (2011) 712-7 [23]

Electrodialysis

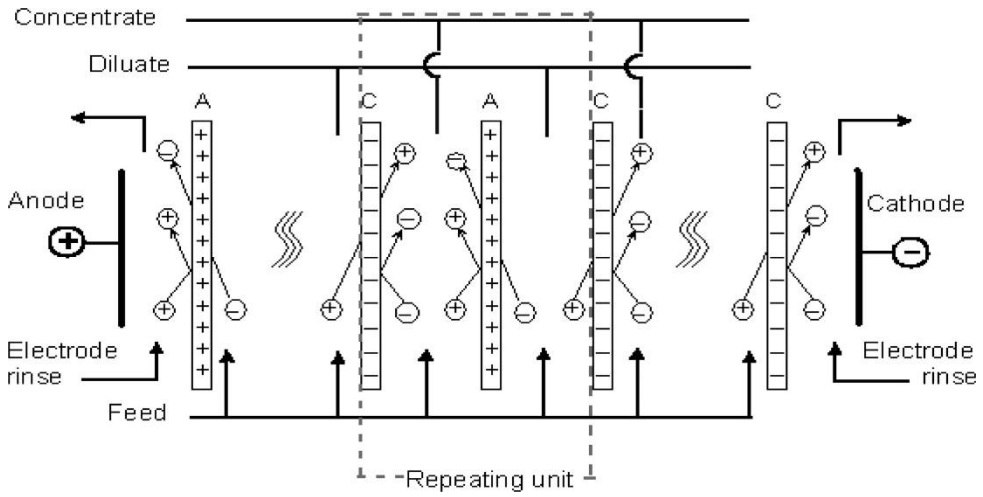

Figure 1.5: Overview of the process of electrodialysis

Figure 1.5 represents the process of electrodialysis. An electrodialysis cell consists of alternately stacked positively charged anion and negatively charged cation exchange membranes, and electrodes - an anode and a cathode. When an electrolyte feed water is pumped through the

cell and an electric potential is applied between the electrodes, the cations from the feed water migrate towards the cathode. They pass through the cation exchange membranes but are retained by the anion exchange membranes. Similarly, the anions move towards the anode passing through the anion exchange membranes but are retained by the cation exchange membranes. The overall result is that the concentrated and diluted electrolytes are separated so that they may be removed and treated. An advantage of the process of electrodialysis over reverse osmosis is that the charged particles deposited on the membranes can be dissolved back into the solution by changing the electrical polarity by electrodialysis reversal. This step can prevent scaling as associated with the reverse osmosis membranes. However, this process is limited to separations of charged species only and neutral contaminants in the feed water such as microorganisms cannot be separated from the feed water [24–26].

1.3.2 Models of membrane processes

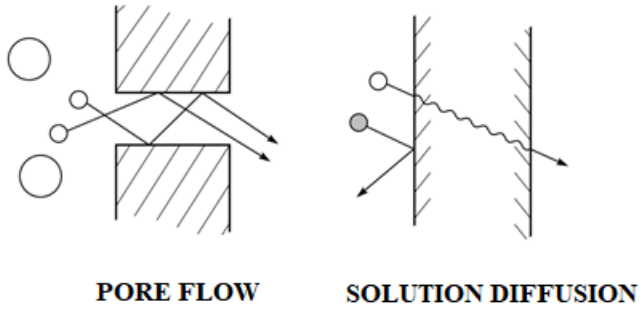

Figure 1.6: The pore slow model and the solution-diffusion model of membrane separation. From R.W. Baker, Membrane Technology and Applications, John Wiley and sons Inc. UK, 2004 [25]

Two models can be used to describe the mechanism of permeation through a membrane: the pore flow model and the solution diffusion model (Figure 1.6) [18,27]. In the pore flow model the separation occurs because one of the permeants is excluded from some of the pores through which other permeants move. The pores are relatively large and do not fluctuate in position or

volume on the time scale of the permeant motion. The membrane fluxes are high compared to those obtained by simple diffusion. Pore flow membranes are used to separate components in the size range of 10-15 Å. Ultrafiltration, microfiltration and microporous Knudsen-flow gas separations employ pore flow membranes.

In the solution diffusion model, the permeants dissolve into the polymer matrix at the high chemical potential face of the membrane and diffuse through the polymer down a chemical potential gradient [28]. The permeants desorb from the downstream side of the polymer film. Diffusion of the molecules through the polymer is the rate limiting step. Diffusion is facilitated by the opening and closing of free volume elements in the polymer matrix. Free volume elements are tiny spaces caused by the thermal motion of the polymer chains. These appear and disappear on about the same time scale as the motion of the permeants across the membrane. The permeants are separated because of differences in their solubilities in the membrane and the difference in the rate at which they diffuse through the membrane. The transport of water through a hydrated membrane can be expressed according to the Fick's law of diffusion (equation 1.1).

$$J_i = -D_i \times \frac{dc_i}{dx} \qquad \text{(Equation 1.1)}$$

Where, J_i = Rate of flux of component i

$\frac{dc_i}{dx}$ = Concentration gradient of component i

D_i = Diffusion coefficient of component i

Reverse osmosis membranes work on the principle of solution diffusion. They do not have any permanent pores and can be used to separate molecules as small as 2-5 Å in diameter (e.g. salts in reverse osmosis membranes).

1.4 Solution diffusion model for transport in reverse osmosis membrane

At steady state, the diffusive permeability of a penetrant, P_i, can be written in terms of the partition or sorption coefficient K_i, and diffusion coefficient, D_i according to equation 1.2 and this equation governs both water and ion transport through the membrane in reverse osmosis

$$P_i = K_i \times D_i \qquad \text{(Equation 1.2)}$$

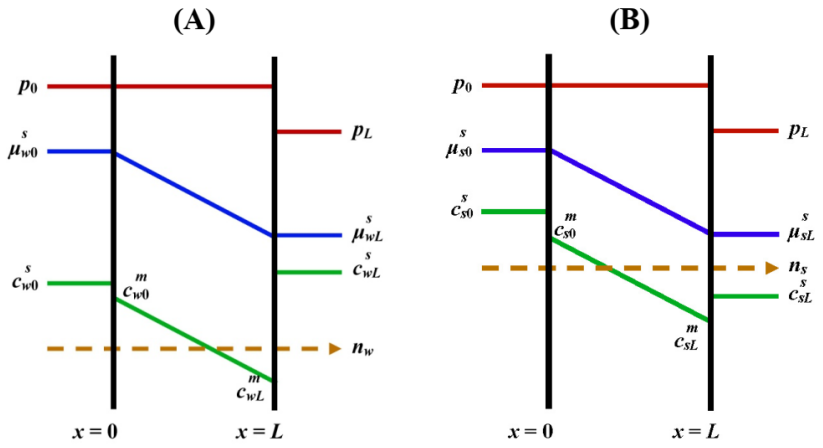

Figure 1.7: Representation of (a) water and (b) salt transport through a solution diffusion membrane. From G.M. Geise, H.B. Park, A.C. Sagle, B.D. Freeman, J.E. Mcgrath, Water permeability and water/salt selectivity tradeoff in polymers for desalination, J. Memb. Sci. 369 (2010) 130–138 [41]

1.4.1 Water Transport

Water sorption

Water uptake, w_u, is defined as the mass of water sorbed by the polymer divided by the mass of the dry polymer and is most commonly used to report water sorption. Water uptake is related to the volume fraction of water in the hydrated polymeric membrane, ϕ_w , as follows:

$$\phi_w = \frac{w_u}{w_u + \rho_w/\rho_p} \qquad \text{(Equation 1.3)}$$

where ρ_w and ρ_p are the densities of the water and dry polymer respectively. In the solution-diffusion model the water sorption coefficient K_w [g (H_2O)/cm^3 (swollen polymer)]/[g (H_2O)/cm^3(solution)] relates to the water sorption by equation 1.4:

$$K_w = \frac{\phi_w M_w}{c_w^s V_w} \quad \text{(Equation 1.4)}$$

where M_w is the molecular weight of water, and c_w^s is the mass concentration of water in the external solution. According to Equation 1.2 a higher water sorption is required for a high permeability. Additionally, water content strongly influences water and salt diffusion coefficients. Some extent of water sorption by the polymers is required to achieve sufficient water permeability for desalination applications. However, increased water sorption can reduce the polymer's ability to separate water and salt as more salt enters the membrane with water. The water sorption increases with increase in the hydrophilicity of the membrane. Highly hydrophilic polymers can be crosslinked to control the water sorption [29–34]. It has been found that crosslinking can reduce the swelling and also the free volume [35–37]. Moreover, crystalline regions in polymers do not absorb small molecules like water. So, all factors remaining equal, increasing the polymer crystallinity decreases the water uptake [38,39].

Water permeability

The driving force for water transport through non-porous membranes is a water concentration gradient across the membrane. In reverse osmosis water flows from the higher osmotic pressure side to the lower osmotic pressure side by application of hydrostatic pressure across the membrane [26,40]. The hydrostatic pressure is constant across the membrane and equal to the upstream pressure. At the downstream face of the membrane the water molecules inside the membrane are exposed to the upstream pressure (P_0) but the ones just outside the

membrane are exposed to downstream pressure (P_L). This discontinuity in pressure creates the water concentration gradient across the membrane and drives the diffusion of water through the film.

Water flux

The flux or permeation rate is the volume of water flowing through the membrane per unit area and time. The water flux through the membrane is given by equation 1.5.

$$J_w = \frac{C_{w0}^m D_w}{\rho_w L} \times \frac{V_w}{RT}(\Delta p - \Delta \pi) = \frac{P_w C_{w0}^s}{\rho_w L} \times \frac{V_w}{RT}(\Delta p - \Delta \pi) \qquad \text{(Equation 1.5)}$$

where J_w, expressed in g/cm^{2}s is the steady state volumetric flux of water, D_w is the average water diffusion coefficient (cm^2/s), and ρ_w is the density of water. L is the film thickness (cm), V_w is the molar volume of water, R is the gas constant, T is the absolute temperature, Δp and $\Delta \pi$ are the pressure and osmotic pressure differences, respectively, across the film. C_{w0}^m (g H_2O/cm^3 of swollen polymer) is the mass concentration of water sorbed in the film at the upstream face. C_{w0}^s (g H_2O /cm^3 solution) is the mass concentration of water in the external solution in contact with the upstream face of the membrane**.**

$$P_w^D = \frac{C_{w0}^m}{C_{w0}^s} D_w = K_w D_w \qquad \text{(Equation 1.6)}$$

K_w is the water partition coefficient, and D_w is the water diffusion coefficient. Water diffusivities in polymers can be low, so high water fluxes require either thin membranes, high water sorption in the polymer, or a large driving force (hydrostatic pressure). The diffusive water permeability of water relates to the diffusive flux of water under a concentration gradient of water and the hydraulic permeability of water relates to the water flux under a hydraulic pressure gradient. Typical units for P_w^H are L µm m^{-2} h^{-1} and that of P_w^D are cm^2/sec. The hydraulic water permeability, P_w^H of a polymer film is defined experimentally by equation 1.7.

$$P_w^H \equiv \frac{J_w L}{\Delta p - \Delta \pi} \quad \text{(Equation 1.7)}$$

For polymers with low water sorption hydraulic water permeability relates to the diffusive water permeability by equation 1.8, and this can be deconvoluted into the water partition coefficient and diffusion coefficient using the solution diffusion model where

$$P_w^D = P_w^H \frac{RT}{V_w} \quad \text{(Equation 1.8)}$$

V_w is the partial molar volume of water, R is the gas constant and T is the absolute temperature.

$$J_w = \frac{P_w^H}{L}(\Delta p - \Delta \pi) = A(\Delta p - \Delta \pi) \quad \text{(Equation 1.9)}$$

In Equation 1.8, A is the water permeance which is commonly reported by the membrane manufacturers. However, water permeance is not an intrinsic material property of a membrane since it depends on the thickness of the membrane. Thus, determining fundamental properties of the membrane becomes difficult for commercial membranes when the thickness of the membranes are not reported by the manufacturer [41].

1.4.2 Salt transport

Salt flux

The difference in salt concentration on either side of the membrane gives rise to a difference in the electrochemical potential of the salt. The potential difference gives rise to a concentration gradient in the polymer that drives salt transport by Fickian diffusion. Unlike water flux, salt flux depends only on the concentration gradient and not on the pressure and temperature. The salt permeability, P_s, can be derived by integrating Fick's law at steady state across the polymer film.

$$J_s = \frac{K_s D_s}{L} \Delta c_s^s = \frac{P_s}{L} \Delta c_s^s = B \Delta c_s^s \quad \text{(Equation 1.10)}$$

where J_s is the mass flux of the salt through the membrane, K_s is the salt sorption coefficient, D_s is the average salt diffusion coefficient, Δc_s^s is the salt concentration difference between the external solutions. Similar to the water permeance, B is the salt permeance.

1.4.3 Membrane selectivity

The ability of polymers to separate water from salt can be characterized in terms of water/salt permeability selectivity, α. This is a material property defined as the ratio of the more permeable penetrant to that of the less permeable one. It was found that increasing the membrane permeability resulted in the loss of membrane selectivity. Geise et al. studied an upper bound relationship for dense water purification membranes to better understand their transport properties [41]. However, the available literature was complicated because most membrane manufacturers report the membrane performance in terms of salt rejection and water flux, neither of which are intrinsic membrane properties. It should be noted that water and salt diffusion coefficients, and water and salt solubility coefficients are intrinsic parameters that can be used to find the selectivity α.

$$\alpha \equiv \frac{P_w}{P_s} = \frac{K_w}{K_s} \times \frac{D_w}{D_s} \qquad \text{(Equation 1.11)}$$

The apparent salt rejection, R, is defined by salt concentrations in the feed and permeate solution and is related to selectivity as follows:

$$R = 1 - \frac{c_{sL}^s}{c_{s0}^s} = \frac{\alpha \frac{V_w}{RT}(\Delta p - \Delta \pi)}{1 + \alpha \frac{V_w}{RT}(\Delta p - \Delta \pi)} \qquad \text{(Equation 1.12)}$$

Salt passage is defined as 1-R, and both salt rejection and passage are typically expressed as a percentage.

1.5 Materials for reverse osmosis membranes

1.5.1 Cellulose acetate

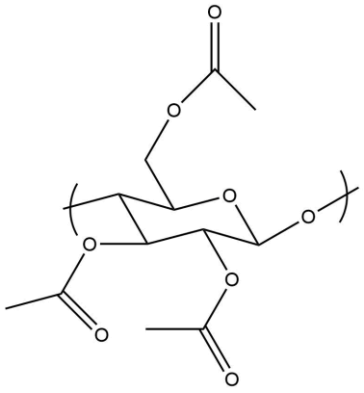

Figure 1.8: Structure of cellulose triacetate

Reid and Breton, in 1959, showed that cellulose acetate membranes can perform as reverse osmosis membranes. They obtained 98% salt rejection with a high pressure of 1000 psi albeit with low permeate flux (less than 10 mL $m^{-2} h^{-1}$) because the membranes were 5-20 µm thick.

A major breakthrough for reverse osmosis membranes was the development of an anisotropic cellulose acetate membrane by Loeb-Sourirajan. With these membranes, water desalination gained the potential to be a practical process and they were the industry standard through the 1960s to mid 1970s. The Loeb-Sourirajan membrane was developed by application of the Gibbs adsorption equation to desalination, the discovery of the semipermability of cellulose acetate (Figure 1.8), and recognition of asymmetry/anisotropy and its importance in obtaining a flux that was greater than that obtained by previously tested homogeneous membranes [21].

The economic utilization of reverse osmosis membranes depended on obtaining high flux without serious loss to electrolyte rejection properties and this was achieved by reducing membrane thickness. These asymmetric cellulose acetate membranes were fabricated by a phase inversion process. This technique leads to an integral structure with the skin and the support layer

made from the same material in a single process. The Loeb-Sourirajan membranes were hand cast using a solution of cellulose acetate, acetone, and aqueous magnesium perchlorate. The solution was evaporated on a glass plate before being immersed in cold water followed by wet annealing to produce asymmetric films [42].

Riley et al. [43] studied the structure of these membranes by transmission electron microscopy and found that they had an asymmetric structure with a thin dense skin, ~100-200 nm in thickness. The skin, which determined the selectvity and flux, was supported by a highly porous structure which provided mechanical strength. In the phase inversion process, the wet annealing step closed the pores and made the membranes dense. Studies on the transport behavior verified the solution-diffusion mechanism for reverse osmosis [44–46]. The water and salt permeability of cellulose acetate membranes were sensitive to the degree of acetylation of the polymer used to make the membrane. While salt rejection increased, the water permeability decreased with increase in the acetyl content [44]. Futher research was carried out to improve membrane transport properties and simplification of manufacturing to bring the technology to industrial applications. Cellulose diacetate (CDA) was replaced by cellulose triacetate (CTA) due to its stability in a wide range of pH and temperature as well as having a higher resistance to chemical and biological attack [47]. Cellulose acetate membranes can tolerate up to 1 ppm of chlorine, so chlorination can be used to sterilize the feed water. However these hydrolyze over time and work best only in a pH range of 4-6 and can operate up to 30 ºC [42]. However, CTA is prone to compaction, resulting in a severe loss of flux even at moderate operating pressures of 30 bar or less [48]. Most commercially used cellulose acetate membranes use a polymer containing about 40 wt% acetate with a degree of acetylation of 2.7. These membranes exhibit a 98-99% sodium chloride rejection and have reasonable fluxes. Some of the best membranes reported are prepared by blends of 39.8

wt% cellulose diacetate with small amounts of cellulose triacetate (44.2% acetate) or cellulose butyrate which exhibit a salt rejection of 99.0-99.5% in SWRO with modest fluxes [27].

1.5.2 Polyamide thin film composite

In the early 1980s John Cadotte developed interfacial polyamide chemistry on thin film composites (TFC) for reverse osmosis applications [49]. Four decades later, it remains the leading technology in the industry. The commercial TFC consists of three distinct layers. The top permselective layer is an ultrathin polyamide. The middle layer is a microporous support (usually polysulfone or poly(vinylidene fluoride)). The bottom layer is a woven or non-woven fabric, usually polyester, to provide additional mechanical support.

For the case of a porous polysulfone support, the polysulfone dissolved in a polar aprotic solvent is cast on a polyester fabric. The fabric is then immersed in a non-solvent (usually water) that precipates the polysulfone. The resulting polysulfone membrane has small pores that are formed upon contact with the non-solvent. The dense polyamide layer on the order of 100 nm thick is formed by interfacial polymerization between a difunctional amine in the aqueous phase and a trifunctional acid chloride in the organic phase. The microporous polysulfone support web is coated with an aqueous solution containing a water soluble monomer. Then, a water immiscible organic solution containing a second monomer is applied on top of the aqueous layer. Monomers in the different layers react only at the interface via diffusion because of the immiscibility of the aqueous and organic solutions. This gives rise to the thin and dense polymer layer. The reaction takes place in a few seconds leading to a crosslinked, three dimensional structure with amine and carboxyl residual groups. The films have a high water flux and salt rejection. The most successful polyamide TFC membranes have been synthesized from trimesoyl chloride and *m*-phenylene

diamine as shown in Figure 1.9. This system known as FT-30 developed by Cadotte at FilmTec has dominated the market.

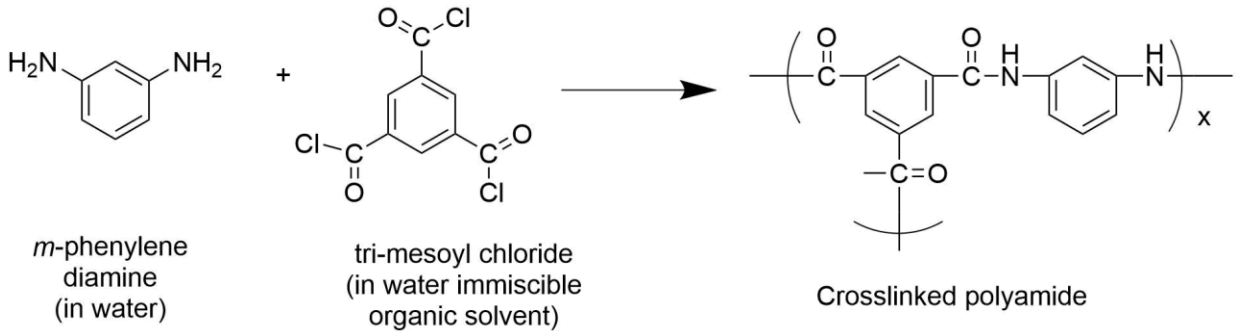

Figure 1.9: Synthesis of crosslinked polyamide membrane by interfacial polymerization [41,49]

Polyamide TFCs were successful in replacing the cellulose acetate membranes because of their excellent transport properties, high water flux and high salt rejection of >99 %, and a wider range of operational pH and temperature. These membranes have excellent transport properties with salt rejections of >99%. There are several key features of polyamide TFCs:

1. The selective layer allows for high water flux because it is very thin but it is unlikely to suffer from any mechanical fatigue because it is supported by the polysulfone layer.
2. The structure is not extremely brittle and weak in spite of being highly crosslinked [49].
3. The top permselective layer and the polysulfone support layer can be independently controlled and optimized to generate high water flux and salt rejection.
4. Polyamide membranes may also be modified post polymerization to further improve the transport properties.

Polyamide TFCs have an extraordinarily rough surface. This phenomenon was investigated by studying the kinetics and mechanism of the interfacial polymerization reaction to form polyamides [50,51]. Polymerization occurs on the liquid-liquid interface as the diamine

from the aqueous phase and acid chloride from the organic phase contact each other. In the first stage there is growth of the membrane along the water-oil interface as monomers from the aqueous phase diffuse into the organic layer. The polymerization shifts from being diffusion controlled in the organic/aqueous layer to being diffusion controlled in the polymerizing film layer. In the first and second stages, the crosslinking reaction proceeds rapidly. The continued polymerization decreases the diffusion coefficient in the film until the *m*-phenylene diamine can no longer reach the organic layer. However, after the polymerization reaction becomes self limiting in the third stage the crosslinking reaction can continue and is favored by any residual monomers. This phenomenon leads to the formation of the rough surface. The slight solubility of the diamine in the organic phase leading to formation of polymer in what has been termed a perpendicular polymerization (i.e., reaction slightly above the interface in the organic layer) is the major cause of the rough membrane surface.

Elimelech et al. found that the commercial TFC membrane they used fouled due to its high surface roughness [52]. The rough surface makes it susceptible to biofouling as a result of bacterial and organic deposition in the 'valley structures' [53–55]. On the other hand, some studies have shown an increase in flux with an increase in surface roughness because more area was available for transport [56]. However, overall efforts are focused towards developing a smooth surface of the TFC membrane. It has been reported that fouling resistant reverse osmosis membranes could be developed by applying a smooth coating of neutral hydrophilic polymer [57–60].

All natural and waste water treatment involves the use of chlorine as a biocide to prevent biofouoling. However, a major disadvantage associated with the polyamide TFC membranes is that they are subject to oxidative degradation when exposed to trace amounts of chlorine [61–63].

Chlorine solutions and hypochlorite salts are commonly used as disinfectants. Membrane performance deteriorates in long term tests even with low amounts of chlorine [42]. Polyamide membranes are generally treated with 500-2000 ppm h^{-1} sodium hypochlorite. Aqueous chlorine soltuion contains three species in equilibrium. At pH=1, the concentration of Cl_2 is the highest, at pH=7 the solution contains 80% HOCl and 20% OCl^- and at pH>7, the major species is OCl^-. The oxidation strength of these species are in the order of Cl_2 > HOCl > OCl^-. The dependence of aromatic ring chlorination on pH was demonstrated by Soice in a model study [64]. At pH 4, an intermediate concentration of chlorine was sufficient to cause significant chlorination, whereas the same amount of available chlorine at pH 7 only yielded minor ring chlorination. At pH 10, no ring chlorination was observed.

Two mechanisms have been reported for degradation of polyamides by chlorinated species as shown in Figure 1.10. The amidic hydrogen in the -NHCO- moiety is replaced by a chlorine atom followed by Orton rearrangement of the position of the chlorine atom.

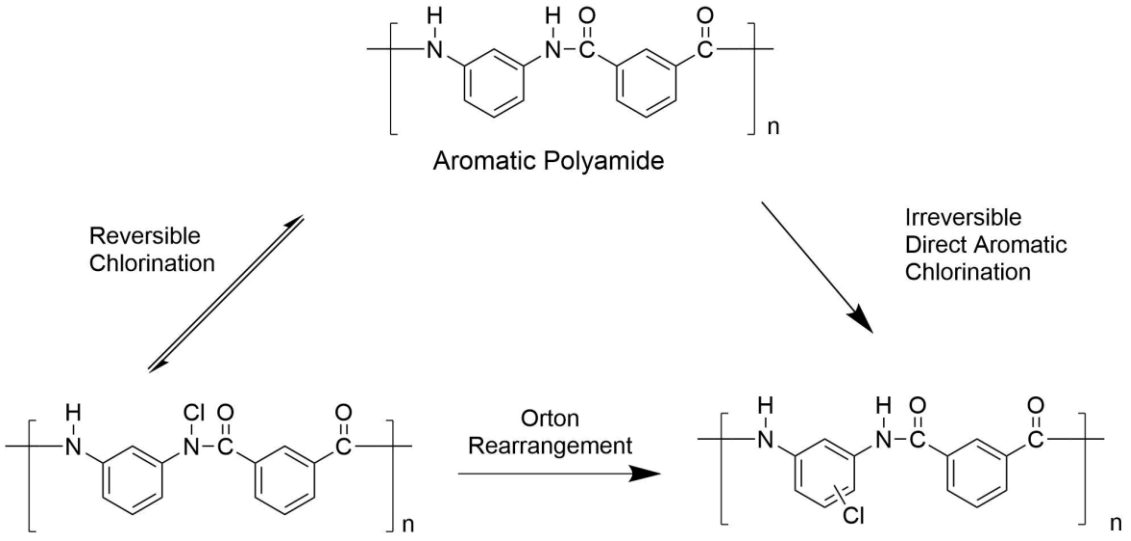

Figure 1.10: Pathways to chlorination in polyamides [41]

The feed water must be chlorinated to prevent biofouling, dechlorinated (reduced using sodium bisulfite) to protect the membrane before permeation and finally rechlorinated after the

water is passed through the membrane to protect against microbes. The treatment steps are expensive and increases the cost of the reverse osmosis systems.

1.5.3 Sulfonated poly(arylene ether sulfone) membranes

Poly(arylene ether sulfone)s exhibit excellent chlorine resistance because of the inherent chemical stability of the arylene ether moieties, but they are intrinsically hydrophobic and exhibit extremely low water permeability. A successful approach to improving water permeabilty is attachment of hydrophilic ionic groups such as sulfonates or carboxylates onto the polymers. The hydrophilicity and water permeability of sulfonated polysulfone can be tailored by controlling the degree of sulfonation. Extensive studies have been carried out on membranes cast from sulfonated polysulfones. A major difference in the method of synthesis of sulfonated polysulfones as compared to polyamide TFCs is that the polymers are first synthesized and then cast into films. Unlike polyamide TFCs the process of interfacial polymerization is not utlilized for the synthesis of the polymers and the membrane. Hence, RO membranes based on sulfonated polysulfones have smooth surfaces that avoid the risk of fouling [53].

1.6 Poly(arylene ether)s

Poly(arylene ether)s are a class of high performance engineering materials with well known thermal, mechanical, oxidative and hydrolytic stability. Poly(arylene ether sulfone)s have a high T_g and are amorphous polymers because the C-S link restricts chain rotation and consequently enhances the chain rigidity. Figure 1.11 depicts the backbone structure of some commercial poly(arylene ether sulfone)s.

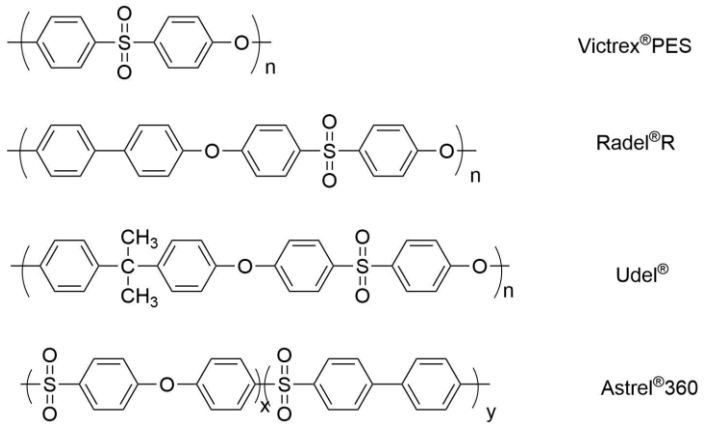

Figure 1.11: Commercial poly(arylene ether sulfone)s

1.6.1 Synthesis of poly(arylene ether sulfone)s

Nucleophlic Aromatic Substitution

Nucleophilic aromatic substitution is the most important route for synthesizing poly(arylene ether)s. This route of synthesis was developed by Johnson and coworkers at Union Carbide in 1967 [65]. They reported the first synthesis of poly(arylene ether sulfone) from 4,4'-dichlorodiphenyl sulfone (DCDPS) and bisphenol A. The reaction involves the condensation of a dialkali metal salt of a dihydric phenol with an activated aromatic dihalide in an anhydrous, aprotic, dipolar solvent. The nucleophilic displacement of a halogen from the activated systems occurs via a two-step addition-elimination mechanism (Figure 1.12).

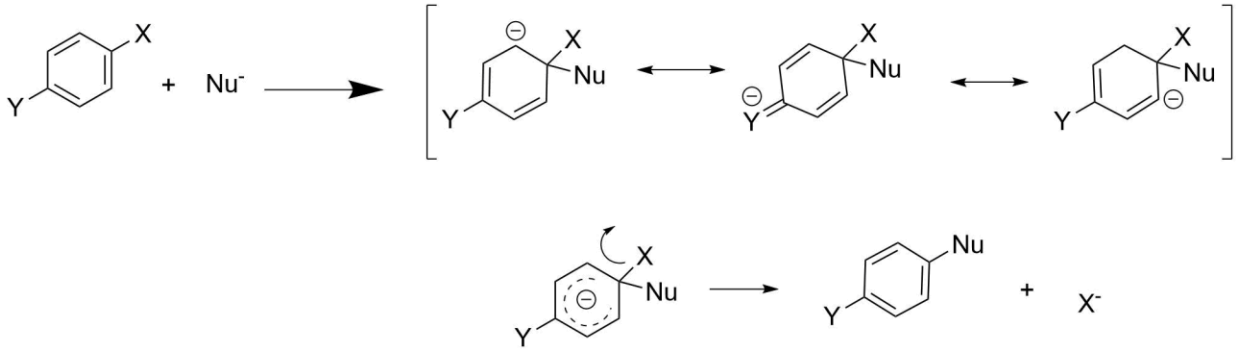

Figure 1.12: Mechanism of nucleophilic aromatic substitution reaction [66]

In the first step the nucleophile (Nu) attacks the electron deficient activated aromatic ring forming a resonance stabilized Meisenheimer complex. This is the slowest and the rate determining step. The Mesisenheimer complex has been well characterized by NMR and crystallographic data [66,67]. The electron withdrawing groups (Y) of the aromatic halides activate the ring. These groups, when positioned at the ortho or the para position to the leaving group accelerate the reaction due to -I effects [68]. The activating power of the electron withdrawing groups in increasing order is NO > NO_2 > SO_2Me > CF_3 > CN > CHO > COR > COOH > F > Cl > Br > I > H > CMe_3 > OMe > NMe_2 > OH > NH_2 [69].

The second step of the reaction involves decomposition of the Meisenheimer complex and release of the leaving group. This step is fast compared to the previous step. The order of the leaving group ability is F > NO_2 > OTs > SOPh > Cl, Br,I > N_3>NR_3^+ > OAr, OR, SR, SO_2R,NH_2. The leaving group order is different than that for SN_1 or SN_2 mechanisms as the reacitivity order in those reactions is I > Br > Cl > F. This difference in the order of reactivity is because breaking of the carbon-halide bond is the limiting factor in the latter cases whereas formation of the Meisenheimer complex is the rate limiting step in the nucleophilic aromatic substitution reaction.

A range of nucleophiles can be used in nucleophilic aromatic substitution reactions and reaction rate increases with an increase in the nucleophilicity. Nucleophilicity increases with increasing base strength. The order of nucleophilicity is ArS^- > RO^- > R_2NH > ArO^- > OH^- > $ArNH_2$ > NH_3 > I^- > Br^- > Cl^- > H_2O > ROH [68].

Polar aprotic solvent with high boiling points are used because they are good solvents for the monomers and the polymers. *N*-methylpyrrolidone (NMP), *N*,*N*-dimethylacetamide (DMAc), *N*,*N*-dimethylformamide (DMF), dimethylsulfoxide (DMSO), and cyclohexylpyrrolidone (CHP) are the commonly used solvents for this reaction.

The nucleophilic aromatic substitution reaction can be performed with either a weak (e.g., K_2CO_3) or a strong base (NaOH). Initial studies focused on using a strong base like NaOH or KOH for the synthesis, commonly known as the caustic process. The main advantage of using a strong base is that high molecular weight polymers can be synthesized in a short time, e.g. 5-6 h. However, a strict stoichiometric amount of the base has to be added because an excess of base can hydrolyse some of the activated aromatic dihalide leading to an offset in the stoichiometry. Also, an excess of the strong base can cleave the activated aromatic-ether linkage of the product polymer. When the amount of strong base is less than the stoichiometric amount required, the reaction stoichiometry is offset. Moreover, the phenolates can form hydrogen bonds with free phenols, thus decreasing the overall nucleophilicity of the phenolates [70,71].

Clendinning et al. reported the use of a weak base, potassium carbonate, for the synthesis of poly(arylene ether sulfone)s [72]. Later, McGrath and coworkers used a weak base to systematically study the synthesis of some novel poly(arylene ether sulfone)s [70,73,74]. The main advantage of the weak base or the carbonate method is that the base need not be added in strictly stoichiometric amounts. It can be used in excess without any undesirable side reactions or hydrolysis of the activated halides. However, adding less than the required stoichiometric amount leads to low molecular weight polymers. Thus, the use of potassium carbonate is preferred over a strong base. K_2CO_3 is found to be better than Na_2CO_3 because it is a stronger base and has a higher solubility in the reaction media. The proposed mechanism for the carbonate process is shown in Figure 1.13. It is postulated that the potassium monophenolate is formed in the first step. The monophenolate then reacts with the dihalo monomer. The potassium bicarbonate disproportionates to potassium carbonate and carbonic acid, producing water and carbon dioxide.

Therefore, an azeotrope forming solvent should be included in the polymerization reaction to remove the water.

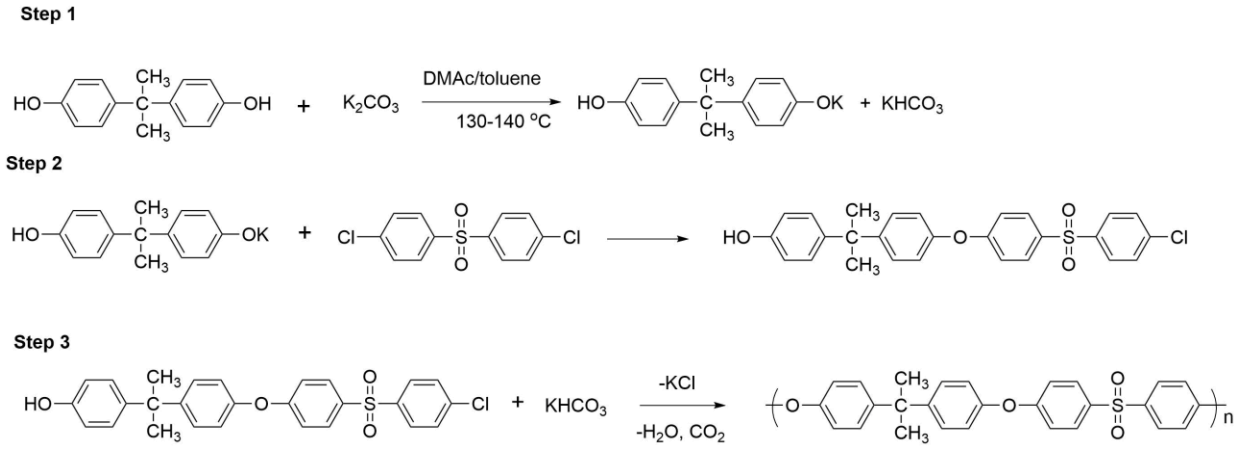

Figure 1.13: Proposed mechanism of the carbonate process [75]

Electrophilic aromatic sulfonation reaction

Electrophilic aromatic sulfonation using a Friedel-Crafts catalyst is another important route for the synthesis of poly(arylene ethers sulfone)s. Astrel 360 was prepared by 3M using this technique. The mechanism involves three steps as represented in Figure 1.14. In the first step the Lewis acid catalyst attacks the sulfonyl halide. Friedel-Crafts catalysts such as $AlCl_3$, $FeCl_3$, $SbCl_5$, $AlBr_3$ and BF_3 can be used effectively. In the second step the electron deficient species, a sulfonylium cation $ArSO_2^+$, is attacked by the π electrons of the aromatic ring to form a positively charged arenium complex. This is the slowest and the rate limiting step. As the arenium ion is highly reactive, in the third step a proton is expelled to afford the final product.

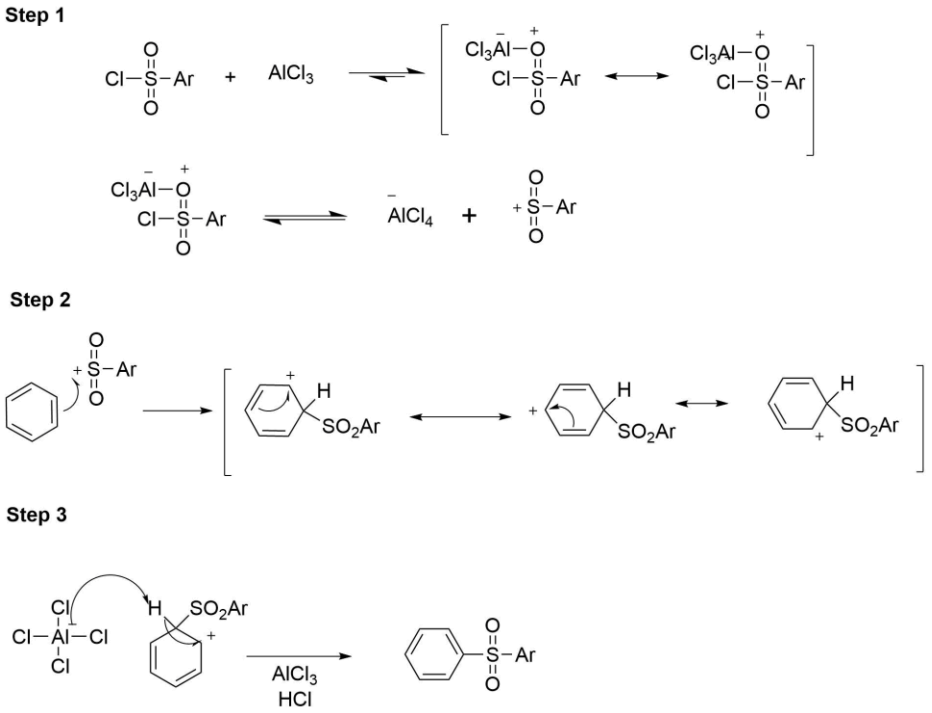

Figure 1.14: Mechanism of electrophilic aromatic sulfonation reaction by a Friedel-Crafts reagent

Other methods

The Ullmann reaction can be used to synthesize poly(arylene ethers)s when the aromatic halide is not activated and a normal nucleophilic aromatic substitution is not possible [77]. The reaction occurs between a double alkali metal salt of a dihydric phenol and aromatic dihalide in the presence of a copper catalyst. However, difficulty in removing the copper salts quantitatively and the need for specialty brominated monomers are some of the disadvantages of this reaction.

The nickel coupling route is another method of synthesis. It uses both activated and deactivated aromatic dihalides for the synthesis of poly(arylene ether)s. This reaction can be performed at a low temperature [78].

1.7 Sulfonated poly(arylene ether sulfone)s

Sulfonated poly(arylene ether sulfone) copolymers can be synthesized by two methods –

i) synthesis of a non-sulfonated polymer followed by post-sulfonation, and ii) direct polymerization of pre-sulfonated monomers. In the second method, the degree of sulfonation is controlled by changing the concentration of the sulfonated co-monomer [79–81]. However, one disadvantage of this process is the need to synthesize the sulfonated monomer.

1.7.1 Post sulfonation of poly(arylene ether sulfone)s

In 1976, Quentin and co-workers at Rhone-Poulenc Industries developed ion exchange membranes for desalination using the commercial polysulfone precursor polymer, Udel™ using the post-polymerization sulfonation reaction as shown in Figure 1.15 [82,83]. These were a potential alternative to cellulose acetate membranes in terms of biological and chemical inertness.

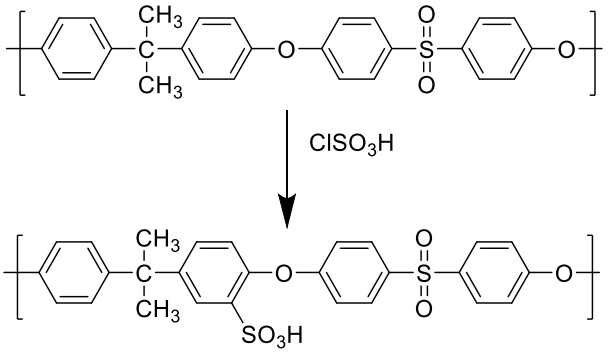

Figure 1.15: Post-sulfontion of Udel™

The reaction involved sulfonation of an aromatic polysulfone, Udel™ in an organic medium with chlorosulfonic acid. The monosulfonated derivative was produced in low yields. These membranes were reported to be equal or superior to the cellulose membranes in some ways. The highest % rejection obtained was 97.5% using a 35000 ppm brine solution at 100 bar [83]. This work did not report the molecular weights or the kinetics of the reaction and focused on polymers with a moderate degree of sulfonaton and low molecular weight (a restriction imposed by the technique of post-sulfonation which may cause chain degradation) [84]. There was a possibility of the chlorosulfonic acid treatment being capable of cleaving the bisphenol-A

polysulfone at the isopropylidene linkage with the risk of branching and crosslinking of the intermediate sulfonic acid group. A partially branched or crosslinked sulfone unit was later reported by McGrath et al. [85] as shown in Figures 1.16 and 1.17.

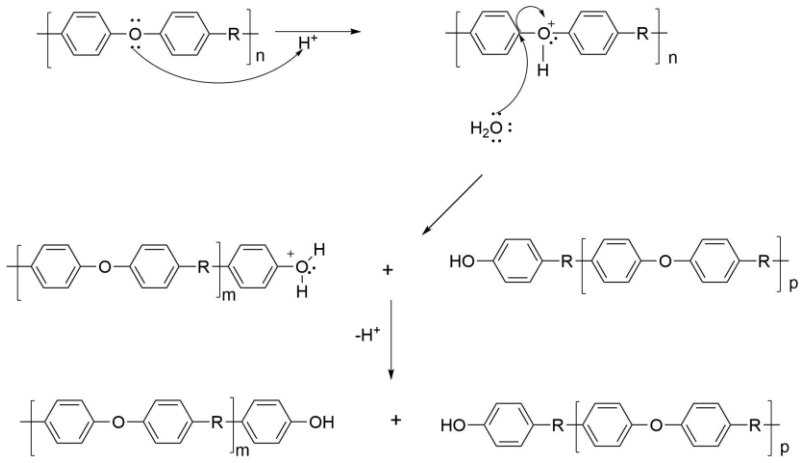

Figure 1.16: Mechanism of chain cleavage of sulfonated poly(arylene ether sulfone) by acid hydrolysis [88]

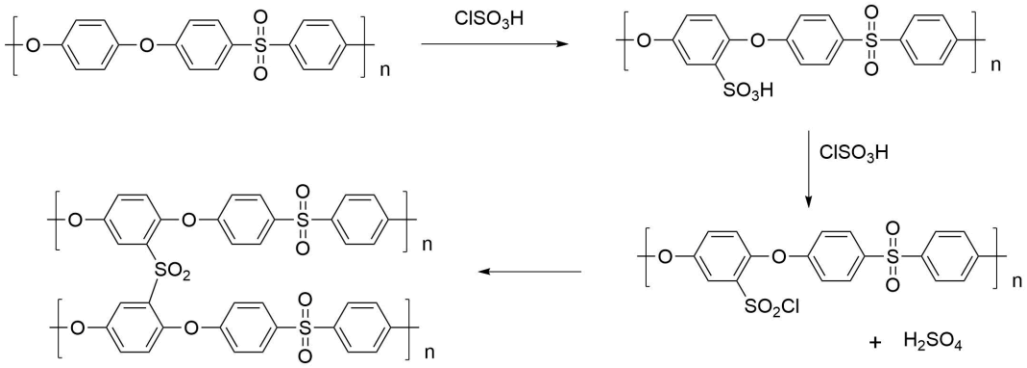

Figure 1.17: Possible interchain crosslinking during post-sulfonation [86]

Noshay and Robeson, in 1976, introduced a mild sulfonation procedure using a complex of SO_3 and triethyl phosphate (SO_3/TEP) at RT. The high reactivity of the SO_3 was controlled by varying the SO_3/TEP ratio. Also, this complex minimized crosslinking due to sulfone-forming side reactions. Johnson et al. used this route to prepare materials intended for applications as desalination membranes [85]. At 50% degrees of sulfonation, these membranes from bisphenol

A polysulfone showed a highest salt rejection of 95% with a good permeate flux when tested with 0.1M NaCl at a pressure of 1500 psi. It was suggested that the mild reaction conditions minimized side reactions [85]. Their results indicated that the degree of sulfonation must be optimized at some moderate value to optimize the strength/stability and flux/separation. The process was cumbersome due to the reactivity and toxicity of SO_3 and the exothermic reaction of SO_3 with TEP. Alternatively, substitution of polysulfones by metalation was also studied [87]. Kerres and coworkers demonstrated sulfonation of arylene polymers by lithiating Udel™ with n-butyllithium at low temperatures, followed by sulfonating the metallated aromatic ring with sulfur dioxide, and oxidizing it to synthesize the modified sulfonated poly(arylene ether sulfone) [88,89].

Allegreza and co-workers found that the sulfonated poly(arylene ether sulfone) membranes were resistant to chlorine (100 ppm free chlorine) and exhibited >95% salt rejection at 400 psi pressure [90]. The pH operation range was 4-11. However, these membranes showed a decreased NaCl rejection with an increase in the Ca^{2+} concentration in mixed feeds.

Alternatively, Rose and coworkers reported controlled post-sulfonation of poly(arylene ether sulfone)s that contained hydroquinone units [91]. The sulfonation reaction proceeded only at the hydroquinone because all of the other rings were deactivated toward electrophilic aromatic sulfonation by the electron withdrawing sulfone groups. A number of investigations on this class of materials have been published [91–95]. The advantage of this method was that the degree of sulfonation could be controlled without the need to synthesize a pre-sulfonated monomer. This modification may provide a novel alternative material for reverse osmosis applications.

Post-sulfonation as an approach for sulfonating poly(arylene ether sulfone)s was abandoned due to poor control over the extent of sulfonation, inability to control the microstructure of the sulfonated units, and decrease in molecular weight due to chain scission

during sulfonation [70]. Moreover, post sulfonated polysulfone membranes were found to be resistant to chlorine but showed a compromised rejection of monovalent cations (Na^+) in the presence of divalent cations (Ca^{2+}) [90]. In the 1980s, these synthetic challenges prevented the preparation of sulfonated polysulfone membranes with flux/rejection capabilities equivalent to those of polyamide membranes. Therefore, sulfonated polysulfones were not used extensively for water desalination despite having promising desalination properties and excellent chlorine resistance.

1.7.2 Directly polymerized sulfonated poly(arylene ether sulfone) membranes

Several researchers explored monomer sulfonations and subsequently controlled the polymerization reactions to form poly(arylene ethers) for applications in proton exchange membranes and fuel cells [96–99]. In the early 2000s McGrath et al. developed a sulfonated monomer [100,101] by disulfonation of the commercially available activated aromatic dihalide monomer, 4,4'-dichlorodiphenyl sulfone (DCDPS) as shown in Figure 1.18.

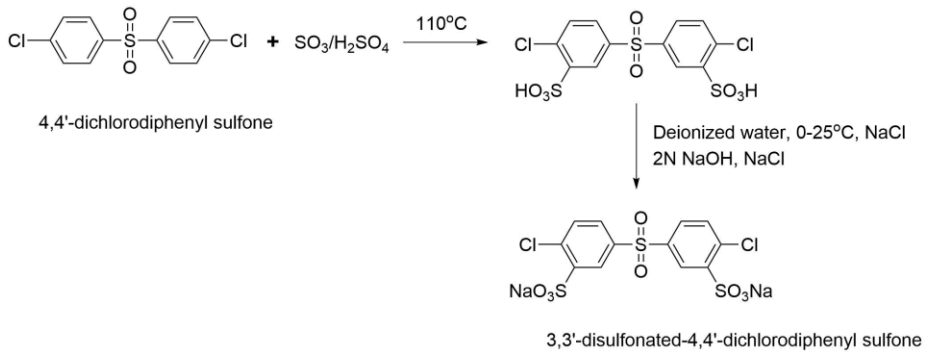

Figure 1.18*:* Synthesis of the disulfonated monomer- 3,3'-disulfonated-4,4'-dichlorodiphenyl sulfone

Random copolymers were synthesized from the direct aromatic nucleophilic substitution step polymerization of the sulfonated monomer, 3,3'-disulfonated,4,4'dichlorodiphenyl sulfone (SDCDPS), 4,4'dichlorodiphenyl sulfone (DCDPS), and biphenol. This route of synthesis of

sulfonated polysulfones avoided the disadvantages traditionally associated with the post sulfonation reaction. There was reproducibility and control over the degree of sulfonation, control of the molecular weight and the polymers had a well-defined morphology, all of which are important for desalination [102].

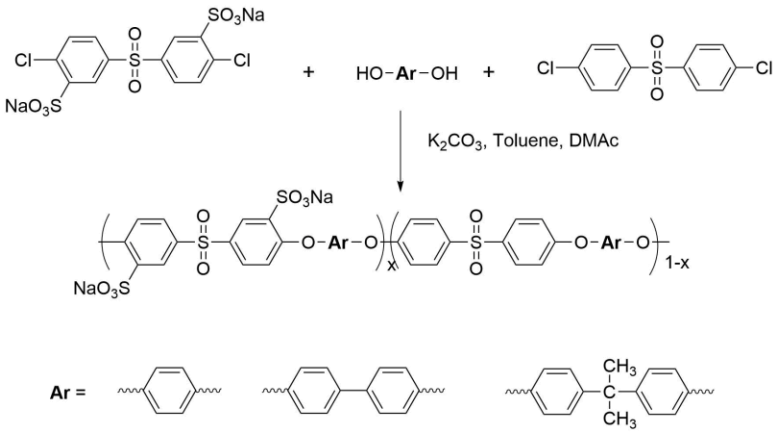

Figure 1.19: Synthesis of sulfonated poly(arylene ether sulfone)s using pre-sulfonated monomer by nucleophilic aromatic substitution reaction

SDCDPS has sulfonate groups on the deactivated phenyl rings ortho to the chlorine atoms and meta to the electron withdrawing sulfone group. Thus, the polymers prepared by this route were more chemically stable than the previous post-polymerization sulfonated polysulfones. This was important for use in proton exchange membranes. However, studies on water uptakes and transport properties were encouraging enough to reopen studies on its applications in reverse osmosis membranes.

McGrath et al. and Freeman et al. studied the transport characteristics of these polymers and synthesized several novel structures with systematically varying levels of sulfonation. The hydrophilicity of the membranes could be tailored by changing the concentration of the sulfonated comonomer. It was found that altering the hydrophilicity of these materials had a pronounced effect on the transport properties [102,103]

It was already established by Allegreza et al., that post-sulfonated polysulfone membranes [90] were highly chlorine resistant. The sulfonated polysulfone membranes synthesized from pre-sulfonated monomers also exhibited good chlorine tolerance at both low and high pH [34,53,104] due to the absence of amide linkages, and water permeability and salt rejection remained unaffected even after continuous exposure to highly chlorinated water over a wide pH range (4-10) (Figure 1.20). Thus, these chlorine resistant membranes could potentially remove the additional steps of de-chlorination and re-chlorination of feed water (as required by the current state of the art polyamide TFC membranes) and decrease the operational costs [53].

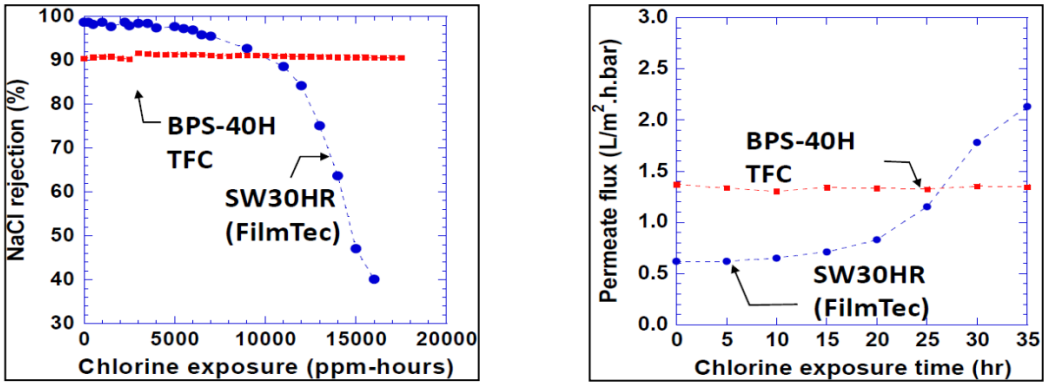

Figure 1.20: Degradation of commercial polyamide thin film composite membrane (SW30HR) compared to sulfonated polysulfone membrane (BPS-40H) From Park, H. B.; Freeman, B. D.; Zhang, Z.-B.; Sankir, M.; McGrath, J. E. Highly Chlorine-Tolerant Polymers for Desalination. Angew. Chemie Int. Ed [104]:

AFM studies showed that the polyamide TFCs have an extraordinarily rough surface which can be susceptible to fouling as a result of bacterial and organic entrapment. On the contrary, the sulfonated polysulfone membranes had smooth surfaces regardless of their degree of sulfonation (Figure 1.21). The smooth sulfonated polysulfone membrane surface morphology could be expected to improve fouling resistance [53].

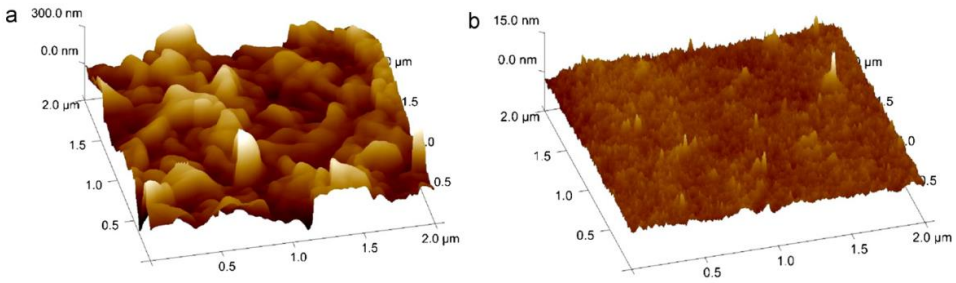

Figure 1.21: AFM image (a) rough surface of polyamide thin film composite (b) smooth surface of the sulfonated polysulfone membranes [53]

Morphological studies by AFM on the sulfonated polysulfones for polyelectrolyte membranes revealed that the polymers have two distinct phase separated nanoscale morphologies [105]. The ionic regions in the membranes aggregate to form hydrophilic domains against a matrix of hydrophobic domains. Water contained in the hydrophilic domains bound to the sulfonic acid groups is critical for the transport of water and ions through the membranes. As the degree of sulfonation is increased, the hydrophilic regions expand. Above a critical value of ion exchange capacity, the hydrophilic regions form a continuous channel through the membrane due to formation of free water. This phenomenon leads to a faster increase in absorption of water with increases in the degree of sulfonation above that critical point [106].

Sulfonate groups on the polymer backbone repels co-ions/salt by Donnan exclusion. However, increasing the sulfonate ions on the backbone also increases the polarity of the membranes leading to higher water uptakes [107,108], causing the membrane to swell and lowering the mechanical strength. The transport properties of the membranes strongly depend on the free volume cavity size. Samples with larger free volume elements have higher water and salt solubility, diffusivity and permeability, and lower water/salt permeability selectivity. Water molecules occupy the free volume in the initially dry polymer. As the water swells the polymer matrix the mean free volume size increases and leads to plasticization of the polymer chain [109].

Paul et al. concluded that the ratio of free water to bound water can be decreased in polyelectrolyte membranes by crosslinking the polymer chain. The crosslinking reaction altered the transport properties without changing the ionic content of the polymer. Crosslinking decreased the ratio of free water to bound water and increased the self-diffusion coefficient of water to improve the transport properties of the membranes [34]. A significant reduction in swelling was also observed for crosslinked membranes. However, crosslinking the polymers did not have a pronounced effect at low ion exchange capacities because the copolymers do not have free water [78]. Sundell et al. [110] and Daryaei et al. [31] found significant reductions in water uptake after crosslinking especially with materials with high ion exchange capacities for reverse osmosis applications [31,33]. Thus, it has been established that crosslinking increases salt rejection and improves transport properties.

1.8 Crosslinking of Poly(arylene ether)s

Crosslinking reactions are important to improve transport properties at high ion exchange capacities without compromising water flux and permeability in membranes. As discussed in the previous section, crosslinks can increase salt rejection by decreasing membrane swelling and reducing the ratio of free to bound water, thereby reducing water uptake. Improved transport properties can be achieved in membranes without increasing the membrane polarity, thereby maintaining an optimum water flux and permeability. Moreover, the excellent transport properties of the polyamide water purification membranes have been attributed to the network structure of these membranes [111].

1.8.1 Covalent

In 1993, Nolte et al. functionalized commercial poly(arylene ether sulfone)s including Udel™ (PSU) and Victrex™ (PES) to reduce swelling in membranes. These were evaluated as solid polymer electrolytes in electrolysers and fuel cells [112]. The polymers were sulfonated and covalently crosslinked in-situ during membrane processing. Some of the pendant sulfonic acid groups of the polymer were reacted with 1,1'-carbonyldiimidazole. The activated groups, *N*-sulfonylimidazoles were reacted with 4,4'-diaminodiphenylsulfone forming sulfonamide crosslink bridges as shown in Figure 1.22. The crosslinked membranes showed a remarkable reduction in swelling in water compared to the non-crosslinked counterparts.

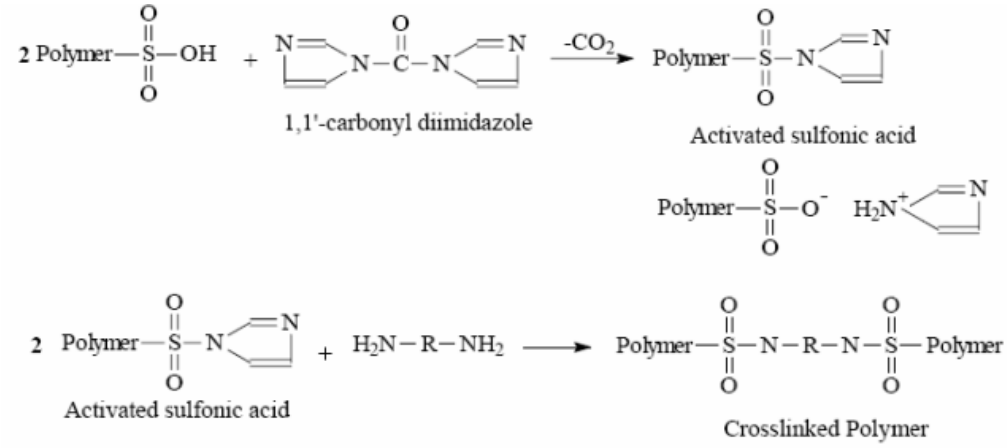

Figure 1.22: Crosslinking of sulfonated poly(arylene ether sulfone) by 1,1'-carbonyldiimidazole [116]

Covalent crosslinking of polysulfones can be achieved by incorporating sulfonate groups into the polymer backbone. The sulfonate groups can undergo crosslinking by disproportionation as shown in Figure 1.23. Kerres et al. demonstrated inter- and intra-molecular crosslinking of sulfinate functional groups by disproportionation [113]. The crosslinking was conducted in a series of steps. The polysulfone sulfinate and polysulfone sulfonate chains were mixed with each other in their salt forms in *N*-methylpyrrolidone to form a homogeneous blend. The strongly acidic cation exchange resin was added in excess to convert the sulfinate and the sulfonate groups

into their acidic form. As the solvent was evaporated the crosslinking took place through disproportionation of the sulfinic acid groups forming a $S(O)_2$-S-crosslinking bridge. Crosslinking through disproportionation occurs when one sulfinate group acts as the nucleophile and another sulfonate group acts as an electrophile. The sulfonate groups do not take part in the crosslinking reaction and become entangled in the crosslinked sulfinate network. These membranes had good thermal stability and were suitable for electrodialysis.

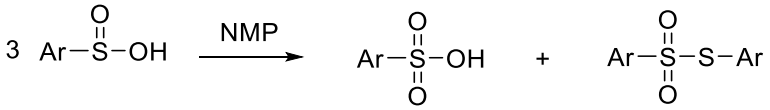

Figure 1.23: Crosslinking by disproportionation of sulfinic acid groups

Kerres et al. also demonstrated a second method of crosslinking the polysulfones [87] as shown in Figure 1.24. The sulfinate groups could be crosslinked by S-alkylation with halogenalkanes. The S-alkylation route required lithiation of the sulfinated group before crosslinking can occur. In this route the lithiated sulfinate groups can attack the α,ω-dihalogen alkane by nucleophilic substitution reaction resulting in a crosslinked network. The sulfinate group is an ambient nucleophile- the sulfinate can be alkylated at the oxygen or the sulfur atom. The sulfur atom is the preferred nucleophile because as per hard-soft/acid-base theory sulfur atom is a softer nucleophile than the oxygen atom, and thus its electron shell is more easily perturbed. One of the key steps in this process is the choice of counterion of the sulfinate group and the crosslinking halogen alkane component. For a successful alkylation at the soft nucleophile center, sulfur, the counterion should be a "hard" cation such as Na^+, Li^+ and the halogen alkane should be a "soft" dibromo or diiodoalkane. The "hard" Lewis acid (Na^+, Li^+) has a weaker interaction with the "soft" S and a stronger interaction with "hard" O leading to S-alkylation. The crosslinked membranes generated in this way showed good thermal properties and low degrees of swelling, thus were promising candidates for fuel cell membranes.

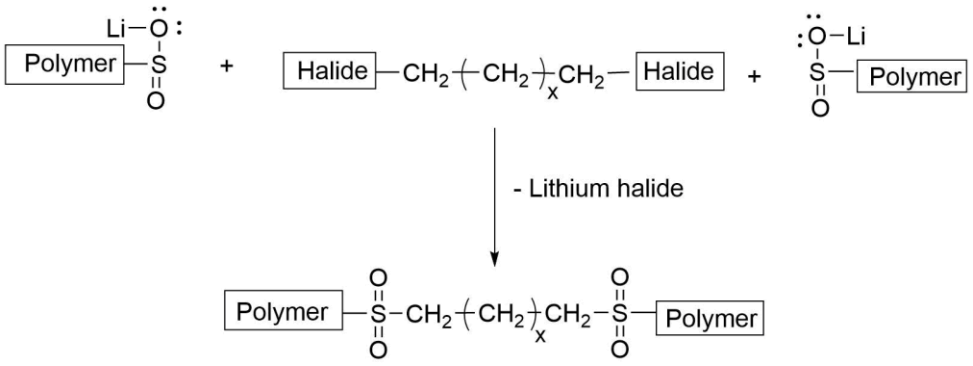

Figure 1.24: Crosslinking by S-alkylation

Delfort et al. synthesized controlled molecular weight oligomers of ethynyl terminated controlled molecular weight oligomers of polyethers with acetylene end groups [87]. The acetylene groups of the oligomers were thermally cured and the resulting networks had a high T_g, improved solvent resistance, good thermostability and good fracture toughness increasing with the oligomers' precursors molecular weights. More recently, Paul et al. crosslinked highly sulfonated polysulfones which showed potential applications in H_2/O_2 fuel cell membranes

Epoxy curing

Epoxy networks have high tensile strengths and moduli, excellent chemical and corrosion resistance and good dimensional stability. Consequently, these materials are widely used for many important applications such as coatings, structural adhesives, reinforced plastics and matrix resins for advanced composite materials. McGrath et al. [114] studied crosslinking of polysulfones with epoxy resins wherein functional polysulfone oligomers acted as modifiers to improve the mechanical toughness of epoxy networks. Polysulfone oligomers were functionalized with either phenolic hydroxyl groups or aromatic amine groups [65,114]. The end terminated polysulfone oligomer and an aromatic diamine were used to thermally cure epoxy resin as shown

in Figure 1.25. The resulting epoxy networks displayed improved fracture toughness that was twice as high as the control epoxy networks.

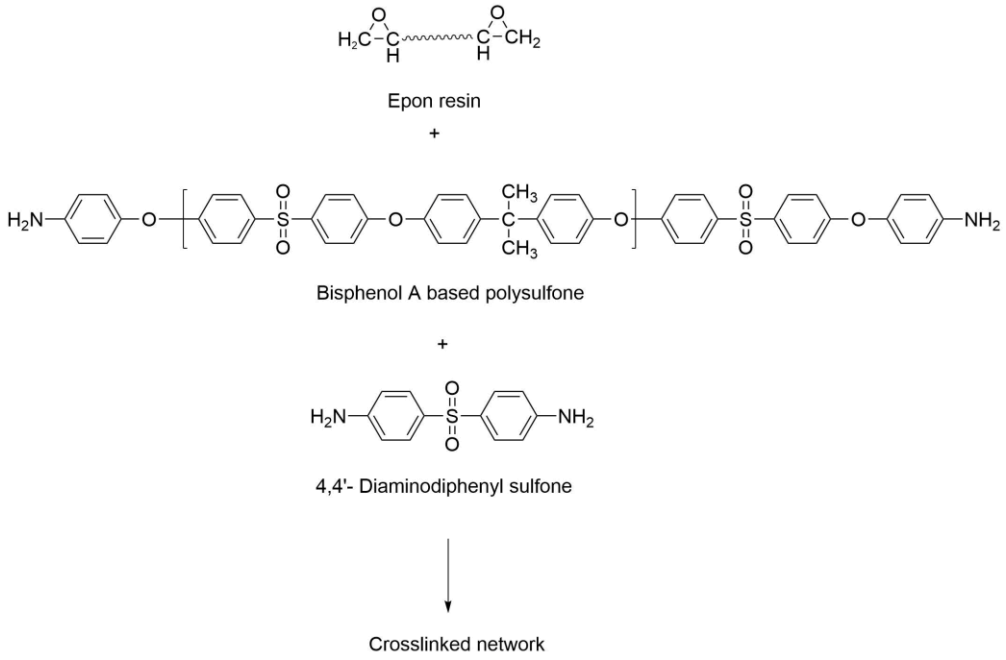

Figure 1.25: Epoxy resin modified with polysulfones to form tough crosslinked networks

Paul et al. produced sulfonated polysulfone oligomers that were phenoxide terminated and crosslinked with a multifunctional epoxide at elevated temperatures [34]. High gel fractions were obtained and the crosslinks produced films with less swelling with improved transport properties of the desalination membranes. Sundell et al. and Daryaei et al. crosslinked amine terminated polysulfone oligomers containing a pre-disulfonated monomer with a tetra-epoxide to obtain membranes with high gel fractions [31,33,110]. These crosslinked membranes had higher levels of salt rejection, with enhanced water permeability, compared to linear disulfonated membranes at a fixed anionic group concentration in the backbone.

1.8.2 Ionic crosslinking

Ionomers such as sulfonated polysulfones can be physically crosslinked via ionic interactions of polymeric bases and polymeric sulfonic acids [115–117]. For example, the acidic polymers like sulfonated polymers could be crosslinked with basic polymers that contained nitrogen bases (Figure 1.26). The sulfonic acid groups interacted with the bases by forming hydrogen bridges and protonation of the basic nitrogen. It was reported that the thermal decomposition temperature of the blends was above 300 ºC. Physical crosslinking limited the water uptake and swelling similar to the materials with covalent crosslinking. However, the physical crosslinking was temperature dependent as the ionic crosslinks and the hydrogen bonds began to break up at high temperatures.

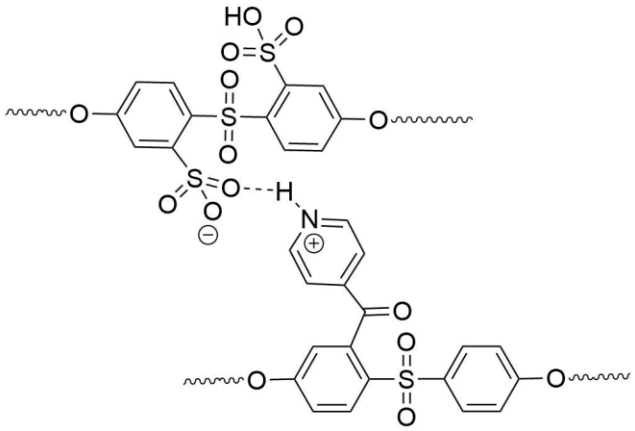

Figure 1.26: Physically crosslinked poly(arylene ether sulfone)s by the formation of acid-base complex [75]

Summary

Water desalination is important to combat global water crisis. Sulfonated polysulfone membranes are a potential alternative to the state-of-the-art polyamide reverse osmosis membranes because they are resistant to chlorinated species and not prone to fouling. Sulfonated poly(arylene ether sulfone)s are most commonly synthesized by nucleophilic aromatic substitution reaction using

disulfonated monomer. Selective post polymerization sulfonation in mild reaction condition has also proved to be an efficient route for synthesis but application of such membranes in reverse osmosis is yet to be studied. Crosslinking the membranes is an efficient way to improve transport properties and various crosslinking reactions have been studied with sulfonated polysulfones. In this dissertation selective post polymerization sulfonation reaction is used to synthesize the sulfonated polysulfone membranes and crosslinking of such membranes have been studied.

References

[1] World Economic Forum, The Global Risks Report 2018- 13th Edition, 2018.

[2] H.K. Lonsdale, H. Podall, Reverse Osmosis Membrane Research, Plenum press, New York, 1972.

[3] R.F. Service, Desalination freshens up., Science. 313 (2006) 1088–90.

[4] K.T. Sanders, M.E. Webber, Evaluating the energy consumed for water use in the United States, Environ. Res. Lett. 7 (2012) 034034.

[5] N.R. Armstrong, R.C. Shallcross, K. Ogden, S. Snyder, A. Achilli, E.L. Armstrong, Challenges and opportunities at the nexus of energy, water, and food: A perspective from the southwest United States, MRS Energy Sustain. 5 (2018) 1–18.

[6] Healy RW, Alley WM, Engle MA, McMahon PB, Bales JD, The Water-Energy Nexus: An Earth Science Perspective, U.S. Geological Survey Circular 1407 (2015) 107.

[7] M.E. Webber, Catch-22: Water vs. Energy, Sci. Am. 18 (2008) 34–41.

[8] USGS-Water School Science, Freshwater - The Water Cycle, (2017). https://water.usgs.gov/edu/watercyclefreshstorage.html.

[9] L.F. Greenlee, D.F. Lawler, B.D. Freeman, B. Marrot, P. Moulin, Reverse osmosis desalination: Water sources, technology, and today's challenges, Water Res. 43 (2009) 2317–2348.

[10] California Office of Administrative Law, Titles 17 and 22 California code of Regulations related to Drinking Water, 2016.

[11] Utah Office of Administrative Rules, R309-200. Monitoring and water quality: Drinking water standards, Utah Administrative Code, 2018.

[12] World Health Organization, European Standards for Drinking Water, 1970.

[13] I.C. Watson, O.J. Morin, L. Henthorne, Desalting Handbook for Planners, 2003.

[14] H.J. Krishna, Introduction to Desalination Technologies, 2004.

[15] B. Van der Bruggen, C. Vandecasteele, Distillation vs. membrane filtration: overview of process evolutions in seawater desalination, Desalination. 143 (2002) 207–218.

[16] P.H. Gleick, H. Cooley, The world's water, 2006-2007 : the biennial report on freshwater resources, Island Press, 2006.

[17] S. Sethi, G. Wetterau, Seawater Desalination Overview, in: Desalin. Seawater - Man. Water Supply Pract. M61, (2011) 1–13.

[18] H. Strathmann, L. Giorno, E. Drioli, Principles of Membrane Separation Processes, in: An Introd. to Membr. Sci. Technol. (Wiley, Weinheim, Germany, 2006) 64–66.

[19] T.A.S. on P.P. of the M.P. Committee, Microfiltration and ultrafiltration membranes for drinking water, J. Am. Water Work. Assoc. 100 (2008) 84–97.

[20] M. Paul, S.D. Jons, Chemistry and fabrication of polymeric nanofiltration membranes: A review, Polymer. 103 (2016) 417–456.

[21] C. Alì Egre, P. Moulin, M. Maisseu, F. Charbit, Treatment and reuse of reactive dyeing effluents, J. Memb. Sci. 269 (2006) 15–34.

[22] J.A. Nollet, Lessons in Experimental Physics, 1743.

[23] M. Elimelech, W.A. Phillip, The future of seawater desalination: energy, technology, and the environment., Science. 333 (2011) 712–7.

[24] H. Strathmann, Electrodialysis, a mature technology with a multitude of new applications, Desalination. 264 (2010) 268–288.

[25] A.H. Galama, M. Saakes, H. Bruning, H.H.M. Rijnaarts, J.W. Post, Seawater predesalination with electrodialysis, Desalination. 342 (2014) 61–69.

[26] J. Kamcev, B.D. Freeman, Charged Polymer Membranes for Environmental/Energy Applications, Annu. Rev. Chem. Biomol. Eng. 7 (2016) 111–133.

[27] R.W. Baker, Membrane Transport Theory, in: Membr. Technol. Appl., Second, John Wiley & Sons, Ltd, Chichester, UK, 2004: pp. 15–84.

[28] J.G. Wijmans, R.W. Baker, The solution-diffusion model: a review, J. Memb. Sci. 107 (1995) 1–21.

[29] A.C. Sagle, H. Ju, B.D. Freeman, M.M. Sharma, PEG-based hydrogel membrane coatings, Polymer. 50 (2009) 756–766.

[30] H. Ju, B.D. McCloskey, A.C. Sagle, Y.-H. Wu, V.A. Kusuma, B.D. Freeman, Crosslinked poly(ethylene oxide) fouling resistant coating materials for oil/water separation, J. Memb. Sci. 307 (2008) 260–267.

[31] A. Daryaei, E.S. Jang, S. Roy Choudhury, D. Kazerooni, J.J. Lesko, B.D. Freeman, J.S.

Riffle, J.E. McGrath, Structure-property relationships of crosslinked disulfonated poly(arylene ether sulfone) membranes for desalination of water, Polymer (Guildf). 132 (2017) 286–293.

[32] A. Nebipasagil, B.J. Sundell, O.R. Lane, S.J. Mecham, J.S. Riffle, J.E. McGrath, Synthesis and photocrosslinking of disulfonated poly(arylene ether sulfone) copolymers for potential reverse osmosis membrane materials, Polymer. 93 (2016) 14–22.

[33] B.J. Sundell, K.-S. Lee, A. Nebipasagil, A. Shaver, J.RCook, E.-S. Jang, B.D. Freeman, J.E. McGrath, Cross-linking disulfonated poly(arylene ether sulfone) telechelic oligomers. 1. Synthesis, characterization, and membrane preparation, Ind. Eng. Chem. Res. 53 (2014) 2583–2593.

[34] M. Paul, H.B. Park, B.D. Freeman, A. Roy, J.E. McGrath, J.S. Riffle, Synthesis and crosslinking of partially disulfonated poly(arylene ether sulfone) random copolymers as candidates for chlorine resistant reverse osmosis membranes, Polymer. 49 (2008) 2243–2252.

[35] W. Xie, H. Ju, G.M. Geise, B.D. Freeman, J.I. Mardel, A.J. Hill, J.E. McGrath, Effect of Free Volume on Water and Salt Transport Properties in Directly Copolymerized Disulfonated Poly(arylene ether sulfone) Random Copolymers, Macromolecules. 44 (2011) 4428–4438.

[36] H.B. Park, J. Kamcev, L.M. Robeson, M. Elimelech, B.D. Freeman, Maximizing the right stuff: The trade-off between membrane permeability and selectivity, Science. 356 (2017) 1137.

[37] G.M. Geise, C.L. Willis, C.M. Doherty, A.J. Hill, T.J. Bastow, J. Ford, K.I. Winey, B.D. Freeman, D.R. Paul, Characterization of aluminum-neutralized sulfonated styrenic pentablock copolymer films, Ind. Eng. Chem. Res. 52 (2013) 1056–1068.

[38] R.M. Hodge, T.J. Bastow, G.H. Edward, G.P. Simon, A.J. Hill, Free volume and the mechanism of plasticization in water-swollen poly(vinyl alcohol), Macromolecules. 29 (1996) 8137–8143.

[39] R.M. Hodge, G.H. Edward, G.P. Simon, Water absorption and states of water in semicrystalline poly(vinyl alcohol) films, Polymer (Guildf). 37 (1996) 1371–1376.

[40] G.M. Geise, D.R. Paul, B.D. Freeman, Fundamental water and salt transport properties of polymeric materials, Prog. Polym. Sci. 39 (2014) 1–24.

[41] G.M. Geise, H.B. Park, A.C. Sagle, B.D. Freeman, J.E. Mcgrath, Water permeability and water/salt selectivity tradeoff in polymers for desalination, J. Memb. Sci. 369 (2010) 130–138.

[42] G.M. Geise, H.-S. Lee, D.J. Miller, B.D. Freeman, J.E. McGrath, D.R. Paul, Water

purification by membranes: The role of polymer science, J. Polym. Sci. Part B Polym. Phys. 48 (2010) 1685–1718.

[43] R. Riley, J.O. Gardner, U. Merten, Cellulose Acetate Membranes: Electron Microscopy of Structure., Science. 143 (1964) 801–3.

[44] H.K. Lonsdale, U. Merten, R.L. Riley, Transport properties of cellulose acetate osmotic membranes, J. Appl. Polym. Sci. 9 (1965) 1341–1362.

[45] H.K. Lonsdale, U. Merten, M. Tagami, Phenol transport in cellulose acetate membranes, J. Appl. Polym. Sci. 11 (1967) 1807–1820. doi:10.1002/app.1967.070110917.

[46] U. Merten, Flow Relationships in Reverse Osmosis, Ind. Eng. Chem. Fundam. 2 (1963)

[47] W.M. King, P.A. Cantor, L.W. Schoellenbach, C.R. Cannon, High-retention, reverse-osmosis desalination membranes from cellulose acetate, J. Appl. Polym. Sci. (1970) 17-19.

[48] K.P. Lee, T.C. Arnot, D. Mattia, A review of reverse osmosis membrane materials for desalination—Development to date and future potential, J. Memb. Sci. 370 (2011) 1–22.

[49] J.E. Cadotte, R.J. Petersen, R.E. Larson, E.E. Erickson, A new thin-film composite seawater reverse osmosis membrane, Desalination. 32 (1980) 25–31.

[50] Y. Song, P. Sun, L.L. Henry, B. Sun, Mechanisms of structure and performance controlled thin film composite membrane formation via interfacial polymerization process, J. Memb. Sci. 251 (2005) 67–79.

[51] G.-Y.Y. Chai, W.B. Krantz, Formation and characterization of polyamide membranes via interfacial polymerization, J. Memb. Sci. 93 (1994) 175–192.

[52] M. Elimelech, Xiaohua Zhu, A.E. Childress, Seungkwan Hong, Role of membrane surface morphology in colloidal fouling of cellulose acetate and composite aromatic polyamide reverse osmosis membranes, J. Memb. Sci. 127 (1997) 101–109.

[53] C.H. Lee, B.D. McCloskey, J. Cook, O. Lane, W. Xie, B.D. Freeman, Y.M. Lee, J.E. McGrath, Disulfonated poly(arylene ether sulfone) random copolymer thin film composite membrane fabricated using a benign solvent for reverse osmosis applications, J. Memb. Sci. 389 (2012) 363–371.

[54] C.Y. Tang, Y.-N. Kwon, J.O. Leckie, Probing the nano- and micro-scales of reverse osmosis membranes—A comprehensive characterization of physiochemical properties of uncoated and coated membranes by XPS, TEM, ATR-FTIR, and streaming potential measurements, J. Memb. Sci. 287 (2007) 146–156.

[55] E.M. Vrijenhoek, S. Hong, M. Elimelech, Influence of membrane surface properties on

initial rate of colloidal fouling of reverse osmosis and nanofiltration membranes, J. Memb. Sci. 188 (2001) 115–128. doi:10.1016/S0376-7388(01)00376-3.

[56] M. Hirose, H. Ito, Y. Kamiyama, Effect of skin layer surface structures on the flux behaviour of RO membranes, J. Memb. Sci. 121 (1996) 209–215.

[57] A.C. Sagle, E.M. Van Wagner, H. Ju, B.D. McCloskey, B.D. Freeman, M.M. Sharma, PEG-coated reverse osmosis membranes: Desalination properties and fouling resistance, J. Memb. Sci. 340 (2009) 92–108.

[58] I.-C. Kim, K.-H. Lee, Dyeing process wastewater treatment using fouling resistant nanofiltration and reverse osmosis membranes, Desalination. 192 (2006) 246–251.

[59] D. Rana, T. Matsuura, Surface Modifications for Antifouling Membranes, Chem. Rev. 110 2448–2471.

[60] G. Kang, Y. Cao, Development of antifouling reverse osmosis membranes for water treatment: A review, Water Res. 46 (2012) 584–600.

[61] S. Konagaya, O. Watanabe, Influence of chemical structure of isophthaloyl dichloride and aliphatic, cycloaliphatic, and aromatic diamine compound polyamides on their chlorine resistance, J. Appl. Polym. Sci. 76 (2000) 201–207.

[62] T. Kawaguchi, H. Tamura, Chlorine-resistant membrane for reverse osmosis. I. Correlation between chemical structures and chlorine resistance of polyamides, J. Appl. Polym. Sci. 29 (1984) 3359–3367.

[63] J. Glater, S. Hong, M. Elimelech, The search for a chlorine-resistant reverse osmosis membrane, Desalination. 95 (1994) 325–345.

[64] N.P. Soice, A.C. Maladono, D.Y. Takigawa, A.D. Norman, W.B. Krantz, A.R. Greenberg, Oxidative degradation of polyamide reverse osmosis membranes: Studies of molecular model compounds and selected membranes, J. Appl. Polym. Sci. 90 (2003) 1173–1184.

[65] T.H. Yoon, D.B. Priddy, G.D. Lyle, J.E. McGrath, Mechanical and morphological investigations of reactive polysulfone toughened epoxy networks, Macromol. Symp. 98 (1995) 673–686.

[66] G.G. Messmer, G.J. Palenik, The crystal structure of a Meisenheimer complex: the potassium methoxide adduct of 4-methoxy-5,7-dinitrobenzofurazan, J. Chem. Soc. D Chem. Commun. 0 (1969) 470.

[67] C.A. Fyfe, A. Koll, S.W.H. Damji, C.D. Malkiewich, P.A. Forte, Low temperature flow nuclear magnetic resonance detection of transient intermediates on the actual reaction pathway in nucleophilic aromatic substitution, J. Chem. Soc. Chem. Commun. 10 (1977) 335.

[68] M. Smith, J. March, J. March, March's advanced organic chemistry : reactions, mechanisms, and structure., Wiley, 2001.

[69] E. Berliner, L.C. Monack, Nucleophilic Displacement in the Benzene Series, J. Am. Chem. Soc. 74 (1952) 1574–1579.

[70] W.L. Harrison, Synthesis and Characterization of Sulfonated Poly(arylene ether sulfone) copolymers via direct copolymerization: Candidates for Proton Exchange Membrane Fuel Cells., Virginia Polytechnic and State University, 2002.

[71] S. Wang, Q. Ji, C.N. Tchatchoua, A.R. Shultz, J.E. Mcgrath, Phosphonyl/hydroxyl hydrogen bonding-induced miscibility of poly(arylene ether phosphine oxide/sulfone) statistical copolymers with poly(hydroxy ether) (phenoxy resin): Synthesis and characterization, J. Polym. Sci. Part B Polym. Phys. 37 (1999) 1849–1862.

[72] R.A. Clendinning, A.G. Farnham, R.N. Johnson, The Development of Polysulfone and Other Polyarylethers, in: High Perform. Polym. Their Orig. Dev., Springer Netherlands, Dordrecht, 1986: pp. 149–158.

[73] J.L. Hedrick, J.J. Dumais, L.W. Jelinski, R.A. Patsiga, J.E. McGrath, Synthesis and characterization of deuterated poly(arylene ether sulfones), J. Polym. Sci. Part A Polym. Chem. 25 (1987) 2289–2300.

[74] J.L. Hedrick, D.K. Mohanty, B.C. Johnson, R. Viswanathan, J.A. Hinkley, J.E. McGrath, Radiation resistant amorphous–all aromatic polyarylene ether sulfones: Synthesis, characterization, and mechanical properties, J. Polym. Sci. Part A Polym. Chem. 24 (1986) 287–300.

[75] R. Guo, J.E. McGrath, Aromatic Polyethers, Polyetherketones, Polysulfides, and Polysulfones, Polym. Sci. A Compr. Ref. (2012) 377–430.

[76] Olah George, Reddy Prakash, Prakash Surya, Friedel Crafts Reactions, in: Kirk-Othmer Encycl. Chem. Technol., John Wiley and Sons. pp. 1–49.

[77] A. Farnham, R. Johnson, Polyarylene polyethers, US3332909A, 1965.

[78] M. Paul, Synthesis, crosslinking and characterization of disulfonated poly(arylene ether sulfone)s for application in reverse osmosis and proton exchange membranes, Ph.D. Dissertation, Virginia Polytechnic and State University, 2008.

[79] F. Wang, M. Hickner, Y.S. Kim, T.A. Zawodzinski, J.E. McGrath, J.E. McGrath, Direct polymerization of sulfonated poly(arylene ether sulfone) random (statistical) copolymers: candidates for new proton exchange membranes, J. Memb. Sci. 197 (2002) 231–242.

[80] A. Daryaei, G.C. Miller, J. Willey, S. Roy Choudhury, B. Vondrasek, D. Kazerooni, M.R. Burtner, C. Mittelsteadt, J.J. Lesko, J.S. Riffle, J.E. McGrath, Synthesis and Membrane

Properties of Sulfonated Poly(arylene ether sulfone) Statistical Copolymers for Electrolysis of Water: Influence of Meta- and Para-Substituted Comonomers, ACS Appl. Mater. Interfaces. 9 (2017) 20067–20075.

[81] J.R. Rowlett, V. Lilavivat, A.T. Shaver, Y. Chen, A. Daryaei, H. Xu, C. Mittelsteadt, S. Shimpalee, J.S. Riffle, J.E. McGrath, Multiblock poly(arylene ether nitrile) disulfonated poly(arylene ether sulfone) copolymers for proton exchange membranes: Part 2 electrochemical and H_2/Air fuel cell analysis, Polymer. 122 (2017) 296–302.

[82] C. Brousse, R. Chapurlat, J.P. Quentin, New membranes for reverse osmosis I. Characteristics of the base polymer: sulphonated polysulphones, Desalination. 18 (1976) 137–153.

[83] J. Quentin, Sulfonated polyarylethersulfones, US3709841A, 1970.

[84] D.R. Lloyd, L.E. Gerlowski, C.D. Sunderland, J.P. Wightman, J.E. Mcgrath, M. Igbal, Y. Kang, Poly(aryl ether) Membranes for Reverse Osmosis Sulfonation of Poly(Aryl Ethers), Synth. Membr. ACS Symp. Ser. (1981).

[85] B.C. Johnson, İ. Yilgör, C. Tran, M. Iqbal, J.P. Wightman, D.R. Lloyd, J.E. McGrath, Synthesis and characterization of sulfonated poly(acrylene ether sulfones), J. Polym. Sci. Polym. Chem. Ed. 22 (1984) 721–737.

[86] R.T.S.M. Lakshmi, J. Meier-Haack, K. Schlenstedt, H. Komber, V. Choudhary, I.K. Varma, Synthesis, characterisation and membrane properties of sulphonated poly(aryl ether sulphone) copolymers, React. Funct. Polym. 66 (2006) 634–644.

[87] J. Kerres, W. Cui, M. Junginger, Development and characterization of crosslinked ionomer membranes based upon sulfinated and sulfonated PSU crosslinked PSU blend membranes by alkylation of sulfinate groups with dihalogenoalkanes, J. Memb. Sci. 139 (1998) 227–241.

[88] J. Kerres, W. Zhang, W. Cui, New sulfonated engineering polymers via the metalation route. II. Sulfinated/sulfonated poly(ether sulfone) PSU Udel and its crosslinking, J. Polym. Sci. Part A Polym. Chem. 36 (1998) 1441–1448.

[89] J. Kerres, W. Cui, S. Reichle, New sulfonated engineering polymers via the metalation route. I. Sulfonated poly(ethersulfone) PSU Udel via metalation-sulfination-oxidation, J. Polym. Sci. Part A Polym. Chem. 34 (1996) 2421–2438.

[90] A.E. Allegrezza, B.S. Parekh, P.L. Parise, E.J. Swiniarski, J.L. White, Chlorine resistant polysulfone reverse osmosis modules, Desalination. 64 (1987) 285–304.

[91] J. Rose, Sulphonated polyaryletherketones and process for the manufacture thereof, EP0008895A1, 1978.

[92] J. Rose, Sulphonated polyaryletherketones, EP0041780A1, 1981.

[93] J.B. Rose, Sulphonated polyarylethersulphone copolymers, US4273903, 1978.

[94] A. Bunn, Rose John B, Sulphonation of poly(phenylene ether sulphone)s containing hydroquinone residues, Polymer. 34 (1993) 1992–1994.

[95] A. Al-Omran, J.B. Rose, Synthesis and sulfonation of poly(phenylene ether ether sulfone)s containing methylated hydroquinone residues, Polymer. 37 (1996) 1735–1743.

[96] F. Wang, Y. Qi, T. Chen, Y. Xing, Y. Lin, J. Xu, Disodium 4,4'-difluoro-3,3'-carbonyldibenzenesulfonate hydrofluoride tetrahydrate, Acta Crystallogr. Sect. C Cryst. Struct. Commun. 55 (1999) 871–873.

[97] F. Wang, T. Chen, J. Xu, Sodium sulfonate-functionalized poly(ether ether ketone)s, Macromol. Chem. Phys. 199 (1998) 1421–1426.

[98] C. Genies, R. Mercier, B. Sillion, N. Cornet, G. Gebel, M. Pineri, Soluble sulfonated naphthalenic polyimides as materials for proton exchange membranes, Polymer. 42 (2001) 359–373.

[99] F. Wang, J. Li, T. Chen, J. Xu, Synthesis of poly(ether ether ketone) with high content of sodium sulfonate groups and its membrane characteristics, Polymer (Guildf). 40 (1999) 795–799.

[100] W.L. Harrison, F. Wang, J.B. Mecham, V.A. Bhanu, M. Hill, Y.S. Kim, J.E. McGrath, Influence of the bisphenol structure on the direct synthesis of sulfonated poly(arylene ether) copolymers. I, J. Polym. Sci. Part A Polym. Chem. 41 (2003) 2264–2276.

[101] M. Sankir, V.A. Bhanu, W.L. Harrison, H. Ghassemi, K.B. Wiles, T.E. Glass, A.E. Brink, M.H. Brink, J.E. McGrath, Synthesis and characterization of 3,3′-disulfonated-4,4′-dichlorodiphenyl sulfone (SDCDPS) monomer for proton exchange membranes (PEM) in fuel cell applications, J. Appl. Polym. Sci. 100 (2006) 4595–4602.

[102] W. Xie, H.-B. Park, J. Cook, C.H. Lee, G. Byun, B.D. Freeman, J.E. McGrath, Advances in membrane materials: desalination membranes based on directly copolymerized disulfonated poly(arylene ether sulfone) random copolymers, Water Sci. Technol. 61 (2010) 619–624.

[103] W. Xie, J. Cook, H.B. Park, B.D. Freeman, C.H. Lee, J.E. McGrath, Fundamental salt and water transport properties in directly copolymerized disulfonated poly(arylene ether sulfone) random copolymers, Polymer. 52 (2011) 2032–2043.

[104] H.B. Park, B.D. Freeman, Z.-B. Zhang, M. Sankir, J.E. McGrath, Highly Chlorine-Tolerant Polymers for Desalination, Angew. Chemie. 120 (2008) 6108–6113.

[105] Yu Seung Kim, Limin Dong, Michael A. Hickner, Thomas E. Glass, A. Vernon Webb, J.E. McGrath*, State of Water in Disulfonated Poly(arylene ether sulfone) Copolymers and a Perfluorosulfonic Acid Copolymer (Nafion) and Its Effect on Physical and Electrochemical Properties, Macromolecules. 36 (2003) 6281–6285.

[106] A. Roy, M.A. Hickner, H.-S. Lee, T. Glass, M. Paul, A. Badami, J.S. Riffle, J.E. McGrath, States of water in proton exchange membranes: Part A - Influence of chemical structure and composition, Polymer. 111 (2017) 297–306.

[107] G.M. Geise, L.P. Falcon, B.D. Freeman, D.R. Paul, Sodium chloride sorption in sulfonated polymers for membrane applications, J. Memb. Sci. (2012) 195–208.

[108] J. Kamcev, M. Galizia, F.M. Benedetti, E.-S. Jang, D.R. Paul, B.D. Freeman, G.S. Manning, Partitioning of mobile ions between ion exchange polymers and aqueous salt solutions: importance of counter-ion condensation, Phyical Chem. Chem. Phys. 18 (2016) 6021–6031.

[109] W. Xie, H. Ju, G.M. Geise, B.D. Freeman, J.I. Mardel, A.J. Hill, J.E. McGrath, Effect of free volume on water and salt transport properties in directly copolymerized disulfonated poly(arylene ether sulfone) random copolymers, Macromolecules. 44 (2011) 4428–4438.

[110] B.J. Sundell, E.-S.S. Jang, J.R. Cook, B.D. Freeman, J.S. Riffle, J.E. McGrath, Cross-Linked Disulfonated Poly(arylene ether sulfone) Telechelic Oligomers. 2. Elevated Transport Performance with Increasing Hydrophilicity, Ind. Eng. Chem. Res. 55 (2016) 1419–1426.

[111] R.J. Petersen, Composite reverse osmosis and nanofiltration membranes, J. Memb. Sci. 83 (1993) 81–150.

[112] R. Nolte, K. Ledjeff, M. Bauer, R. Mülhaupt, Partially sulfonated poly(arylene ether sulfone) - A versatile proton conducting membrane material for modern energy conversion technologies, J. Memb. Sci. 83 (1993) 211–220.

[113] J. Kerres, W. Cui, R. Disson, W. Neubrand, Development and characterization of crosslinked ionomer membranes based upon sulfinated and sulfonated PSU crosslinked PSU blend membranes by disproportionation of sulfinic acid groups, J. Memb. Sci. 139 (1998) 211–225.

[114] J. Hedrick, I. Yilgor, M. Jurek, J.. Hedrick, G.. Wilkes, J. McGrath, Chemical modification of matrix resin networks with engineering thermoplastics: 1. Synthesis, morphology, physical behaviour and toughening mechanisms of poly(arylene ether sulphone) modified epoxy networks, Polymer. 32 (1991) 2020–2032.

[115] W. Zhang, C.-M. Tang, J. Kerres, Development and characterization of sulfonated-unmodiftied and sulfonated-aminated PSU Udel blend membranes, Sep. Purif. Technol. 22–23 (2001) 209–221.

[116] J. Kerres, A. Ullrich, Synthesis of novel engineering polymers containing basic side groups and their application in acid–base polymer blend membranes, Sep. Purif. Technol. 22–23 (2001) 1–15.

[117] J. Kerres, W. Cui, Acid-base polymer blends and their application in membrane processes, US 6,194,474 B1, 2001.

Chapter 2 : Synthesis and characterization of post-sulfonated poly(arylene ether sulfone) membranes for water desalination

Shreya Roy Choudhury, [a] Ozma Lane,[a] Dana Kazerooni,[a,b] Gurtej S. Narang,[a] Benny D. Freeman,[c] John J. Lesko,[b] J. S. Riffle[a*]

[a]Macromolecules Innovation Institute, Virginia Tech, Blacksburg, VA 24061, United States

[b]College of Engineering, Virginia Tech, Blacksburg, VA 24061, United States

[c]Department of Chemical Engineering and the Center for Energy and Environmental Resources, University of Texas at Austin, Austin, TX 78758, United States

(Article in preparation for submission)

Abstract

This study focuses on post-sulfonated polysulfone membranes for potential applications in desalination by reverse osmosis or electrodialysis. A series of controlled molecular weight (5000 and 10,000 g/mole) polysulfones containing hydroquinone and their high molecular weight linear counterparts were synthesized using post-sulfonation of pre-formed polymers under mild conditions. The sulfonic acid groups were substituted on only the hydroquinone units. Amine terminated oligomers were crosslinked with a tetrafunctional epoxy molecule under suitable conditions to form membranes whereas the high molecular weight polymers were cast into linear films by chain entanglements. Fixed charge concentrations of the linear membranes increased from 3.94 to 5.14 meq/mL when the ion exchange capacity was decreased from 1.30 to 0.88 meq/g. The fixed charge concentration of the networks cast from the 5000 g/mol oligomers increased from 4.04 to 6.23 meq/mL with a decrease in the ion exchange capacity from 1.51 to 0.90 meq/g.

2.1 Introduction

Clean water is critical to the safety, security and survivability of mankind. Nearly 41% of the Earth's population lives in water-stressed areas, and the water scarcity will be exacerbated by an increasing population [1–4]. According to the U.S. Geological Survey, ~96.5 % of the Earth's water is located in seas and oceans with the remaining in surface and ground water, mostly frozen in glaciers and ice caps. Thus, ~96% of the total water is saline and only ~0.8% is considered to be accessible fresh water [5]. Thus, saltwater desalination is economically the key to tackle the problem of water scarcity. Thermal desalination methods are not energetically efficient because they rely on an energy-intensive phase change and require a large quantity of fuel to vaporize the water. Membrane based desalination processes have proven to be more economical and energetically efficient than thermal methods, thus playing a key role in the desalination industry [6–8]. This paper reports new membranes that may have potential for desalination by electrodialysis (ED) and reverse osmosis (RO).

ED is applied for demineralization or concentrating salt-containing solutions. In this process, positively charged anion exchange membranes (AEMs) and negatively charged cation exchange membranes (CEMs) are alternately stacked between two electrodes [9–11]. When an electric potential is applied and feed water solution is pumped through the cell, the membranes allow the oppositely charged counterions to pass through but reject similarly charged co-ions. The electrolyte becomes concentrated in alternate compartments, and the other compartments are depleted of ions. ED membranes require high fixed charge concentrations (ion exchange capacity/water uptake) to repel co-ions via Donnan exclusion. However, with an increase in ionic content, there is often an increase in water uptake that is detrimental to the hydrated mechanical

properties of the membranes [12]. Hence, our goal is to develop membranes for ED with high fixed charge concentration and optimum water uptake with primary focus on CEMs in this study.

RO is the most widely utilized membrane technique for commercial desalination [13,14]. RO polymeric membranes are semipermeable and follow the principle of solution diffusion to achieve desalination [15]. Current state-of-the art RO membranes are thin film composites comprised of an interfacially polymerized, crosslinked aromatic polyamide atop a porous polymeric film that provides mechanical support [7,16]. These membranes can provide ~99% salt rejection. The permselective polyamide layer is very thin (~100 nm) to afford high water flux. One of the disadvantages of the polyamide thin film composites is that the process of interfacial polymerization gives rise to a rough surface. This facilitates deposition of salts and other contaminants, leading to scaling and fouling [17–19]. Sulfonated polysulfone membranes are a potential alternative to the polyamide membranes. The polysulfones are polymerized then cast to form membranes with smooth surfaces, and they are also more chemically resistant to disinfectants such as chlorine than the polyamides [20,21].

Sulfonated poly(arylene ether sulfone) copolymers can be synthesized by two methods – i) direct polymerization of pre-sulfonated monomers, and ii) synthesis of a non-sulfonated polymer followed by post-sulfonation. In the first method, the degree of sulfonation is controlled by changing the concentration of the sulfonated comonomer [22–24]. However, one disadvantage of this process is the need to synthesize the sulfonated monomer.

Historically, the second method of employing the post-sulfonation route led to uncontrolled sequences of sulfonic acid groups along the chains unless special compositions were utilized. Most previous work on post-sulfonation of polysulfones utilized rather harsh conditions because the

rings to be sulfonated included both activated and deactivated rings toward the electrophilic aromatic sulfonation reaction. Hence, post-sulfonation as an approach for sulfonating poly(arylene ether sulfone)s was abandoned due to poor control over the extent of sulfonation, inability to control the microstructure of the sulfonated units, and decrease in molecular weight due to chain scission during sulfonation. These post sulfonated polysulfone membranes were found to be resistant to degradation by chlorine but showed relatively low salt rejections relative to the state-of-the-art interfacial polyamides [25]. Alternatively, Rose and coworkers reported controlled post-sulfonation of poly(arylene ether sulfone)s that contained hydroquinone units [26]. The sulfonation reaction proceeded only at the hydroquinone because all of the other rings were deactivated toward electrophilic aromatic sulfonation by the electron withdrawing sulfone groups. A series of investigations on this class of materials has been published [26–30]. In the current research, the reaction kinetics and measurements of molecular weight of a commercial polysulfone containing hydroquinone (Radel A™) were studied to optimize the sulfonation process with a minimal level of chain scission. This information was used as a model study for developing a series of post-sulfonated polymers with varying structures to determine their relationships among structures and properties.

Studies have shown that the crosslink density of RO membranes is vital to achieve the desired transport properties [14,31]. Sundell et al. and Daryaei et al. crosslinked amine terminated polysulfone oligomers containing a pre-disulfonated monomer with a tetra-epoxide to obtain membranes with high gel fractions [32,33]. The crosslinked membranes had higher levels of salt rejection with enhanced water permeability than linear disulfonated membranes at a fixed anionic group concentration in the backbone [34]. It is postulated that the free volume of the system

decreased with an increase in crosslink density since the networks absorbed less water than their linear counterparts.

In this paper, post-sulfonated crosslinked poly(arylene ether sulfone) membranes as potential candidates for RO and ED are described. Novel hydroquinone based, amine terminated oligomers were synthesized with block molecular weights of ~5,000 and ~10,000 g/mole. They were post-sulfonated under controlled conditions, then crosslinked at their termini with epoxy reagents. We have investigated the effect of the degree of monosulfonation of the hydroquinone units on the properties including water uptake, ion exchange capacity, fixed charge concentration, and hydrated mechanical properties. The crosslinked membranes were compared with linear counterparts to investigate the effect of crosslinking on the properties of these membranes.

2.2 Experimental

Materials

Radel-A™ (I) was kindly provided by Solvay Advanced Polymers and used as received.

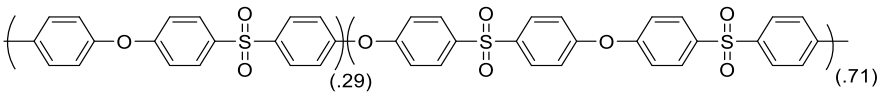

(I)

Concentrated sulfuric acid was obtained from VWR and used as received. 4,4'-Dichlorodiphenylsulfone (DCDPS) was kindly donated by Solvay Advanced Polymers and was recrystallized in toluene. It was dried under vacuum at 110 ºC for 12 h prior to use. Bisphenol sulfone (Bis-S) was provided by Solvay Advanced Polymers. It was recrystallized in methanol and dried under vacuum at 110 ºC for 12 h. Hydroquinone (HQ) was provided by Eastman Chemical Company and was recrystallized in toluene and dried under vacuum at 110 ºC for 12 h. 3-

Aminophenol (*m*-AP, 99%) was purchased from Acros Organics and was recrystallized in ethanol and dried at 70 ºC for 12 h. Potassium carbonate was purchased from Sigma-Aldrich and was dried under vacuum at 160 ºC for 72 h. For the crosslinking reaction of the sulfonated oligomers, triphenylphosphine (TPP, 99%) and tetraglycidyl bis(*p*-aminophenyl)methane (TGBAM, 92%), sulfolane, *N*,*N*-dimethylacetamide (DMAc) and toluene were purchased from Sigma-Aldrich.

Kinetics of Post-Sulfonation of a Poly(arylene ether sulfone) containing Hydroquinone: Post-sulfonation of Radel A

A solution of 30% (w/v) of Radel A in DMAc was prepared and precipitated in deionized water in a blender to provide a high surface area powder. This facilitated rapid dissolution during the sulfonation reaction. The precipitated polymer was filtered, washed with deionized water, dried without vacuum at 100 ºC for 12 h and then under vacuum at 110 ºC for 12 h to remove the solvent.

For the sulfonation reaction, a four-neck flask equipped with an overhead stirrer, nitrogen inlet, condenser and a thermometer was assembled. An oil bath with a thermocouple and temperature controller was used to control the reaction temperature. Radel A powder (15 g) and sulfuric acid (150 mL) were added into the flask. Reactions were performed at 40, 50, and 60 ºC. Time zero was designated when the temperature reached the desired point for the kinetics experiment (~2 min). Aliquots of 5-10 mL were removed at 5, 10, 15, 30, 60, and 120 min. The aliquots were quenched by precipitation in deionized water, followed by washing with copious amounts of deionized water until the pH reached at least 5.

Synthesis of sulfonated poly(arylene ether sulfone)s with isolated sulfonated rings by post-sulfonation

Synthesis of amine terminated hydroquinone containing polysulfone (xx-HQS-y) oligomers (I) with different amounts of hydroquinone relative to Bis-S (where xx = degree of sulfonation, y = targeted molecular weight)

The hydroquinone sulfone (HQS) oligomer series was synthesized using a nucleophilic aromatic substitution reaction. The reaction for the synthesis of a 10,000 g/mol, amine-terminated oligomer with 50 mol % of the bisphenol moieties being hydroquinone (50-HQS-10k) is provided. HQ (2.642 g, 24 mmol), Bis-S (6.006 g, 24 mmol), and *m*-AP (0.436 g, 4 mmol) were dissolved in 67 mL of sulfolane in a 3-neck round bottom flask equipped with a nitrogen inlet, overhead stirrer, and condenser with a Dean Stark trap. The reaction temperature was controlled with a temperature controller connected to a thermocouple in a salt bath. Toluene (34 mL) and K_2CO_3 (8.624 g, 62 mmol) were added and the reaction was refluxed at 180-185 ºC to azeotropically remove any water. After 4 h, the toluene was removed from the Dean Stark trap. DCDPS (14.358 g, 50 mmol) was added into the reaction flask and the reaction temperature was raised to 200-210 ºC. After 36 h of reaction, the mixture was allowed to cool to ~150 ºC and then diluted with 40 mL of DMAc. The solution was filtered hot to remove salts and subsequently precipitated in water. The polymer was boiled with 3 changes of water to remove trace amounts of sulfolane and then dried at 50 ºC for 4 h, followed by 12 h under vacuum at 110 ºC. The other oligomers in the 5,000 and 10,000 g/mol series were synthesized in a similar manner by varying the percentage of hydroquinone and *m*-AP accordingly. The reaction had a yield of 97 %.

Synthesis of high molecular weight hydroquinone sulfone (xx-HQS) polymers

Aromatic nucleophilic substitution step copolymerization was used to synthesize a series of hydroquinone-based, high molecular weight poly(arylene ether sulfone) copolymers (XX-

HQS). 60-HQS with 60% of the repeat units containing hydroquinone was synthesized as follows. HQ (19.85 mmol, 2.186 g), DCDPS (33.08 mmol, 9.501 g), Bis-S (13.235 mmol, 3.312 g) and sulfolane (43 mL) were charged into a 250-mL 3-neck round bottom flask equipped with a mechanical stirrer, condenser, nitrogen inlet, and Dean-Stark trap filled with toluene. The mixture was stirred and heated in an oil bath at 150 ºC until the monomers completely dissolved. K_2CO_3 (38.382 mmol, 5.305 g) and toluene (21 mL) were added into the flask. The reaction was refluxed for 6 h to azeotropically remove water from the system. Toluene was drained from the Dean-Stark trap, and the oil bath temperature was raised to 200 ºC to remove residual toluene from the reaction. The reaction solution was stirred for 36 h at 200 ºC. The reaction mixture was hot filtered to remove salts and precipitated in DI water. The polymer was stirred in boiling DI water for 4 h to remove any residual solvent. The polymer was filtered and dried at 120 ºC under reduced pressure in a vacuum oven. The reaction had a yield of 95%.

Post sulfonation of hydroquinone sulfone oligomers (xx-SHQS-5k and xx-SHQS-10k) and high molecular weight polymers (xx-SHQS)

The sulfonated hydroquinone sulfone (SHQS) oligomer/polymer series was synthesized by electrophilic aromatic sulfonation**.** Ten g of the dried *m*-AP terminated oligomer or high molecular weight polymer was dissolved in 100 mL of concentrated sulfuric acid in a 3-neck round bottom flask equipped with a nitrogen inlet and thermometer, overhead stirrer, and a condenser. An oil bath was used to maintain a reaction temperature of 50 ºC. The reaction was stirred vigorously to promote rapid dissolution and to break up any clumps of acid-swollen polymer. After 2 h of reaction, the solution was precipitated into ice-cold water and rinsed thoroughly to remove the excess acid until litmus paper showed no traces of acid. The oligomer samples were converted to

their salt form by stirring in 0.1 M NaOH for 6 h, filtered, and dried at 50 ºC for 7 h at atmospheric pressure overnight, followed by 12 h under vacuum at 110 ºC.

Characterization

Nuclear magnetic resonance spectroscopy (NMR)

Quantitative ^{1}H NMR and COSY NMR analyses were performed on the oligomeric copolymers and high molecular weight polymers on a Varian Unity Plus spectrometer operating at 400 MHz at a pulse angle of 30º with a pulse delay of 5 s. The spectra of the copolymers were obtained from a 10 % (w/v) solution in DMSO-d_6 with 64 scans.

End group analysis of the oligomers by fluorine derivatization

The amine terminated oligomers with amine and any residual phenolic end groups were reacted with trifluoroacetic anhydride to produce the respective trifluoroacetate derivatives. The reaction for the derivatization of a 5,000 g/mol, amine-terminated oligomer with 50 mol % of the bisphenol moieties being hydroquinone (50-HQS-5k) is provided. 50-HQS-5k oligomer (200 mg, 0.040 mmol), with amine end groups and possibly unreacted hydroxyl end groups, was dissolved in 5 mL of $CHCl_3$ in a 25-mL flask and trifluoroacetic anhydride (0.5 mL, 3.53 mmol) was added. The reaction mixture was held at 25 ºC for 12 h. DI water (100 mL) was added to the reaction mixture to hydrolyze the remaining anhydride, and the mixture was stirred at room temperature for 2 h. The organic phase was analyzed by ^{19}F NMR. ^{19}F NMR spectra were collected utilizing the same NMR spectrometer operating at 376.29 MHz with a pulse width of 45º and a relaxation delay of 3 s with 64 scans.

Size Exclusion Chromatography (SEC)

Molecular weights and polydispersities of the polymers were measured using SEC. The mobile phase was DMAc distilled from CaH_2 containing dry LiCl (0.1 M). The column set consisted of 3 Agilent PLgel 10-mm Mixed B-LS columns 300*7.5 mm (polystyrene/divinylbenzene) connected in series with a guard column having the same stationary phase.

The columns and detectors were maintained at 50 ºC. An isocratic pump (Agilent 1260 infinity, Agilent Technologies) with an online degasser (Agilent 1260), autosampler and column oven were used for mobile phase delivery and sample injection. A system of multiple detectors connected in series was used for the analyses. A multi-angle laser light scattering detector (DAWN-HELEOS II, Wyatt Technology Corp.), operating at a wavelength of 658 nm and a refractive index detector operating at a wavelength of 658 nm (Optilab T-rEX, Wyatt Technology Corp.) provided online results. The system was corrected for interdetector delay and band broadening using a 21,000 g/mole polystyrene standard. Data acquisition and analysis were conducted using Astra 6 software from Wyatt Technology Corp. Validation of the system was performed by monitoring the molar mass of a known molecular weight polystyrene sample by light scattering. The accepted variance of the 21,000 g/mole polystyrene standard was defined as 2 standard deviations (11.5% for M_n and 9% for M_w) derived from a set of 34 runs.

Specific refractive indices were measured offline. Oligomer samples with systematically varying concentrations in DMAc with 0.1M LiCl from ~0.0005 to 0.008 g/L were injected directly into the RI detector using an injection box. The data was plotted on a graph of dRI (differential refractive index) versus concentration. dn/dc of the oligomer solution was determined from the slope of the graph.

Film casting and characterization

Epoxy-amine crosslinking of the oligomers

The crosslinked films were prepared by adding the oligomer and TGBAM in the molar ratio of 1:2.5 respectively. TPP was used in a 3.0 % by weight ratio relative to the weight of TGBAM. The following steps were completed to prepare a crosslinked film containing 10k-50-SHQS. A mixture of 10k-50-SHQS (0.046 mmol, 0.63 g), TGBAM (0.114 mmol, 0.048 g) and TPP (5.5×10^{-3} mmol, 1.44 mg) were dissolved in 8 mL of DMAc in a vial and stirred until a homogeneous solution was obtained. The solution was syringe-filtered through a 0.45 μm PTFE filter into a new vial. The original vial was washed with 7 mL of DMAc and filtered into the new vial to transfer any residual oligomers. The solution was sonicated for 15 min and was cast on a circular Teflon mold with flat edges and a diameter of 10 cm. The mold was placed on a levelled surface inside an oven at 70 ºC. The temperature of the oven was ramped up from 70 to 175 ºC gradually over 6 h and the film was cured at a steady temperature of 175 ºC for 12 h. The temperature of the oven was gradually ramped down to 120 ºC and the film was dried under vacuum for 12 h. The oven was turned off and the film was allowed to cool in the oven to room temperature. The epoxy-cured network was detached from the Teflon mold by immersion in deionized water and dried. The thickness of the film was approximately 70 μm.

Film casting of the high molecular weight polymers

A copolymer (1.2 g) was dissolved in 10 mL of DMAc in a glass vial. The solution was filtered through a 0.45 μm PTFE filter and the vial was washed with 2 mL of DMAc to form a 10 wt/v% polymer solution. The solution was sonicated for 10 min and cast on a level 4” x 4” clean glass plate. The plate was cleaned in a base bath, washed and dried prior to film casting. The films were heated under an IR lamp with a starting temperature of ~45 ºC. The temperature of the IR

lamp was ramped up by 20 ºC every 2 h until the temperature reached ~75 ºC. The plate with the film was kept at that temperature for 8-10 h. The film was dried under vacuum at 110 ºC for 24 h. The film was delaminated from the glass plate by immersion in deionized water. The film, in the acidic form, was stirred in 0.1 N NaCl for 3 days to convert it into the salt form. The film was stirred in deionized water overnight to remove the excess salt and dried under vacuum at 110 ºC overnight. The thickness of the film was ~100 μm.

Gel fraction measurements on the crosslinked films

Crosslinked films were dried at 120 ºC under vacuum overnight. After drying, 0.1−0.2 g of the sample was placed in a 20-mL scintillation vial filled with DMAc and stirred at 100 ºC for ~12 h. The remaining solid was filtered, transferred to a weighed vial, dried to a constant weight at 160 ºC under vacuum for ~12 h, and then weighed. Three measurements were taken for each film and gel fractions were calculated by equation 1.

$$Gel\ Fraction\ (\%) = \frac{Final\ mass\ of\ extracted\ film}{Initial\ mass\ of\ dried\ film} \times 100 \qquad \text{(Equation 1)}$$

Water uptake

The water uptakes of the crosslinked and high molecular weight linear membranes were determined gravimetrically. The membranes in their sodium salt form were dried at 12 ºC under vacuum for 24 h and weighed. The membranes were soaked in water at room temperature for 24 h. Wet membranes were removed from the water, blotted dry to remove surface droplets, and quickly weighed. The water uptake of the membranes was calculated according to equation 2, where $mass_{dry}$ and $mass_{wet}$ refer to the masses of the dry and the wet membranes, respectively.

$$\text{Water Uptake}\ (\%) = \frac{Mass_{wet} - Mass_{dry}}{Mass_{dry}} \times 100 \qquad \text{(Equation 2)}$$

Tensile tests of hydrated membranes

The crosslinked membranes were cut into dogbone samples with a gauge width of 3.18 mm and gauge length of 25 mm, Type V according to ASTM D638-14, using a Cricut Explore One™ cutting machine. Seven samples with uniform thickness of 60-70 μm from each membrane were tested. The thickness of the dogbones were measured at five points along the gauge length using a Mitutoyo digimatic micrometer model MDC-1"SXF. A hydrated testing cell was secured onto the Instron to test samples under fully hydrated conditions. The wet samples were loaded into the hydrated cell of the Instron and the cell was filled with DI water. The samples were immersed in DI water for at least 24 h prior to testing and allowed to equilibrate in the Instron in the water for 3 min. Uniaxial load tests were performed using an Instron ElectroPuls E1000 testing machine equipped with a 250-N Dynacell load cell. The crosshead displacement rate was 10 mm/min and the initial grip separation was 25 mm.

2.3 Results and discussion

Sulfonated polysulfone oligomers with amine end groups prepared from a pre-disulfonated monomer, 3,3'-disulfonate-4,4'-dichlorodiphenylsulfone (III), were previously investigated by Sundell et al. and Daryaei et al. [33,34]. The present work deals with the sulfonic acid groups on isolated rings as opposed to having sulfonates in pairs on adjacent rings so that the placement of ions could be related to water uptake and fixed charge concentration. Moreover, previous studies on sulfonated polysulfone membranes in their acid form have shown that above a critical IEC of ~1.3, the absorption of water increases faster as the fixed charge groups on the polymer backbone is increased.[35] We hypothesize that decreased water uptake per ionic group will lead to higher salt rejection values due to Donnan exclusion. Thus, the series of membranes investigated in this study have been designed with a lower IEC range compared to the previous materials.

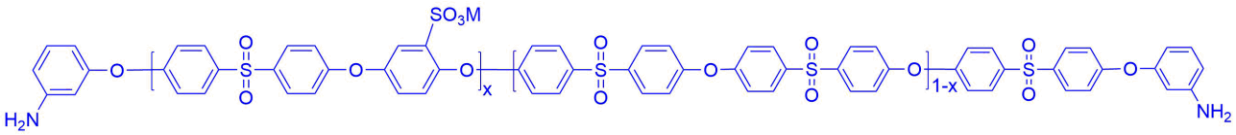

II (SHQS)

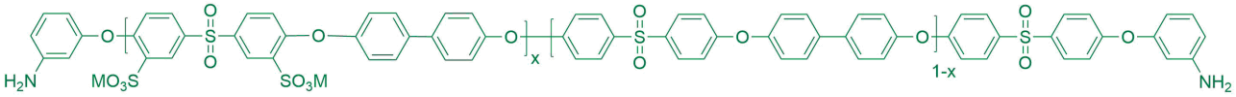

III (BPS)

Synthesis and characterization of controlled molecular weight oligomers

A series of oligomers with controlled molecular weights of ~5,000 and ~10,000 g/mol were synthesized via nucleophilic aromatic substitution step growth polymerization with a weak base in a dipolar aprotic solvent as depicted in Figure 2.1. The reaction was azeotropically dehydrated with toluene to remove water generated from the reaction of the base with the phenol, which might compete with the phenolate nucleophile and hydrolyze the dihalide. Due to the presence of the electron withdrawing sulfone group between the rings, the phenoxide ions of Bis-S are poorly nucleophilic [36]. Hence, the reaction was carried out at a high temperature of 200 ºC for 36 h in a high boiling solvent, sulfolane.

Synthesis of controlled molecular weight oligomers using an end-capping reagent are well known [14,32]. It has been established that *m*-AP acts as a quantitative end-capping agent for poly(arylene ether sulfone)s [32,33,37] that are comprised of structures similar to II. *m*-AP is preferred over *p*-aminophenol because the latter oxidizes to form stable quinone type structures. *m*-AP terminated oligomers produce high gel fractions when cured with multifunctional epoxides [32,38]. The amount of *m*-AP required was calculated using the Carothers equation by offsetting the reaction stoichiometry between the phenols and the dihalide. Although *m*-AP contains both

amine and phenol functionality, the reaction proceeds through nucleophilic aromatic substitution of the more nucleophilic phenolate group, and the amine does not interfere with the polymerization. This paper describes control of molecular weight with *m*-AP end groups on polymers with structure II and varied degrees of sulfonation.

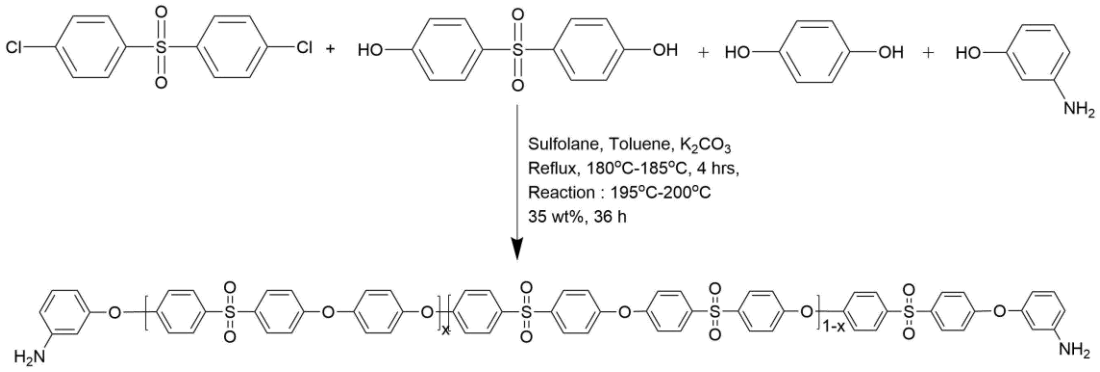

Figure 2.1: Synthesis of controlled molecular wegiht random oligomers by nucleophilic aromatic substitution X=0.4, 0.50, 0.65, 0.80

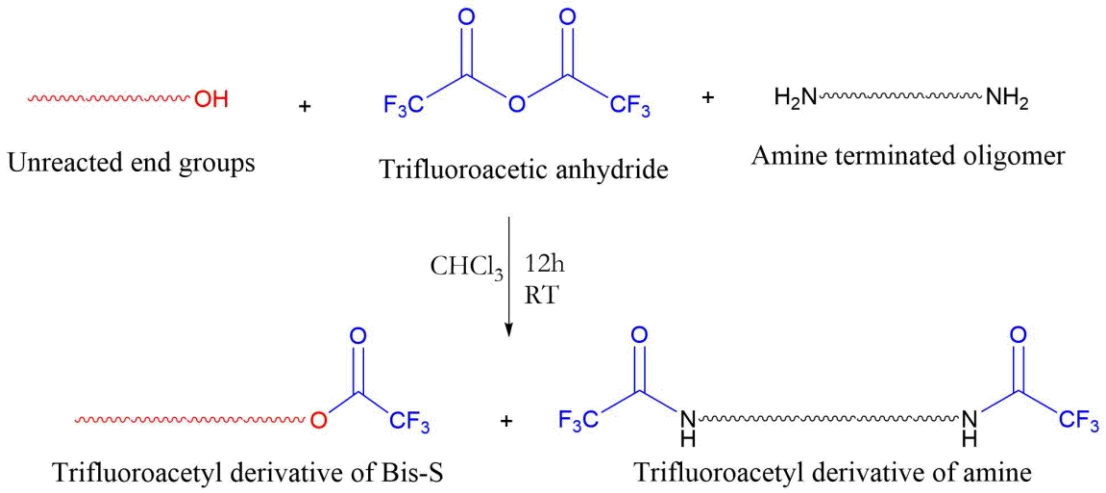

Figure 2.2: Fluorine derivatization of the oligomers to check for unreacted monomers and completion of the reaction

To confirm the absence of undesirable residual phenol or chlorine end groups after the reaction, the oligomer was derivatized with trifluoroacetic anhydride as shown in Figure 2.2 [39].

The anhydride reacts with the amine end groups forming a derivative that resonates at ~ -74 ppm in the ^{19}F NMR spectrum (Figure 2.3). The anhydride also reacts with any unreacted end groups of Bis-S or hydroquinone, resonating downfield from the amine. An aliquot taken at 24 h showed that there was one equivalent of phenol from Bis-S for very five equivalents of amine. However, an aliquot taken at 36 h showed successful completion of the reaction.

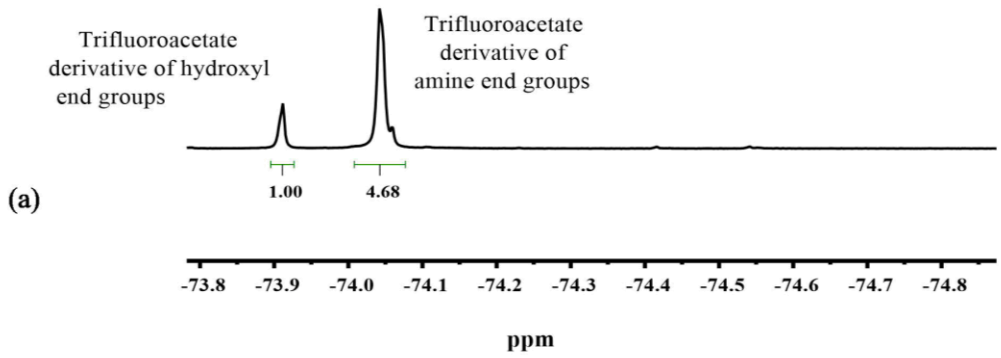

Figure 2.3: ^{19}F NMR spectra of the oligomers showing unreacted hydroxyl end groups and amine groups of the oligomer- aliquot at 24 h of the reaction

Post -sulfonation of structure II

Post-sulfonation of the amine terminated oligomers and the high molecular weight polymers was performed under mild conditions to place the sulfonate ions strategically along the backbone of the polymer chain (Figure 2.4). Only the aromatic rings of the hydroquinone units were sulfonated because all of the other rings were deactivated for electrophilic aromatic sulfonation by the electron withdrawing sulfone groups. Lane optimized the conditions of the reaction [40]. A copolymer containing hydroquinone in 29% of the repeat units was sulfonated at 40, 50 and 60 ºC for various times. Figure 2.5 and Table 2.1 show a comparable degree of sulfonation at 50 and 60 ºC, with the highest molecular weight at 50 ºC. It should be noted that Figure 2.5 shows a degree of sulfonation of 30% for the Radel A at 2 h post-sulfonation at 50 and

60 ºC whereas the NMR of the non sulfonated Radel A indicated that 29% of the repeat units contained HQ. This difference is well within the error of the NMR measurements. The high molecular weight at 50 ºC suggests that minimal degradation of the chains occurs over 2 h, and thus these sulfonation conditions were employed for the polymers in this research.

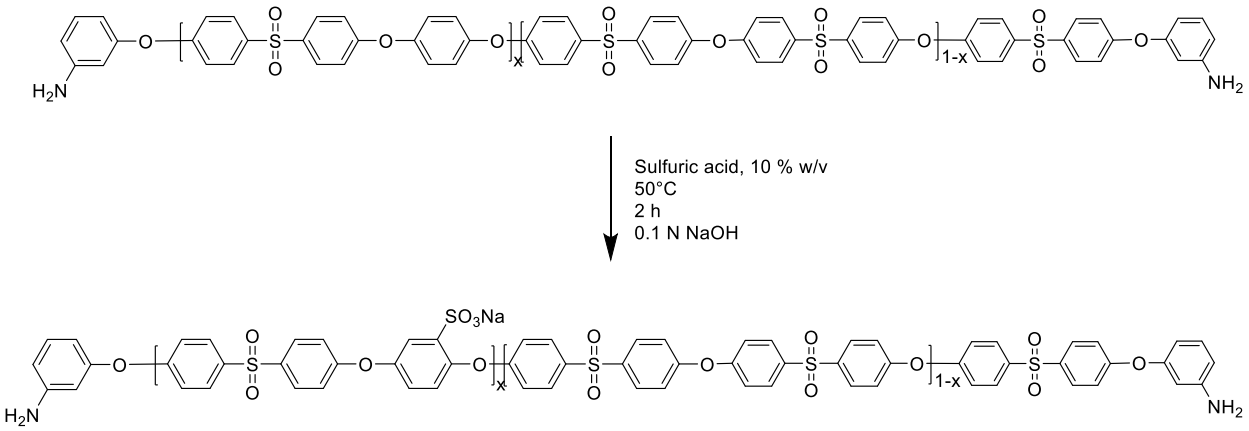

Figure 2.4: Post-sulfonation of hydroquinone-based amine terminated oligomers by electrophilic sulfonation under mild conditions

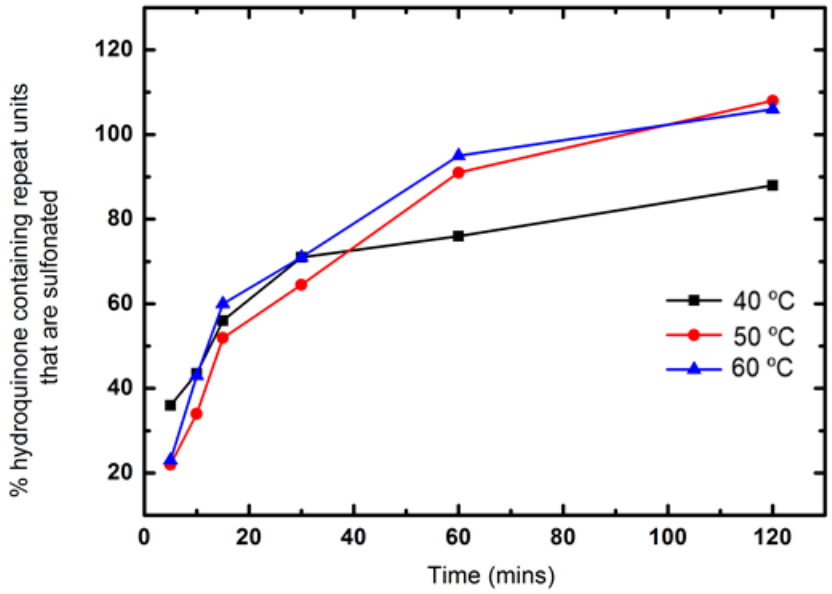

Figure 2.5: Progress of sulfonation of hydroquinone (%) as a function of reaction time and temperature

Time (min)	50 ºC	60 ºC
0	35,000	35,000
60	42,600	36,800
120	56,600	32,300

Table 2.1: M_w of Radel A (g/mole) before and after post-sulfonation at 50 and 60 ºC. M_w obtained by SEC in DMAc with 0.1M LiCl

Structure and molecular weights of the functional oligomers

The non-sulfonated and sulfonated oligomers were characterized by quantitative ^{1}H NMR to calculate the molecular weights and degrees of sulfonation (Figure 2.6). Completion of the reaction was confirmed by the absence of peaks of undesired end groups in the spectra. The spectra were normalized using the peaks from the amine end groups.

The **a_1, a** signals overlapped and resonated at 7.88 to 8.02 ppm. **The i** peaks from the amine end groups resonated at 5.33 ppm. The **c** protons of the hydroquinone resonated at 7.2 ppm. After sulfonation, the **c** protons shifted downfield to 7.45 ppm due to the electron withdrawing nature of the sulfonic acid groups that deshielded the protons. The amine end groups were acidified during the sulfonation at 50 ºC for 2 h, shifting the peaks downfield. Thus, the sulfonated oligomers were

stirred in a solution of 0.1 N NaOH to recover the amine end groups.

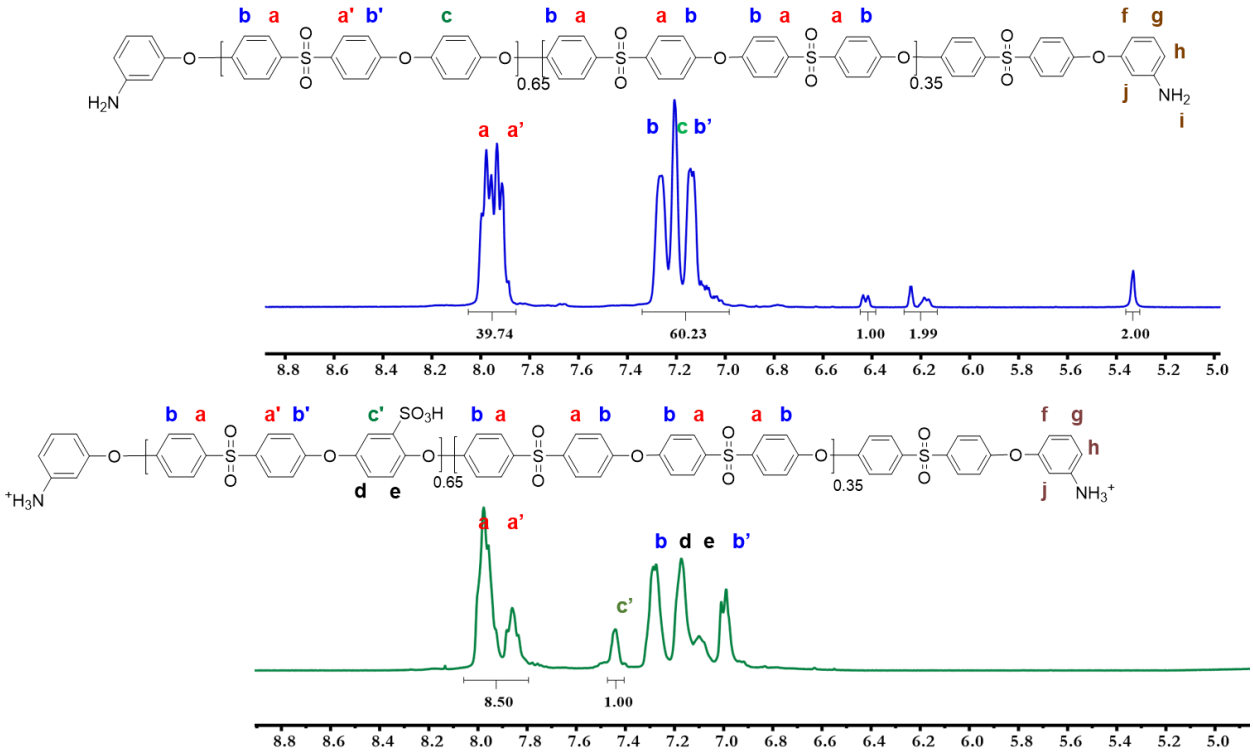

Figure 2.6: ^{1}H NMR of an oligomer with a target molecular weight of ~5000 g/mol and 65% hydroquinone containing repeat units before and after sulfonation

The degree of sulfonation was calculated from the spectra of the sulfonated oligomers, and the ion exchange capacities were calculated using the degrees of sulfonation (Equation 3). In equation 3, DS is the degree of sulfonation, MW_{SRU} is the molecular weight of the sulfonated repeat unit in the Na^+ form, MW_{NSRU} is the molecular weight of the non-sulfonated repeat unit.

$$IEC_{oligomer} = \frac{1000*DS}{(DS*MW_{SRU})+[(1-DS)*MW_{NSRU}]} \quad \text{(Equation 3)}$$

COSY NMR experiments were performed to confirm the structure of the post sulfonated oligomers (Figure 2.7). The **c'** proton correlated only with itself and did not show a three-bond correlation with any other proton. There were no other uncorrelated protons. Thus, there were no

secondary sites of sulfonation and all the hydroquinone moieties were strategically sulfonated by post-sulfonation.

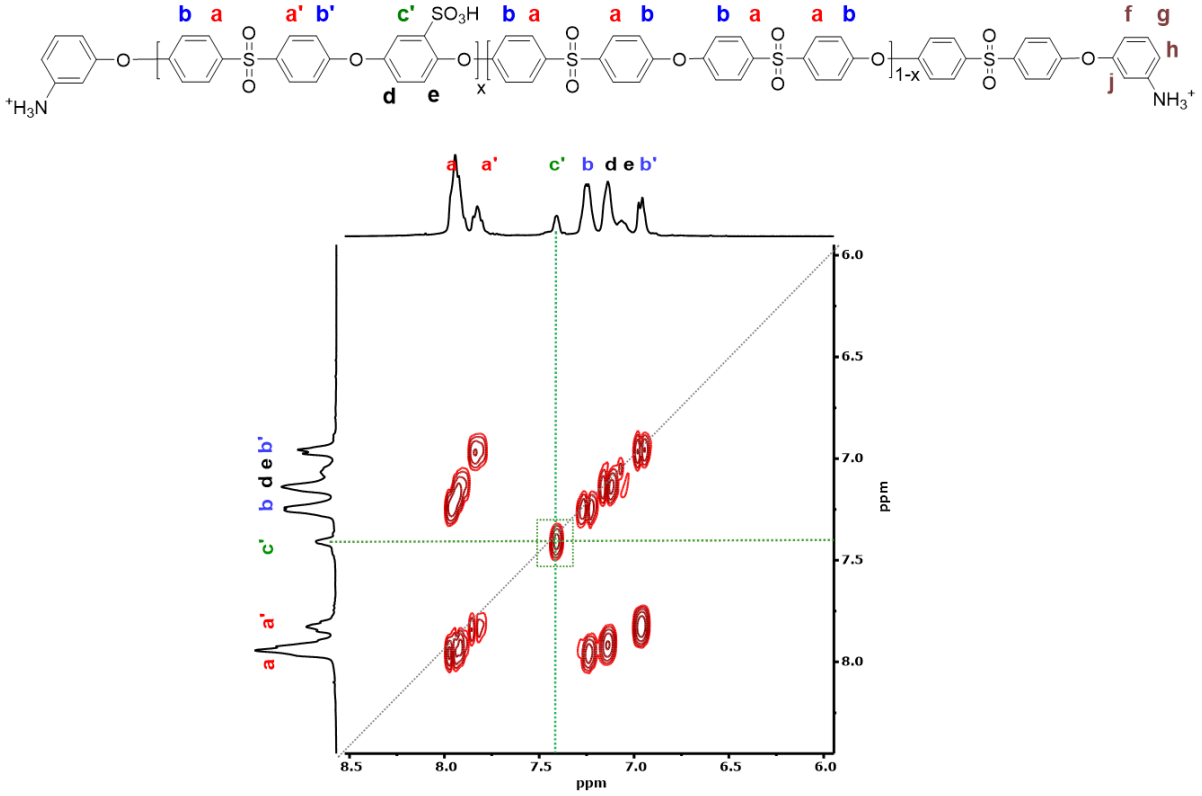

Figure 2.7: COSY-NMR of a sulfonated oligomer with a target molecular weight of ~5,000 g/mol and 65% hydroquinone containing repeat units (65-SHQS-5k)

The molecular weights of the oligomers were analyzed by SEC and ^{1}H NMR. The dn/dc is an essential parameter for analysis of the SEC light scattering data. The dn/dc's of the oligomers were measured, in DMAc with 0.1 M LiCl, offline from the slopes of the plots of the differential refractive indices versus concentration as shown in Figure 2.8. In all cases, the dn/dc's of the sulfonated copolymers were less than their non-sulfonated counterparts. The dn/dc's were then used to determine the weight average molecular weights using the Rayleigh ratio [41].

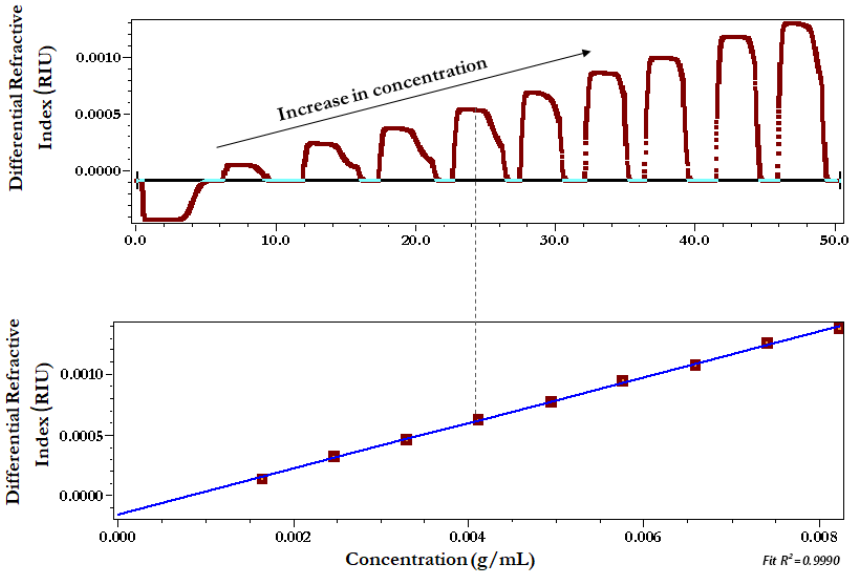

Figure 2.8: Offline measurement of the refractive index of 65-SHQS-5k

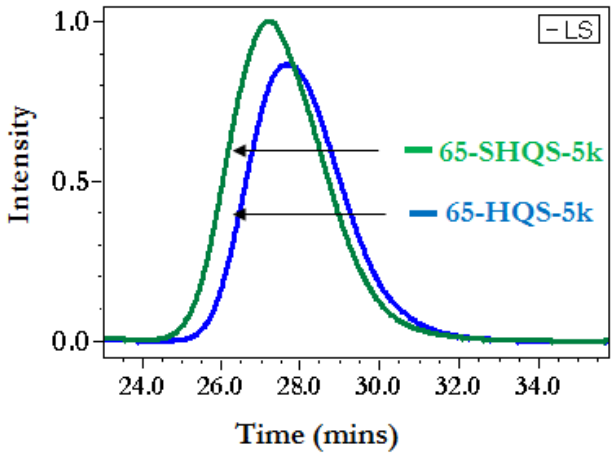

Figure 2.9: SEC light scattering chromatograms of a ~5000 g/mol oligomer before sulfonation (65-HQS-5k) and after sulfonation (65-SHQS-5k)

Oligomer/Polymer	Estimated M_n ^{1}H NMR (kDa)	M_n SEC (kDa)	M_w SEC (kDa)	dn/dc
50-HQS-5k	5.0	6.8	10.2	0.22
50-SHQS-5k	5.4	8.2	12.2	0.20

65-HQS-5k	5.5	7.6	16.5	0.20
65-SHQS-5k	6.3	10.0	19.6	0.19
80-HQS-5k	6.0	10.8	22.1	0.19
80-SHQS-5k	7.3	14.4	28.5	0.18
40-HQS-10k	11.9	12.1	24.3	0.19
40-SHQS-10k	13.0	18.4	30.0	0.15
50-HQS-10k	12.3	13.7	27.5	0.19
50-SHQS-10k	13.8	18.2	35.9	0.16
65-HQS-10k	11.2	9.9	21.5	0.18
65-SHQS-10k	13.0	17.5	38.4	0.15
40-HQS		26.1	50.7	
40-SHQS		28.4	55.2	
50-HQS		20.1	34.2	
50-SHQS		23.3	43.4	
60-HQS		18.4	30.4	
60-SHQS		23.8	37.8	

Table 2.2: Molecular weights and polydispersities of the oligomers and the polymers before and after sulfonation as obtained by SEC

The molecular weights of the oligomers by SEC increased after sulfonation as expected (Figure 2.9 and Table 2.2), but it is not clear what causes the deviation of the molecular weights relative to the targeted molecular weights. It should be noted that ionic interactions could affect the hydrodynamic volume of these sulfonated oligomers even though the SEC solvent contained salt to screen such interactions. Most of the previous studies on post-sulfonation of polysulfones found difficulties with the retention of molecular weight after sulfonation due to degradation of the polymers. None of the oligomers in the present study decreased in molecular weight after

sulfonation using the mild conditions employed. Thus, it is reasoned that sulfonation under these mild conditions should be appropriate for applications such as desalination membranes.

For comparison the number average molecular weights of the non-sulfonated oligomers were estimated from the ^{1}H NMR spectra by considering the relative integrals of the polyether segments next to the end groups and the oligomer backbones (Table 2.2, S-equation 2). These analyses required significant subtractions of integrals and thus the molecular weights by NMR are only considered approximate. The NMR molecular weights of the sulfonated oligomers were approximated from those of the non-sulfonated counterparts and the degree of sulfonation (S-equation 3).

The high molecular weight, linear polymers were also characterized by ^{1}H NMR, COSY NMR and SEC. All the samples yielded 100% sulfonation of the hydroquinone units with no secondary sites of sulfonation. The SEC results confirmed high molecular weight without chain degradation as shown in Table 2.

Film casting

The epoxy amine crosslinking is a well-studied reaction [42–45]. Networks of amine terminated sulfonated polysulfone oligomers prepared with pre-sulfonated monomers with TGBAM have been reported [23,32]. The post-sulfonated oligomers in the salt form were crosslinked with TGBAM (Figure 2.10). TPP catalyzes both the reaction between hydroxyl and epoxy groups and the polyetherification of the epoxy resin [46]. The curing reaction was performed in the presence of DMAc which reduces the T_g. The film was cured as the temperature was ramped from 100 to 175 ºC in a convection oven. The process was continued for 6 h until the mixture became viscous. The crosslinked networks had high gel fractions ranging from 88-93%. Attempts to cast membranes on glass substrates showed that it was difficult to delaminate the film even after

silanizing the glass plate. Hence, the films were cast in a teflon mold with a flat bottom and sharp inner edges such that the films would not recede. It was also found that vacuum drying at 120 ºC after crosslinking played an important role in the process of film casting. It is imperative to remove most of the residual solvent before soaking the films in water to avoid the formation of pinholes. It is hypothesized that water can dissolve the residual DMAc from the films, leading to pinholes.

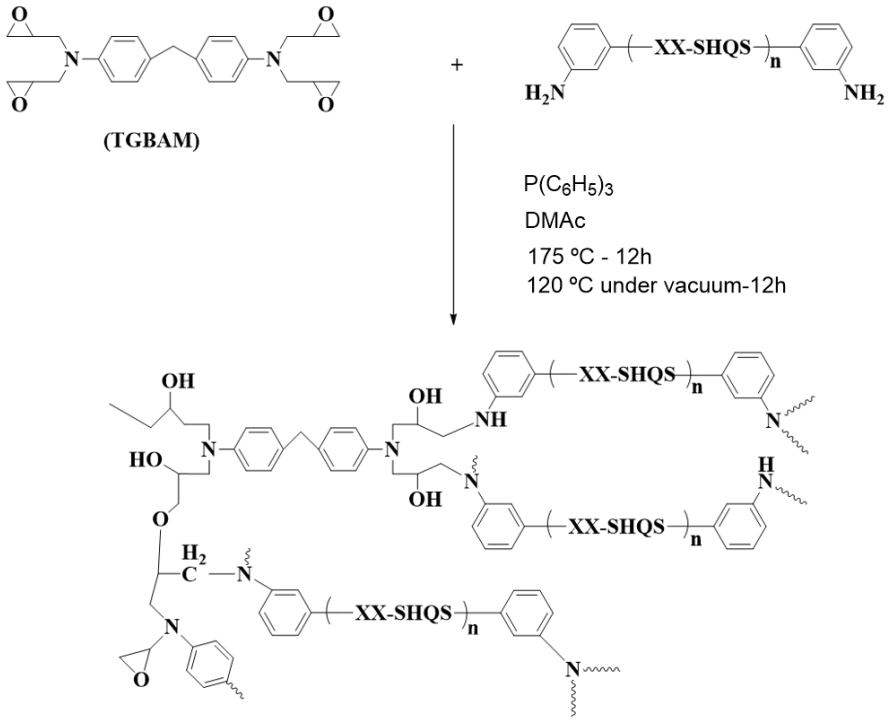

Figure 2.10: Schematic representation of the crosslinking reaction of amine terminated oligomer with an epoxy resin (TGBAM)

Membrane properties

The maximum absorption of water increases with IEC (Figure 2.11, Table S1). The IECs of the crosslinked membranes were calculated from the IECs of the oligomers measured by ^{1}H NMR, by taking into account the addition of the non-ionic crosslinking agent (Equation 4). The water uptakes of crosslinked membranes have been reported to be constrained due to reduced swelling and free volume [47,48]. This is evident for the systems discussed in this paper in Figure

2.10 where, for a given IEC, the water uptakes of the epoxy networks prepared from the 5000 g/mol oligomers are less than the linear counterparts.

$$IEC_{\substack{crosslinked \\ membrane}} = IEC_{oligomer} * weight\ fraction\ of\ oligomer\ in\ the\ membrane$$

(Equation 4)

The fixed charge concentration of the membranes, C_A^m, is defined as the concentration of fixed ions on the polymer per unit of sorbed water (Equation 5 where ρ_w is assumed to be 1 g/cc).

$$C_A^m \approx \frac{IEC \times \rho_w}{water\ uptake} \quad \text{(Equation 5)}$$

Increasing the membrane fixed charge concentration increases the Donnan potential, which should lead to better co-ion and salt rejection. Thus, increasing the fixed charge groups in the polymer matrix can increase the fixed charge concentration. However, increasing the IEC also increases the water uptake of the membranes which acts to reduce the fixed charge concentration. Figure 2.11 shows the fixed charge concentrations of the linear and crosslinked SHQS membranes with respect to IEC. It is clear that the crosslinked membranes have higher fixed charge concentrations than the linear counterparts. Thus, it is hypothesized that these crosslinked membranes will also show improved salt rejection. The effect of crosslinking on constraining the membranes made from the 10,000 g/mole oligomers was not as prominent, likely due to their lower crosslink densities. It should also be noted that all of the SHQS membranes had higher fixed charge concentrations than those of some commercial GE Electrodialysis membranes as described in reference [33].

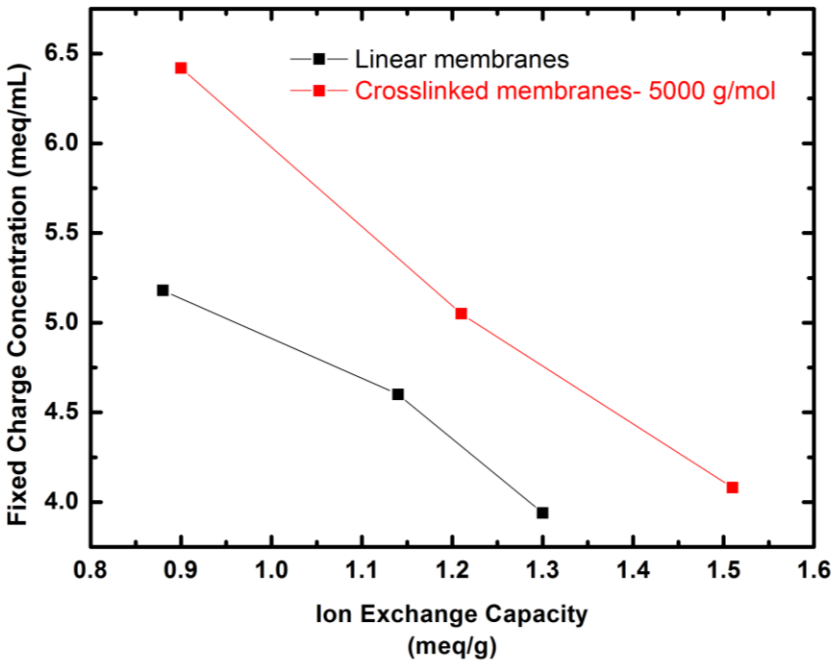

Figure 2.11: Fixed charge concentrations of the linear and the crosslinked (~5000 g/mole) membranes as a function of their ion exchange capacities.

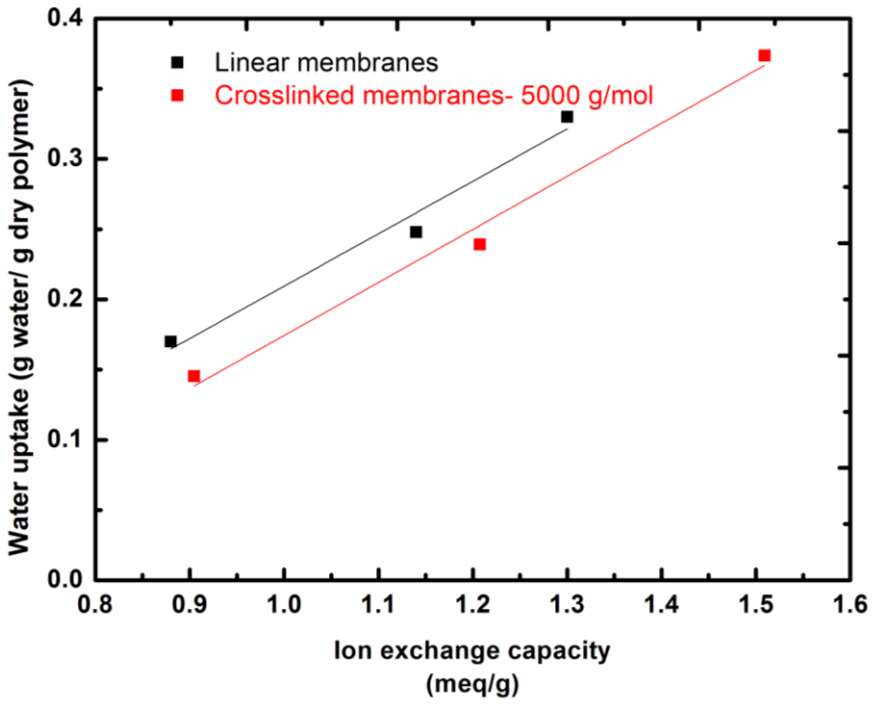

Figure 2.12: Water uptake of the linear and the crosslinked membranes (~5000 g/mole) as a function of their ion exchange capacities

Hydrated mechanical properties of the membranes

One of the objectives of this work is to develop membranes that have superior mechanical properties in fully hydrated conditions to withstand high applied pressure in reverse osmosis. The linear and the crosslinked SHQS membranes are in the glassy state under fully hydrated conditions. The tensile data (Figure 2.13) showed that increasing water uptake decreased the elastic modulus and the yield stress in the crosslinked networks. This phenomenon occurred due to the plasticization effect of water independent of the degree of crosslinking. The high dielectric constant of the water reduces the van der Waals forces between the polymer chains, leading to an increase in the free volume and chain mobility. Interestingly, a similar trend was observed in the linear samples as shown in Figure 2.13. Therefore, it can be concluded that the effect of water content superseded the effect of block length and crosslinking. This could have happened because

the crosslinked membranes were designed for controlled crosslinking only at the ends and the crosslink density was low. The 50-SHQS-5k network showed the highest yield stress due to the lowest amount of water uptake (0.14)

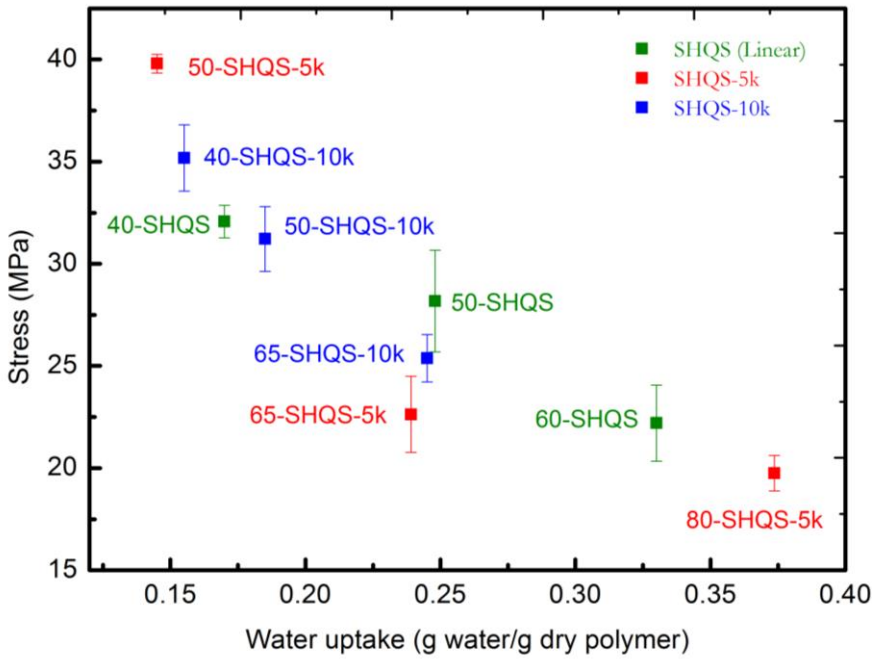

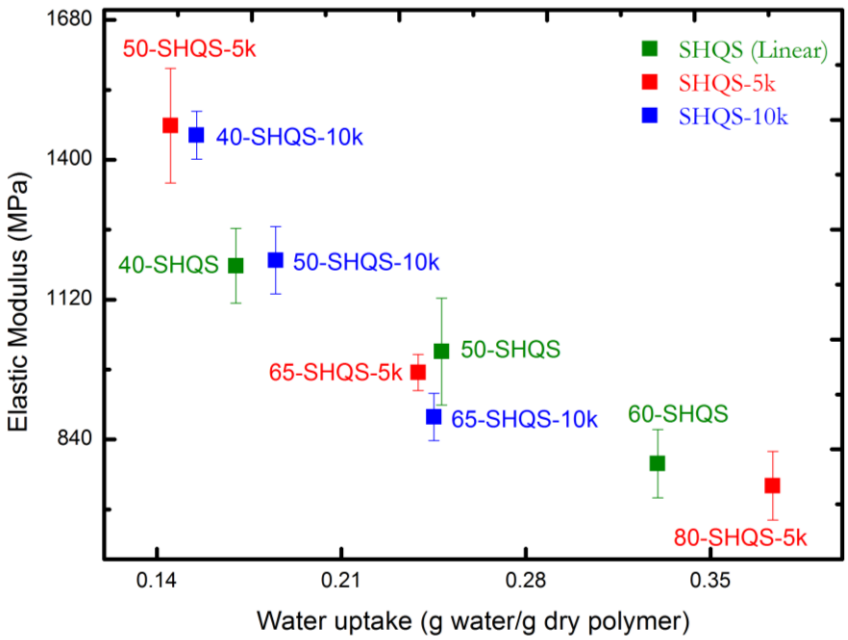

Figure 2.13: Yield stress and elastic modulus decreases with an increase in water uptake for the crosslinked and linear SHQS membranes

2.4 Conclusions

It is now clear that sulfonated poly(arylene ether sulfone)s can be prepared with control over both the level of sulfonation and the distribution of sulfonate groups along the chains, and that this can be achieved by using either pre-sulfonated monomers or by post-sulfonation. Post-sulfonation is likely preferable economically since sulfonated monomers would not be required. The work reported herein shows that controlled molecular weight oligomers with functional end groups can be post-sulfonated in a controlled manner, then crosslinked. This has enabled a comparison between linear and crosslinked networks prepared by the post-sulfonation route.

In general, the crosslinked networks absorb less water than the linear polymers at a given IEC. This can likely be attributed to constraints that result in higher fixed charge concentrations. It is thus anticipated that the transport properties, including salt rejection and water to salt

permeability selectivity, will be improved in the crosslinked materials. The transport properties will be a focus of a second publication.

References

[1] R.F. Service, Desalination freshens up., Science. 313 (2006) 1088–90.

[2] M. Elimelech, W.A. Phillip, The future of seawater desalination: energy, technology, and the environment., Science. 333 (2011) 712–7.

[3] M.A. Shannon, P.W. Bohn, M. Elimelech, J.G. Georgiadis, B.J. Mariñas, A.M. Mayes, Science and technology for water purification in the coming decades, Nature. 452 (2008) 301–310.

[4] G. Kang, Y. Cao, Development of antifouling reverse osmosis membranes for water treatment: A review, Water Res. 46 (2012) 584–600.

[5] L.F. Greenlee, D.F. Lawler, B.D. Freeman, B. Marrot, P. Moulin, Reverse osmosis desalination: Water sources, technology, and today's challenges, Water Res. 43 (2009) 2317–2348.

[6] I.C. Karagiannis, P.G. Soldatos, Water desalination cost literature: review and assessment, Desalination. 223 (2008) 448–456.

[7] G.M. Geise, H.-S. Lee, D.J. Miller, B.D. Freeman, J.E. McGrath, D.R. Paul, Water purification by membranes: The role of polymer science, J. Polym. Sci. Part B Polym. Phys. 48 (2010) 1685–1718.

[8] H. Luo, J. Aboki, Y. Ji, R. Guo, G.M. Geise, Water and Salt Transport Properties of Triptycene-Containing Sulfonated Polysulfone Materials for Desalination Membrane Applications, ACS Appl. Mater. Interfaces. 10 (2018) 4102–4112.

[9] Y. Tanaka, Ion-Exchange Membrane Electrodialysis for Saline Water Desalination and Its Application to Seawater Concentration, Ind. Eng. Chem. Res. 50 (2011) 7494–7503.

[10] H. Strathmann, Electrodialysis, a mature technology with a multitude of new applications, Desalination. 264 (2010) 268–288.

[11] J. Kamcev, B.D. Freeman, Charged Polymer Membranes for Environmental/Energy Applications, Annu. Rev. Chem. Biomol. Eng. 7 (2016) 111–133.

[12] J. Kamcev, D.R. Paul, B.D. Freeman, M. Elimelech, C. Gavach, M.G. Mclin, J.J. Fontanella, Effect of fixed charge group concentration on equilibrium ion sorption in ion exchange membranes, J. Mater. Chem. A. 5 (2017) 4638–4650.

[13] D.M. Stevens, J.Y. Shu, M. Reichert, A. Roy, Next-Generation Nanoporous Materials: Progress and Prospects for Reverse Osmosis and Nanofiltration, Ind. Eng. Chem. Res. 56 (2017) 10526–10551.

[14] M. Paul, H.B. Park, B.D. Freeman, A. Roy, J.E. McGrath, J.S. Riffle, Synthesis and crosslinking of partially disulfonated poly(arylene ether sulfone) random copolymers as candidates for chlorine resistant reverse osmosis membranes, Polymer. 49 (2008) 2243–2252.

[15] J.G. Wijmans, R.W. Baker, The solution-diffusion model: a review, J. Memb. Sci. 107 (1995) 1–21.

[16] W. Xie, G.M. Geise, B.D. Freeman, H.-S. Lee, G. Byun, J.E. McGrath, Polyamide interfacial composite membranes prepared from m-phenylene diamine, trimesoyl chloride and a new disulfonated diamine, J. Memb. Sci. 403–404 (2012) 152–161.

[17] C.H. Lee, B.D. McCloskey, J. Cook, O. Lane, W. Xie, B.D. Freeman, Y.M. Lee, J.E. McGrath, Disulfonated poly(arylene ether sulfone) random copolymer thin film composite membrane fabricated using a benign solvent for reverse osmosis applications, J. Memb. Sci. 389 (2012) 363–371.

[18] W. Choi, S. Jeon, S.J. Kwon, H. Park, Y.-I. Park, S.-E. Nam, P.S. Lee, J.S. Lee, J. Choi, S. Hong, E.P. Chan, J.-H. Lee, Thin film composite reverse osmosis membranes prepared via layered interfacial polymerization, J. Memb. Sci. 527 (2017) 121–128.

[19] Y. Song, P. Sun, L.L. Henry, B. Sun, Mechanisms of structure and performance controlled thin film composite membrane formation via interfacial polymerization process, J. Memb. Sci. 251 (2005) 67–79.

[20] B.D. McGrath, J. E.; Park, H. B.; Freeman, Chlorine resistant desalination membranes based on directly sulfonated poly(arylene ether sulfone) copolymers, US 8,028,842 B2, 2011.

[21] H.B. Park, B.D. Freeman, Z.-B. Zhang, M. Sankir, J.E. McGrath, Highly Chlorine-Tolerant Polymers for Desalination, Angew. Chemie. 120 (2008) 6108–6113.

[22] F. Wang, M. Hickner, Y.S. Kim, T.A. Zawodzinski, J.E. McGrath, J.E. McGrath, Direct polymerization of sulfonated poly(arylene ether sulfone) random (statistical) copolymers: candidates for new proton exchange membranes, J. Memb. Sci. 197 (2002) 231–242.

[23] A. Daryaei, G.C. Miller, J. Willey, S. Roy Choudhury, B. Vondrasek, D. Kazerooni, M.R. Burtner, C. Mittelsteadt, J.J. Lesko, J.S. Riffle, J.E. McGrath, Synthesis and Membrane Properties of Sulfonated Poly(arylene ether sulfone) Statistical Copolymers for Electrolysis of Water: Influence of Meta- and Para-Substituted Comonomers, ACS Appl. Mater. Interfaces. 9 (2017) 20067–20075.

[24] J.R. Rowlett, V. Lilavivat, A.T. Shaver, Y. Chen, A. Daryaei, H. Xu, C. Mittelsteadt, S. Shimpalee, J.S. Riffle, J.E. McGrath, Multiblock poly(arylene ether nitrile) disulfonated poly(arylene ether sulfone) copolymers for proton exchange membranes: Part 2 electrochemical and H_2/Air fuel cell analysis, Polymer. 122 (2017) 296–302.

[25] A.E. Allegrezza, B.S. Parekh, P.L. Parise, E.J. Swiniarski, J.L. White, Chlorine resistant polysulfone reverse osmosis modules, Desalination. 64 (1987) 285–304.

[26] J. Rose, Sulphonated polyaryletherketones and process for the manufacture thereof, EP0008895A1, 1978.

[27] J. Rose, Sulphonated polyaryletherketones, EP0041780A1, 1981.

[28] J. Rose, Sulphonated polyarylethersulphone copolymers, EP0008894B1, 1978.

[29] J.B. Rose, Sulphonated polyarylethersulphone copolymers, US4273903, 1978.

[30] J. Rose, Sulphonated polyaryletherketones, US4268650, 1979.

[31] R.J. Petersen, Composite reverse osmosis and nanofiltration membranes, J. Memb. Sci. 83 (1993) 81–150.

[32] B.J. Sundell, K. Lee, A. Nebipasagil, A. Shaver, J.R. Cook, E.-S. Jang, B.D. Freeman, J.E. McGrath, Cross-linking disulfonated poly(arylene ether sulfone) telechelic oligomers. 1. Synthesis, characterization, and membrane preparation, Ind. Eng. Chem. Res. 53 (2014) 2583–2593.

[33] A. Daryaei, E.S. Jang, S. Roy Choudhury, D. Kazerooni, J.J. Lesko, B.D. Freeman, J.S. Riffle, J.E. McGrath, Structure-property relationships of crosslinked disulfonated poly(arylene ether sulfone) membranes for desalination of water, Polymer. 132 (2017) 286–293.

[34] B.J. Sundell, E.-S.S. Jang, J.R. Cook, B.D. Freeman, J.S. Riffle, J.E. McGrath, Cross-Linked Disulfonated Poly(arylene ether sulfone) Telechelic Oligomers. 2. Elevated Transport Performance with Increasing Hydrophilicity, Ind. Eng. Chem. Res. 55 (2016) 1419–1426.

[35] A. Roy, M.A. Hickner, H.-S. Lee, T. Glass, M. Paul, A. Badami, J.S. Riffle, J.E. McGrath, States of water in proton exchange membranes: Part A - Influence of chemical structure and composition, Polymer. 111 (2017) 297–306.

[36] S. Maiti, B.K. Mandal, Aromatic polyethers by nucleophilic displacement polymerization, Prog. Polym. Sci. 12 (1986) 111–153.

[37] M.J. Jurek, J.E. McGrath, Synthesis and characterization of amine terminated poly(arylene ether sulphone) oligomers, Polymer. 30 (1989) 1552–1557.

[38] A. Nebipasagil, B.J. Sundell, O.R. Lane, S.J. Mecham, J.S. Riffle, J.E. McGrath, Synthesis and photocrosslinking of disulfonated poly(arylene ether sulfone) copolymers for potential reverse osmosis membrane materials, Polymer. 93 (2016) 14–22.

[39] J.C. Ronda, A. Serra, A. Mantecón, V. Cádiz, End-group analysis of poly(phenyl glycidyl

ether), 2. Hydroxylic groups using 19F nuclear magnetic resonance, Macromol. Chem. Phys. 195 (1994) 3459–3468.

[40] O. Lane, Synthesis, Characterization and modifications of Sulfonated Poly(arylene ether sulfone)s for Membrane Separations, PhD Thesis Virginia Polytechnic and State University, 2015.

[41] S. Podzimek, Light scattering, in: Light Scattering, Size Exclusion Chromatography and Asymmetric Field Flow Fractionation, John Wiley and Sons, 2010: pp. 37–98.

[42] S. Vyazovkin, Mechanism and Kinetics of Epoxy - Amine Cure Studied by Differential Scanning Calorimetry, Macromolecules. 29 (1996) 1867–1873.

[43] M. Sharifi, C.W. Jang, C.F. Abrams, G.R. Palmese, Toughened epoxy polymers via rearrangement of network topology, J. Mater. Chem. A. 2 (2014) 16071–16082.

[44] S. Han, W.G. Kim, H.G. Yoon, T.J. Moon, Kinetic study of the effect of catalysts on the curing of biphenyl epoxy resin, J. Appl. Polym. Sci. 68 (1998) 1125–1137.

[45] J.. Hedrick, I. Yilgor, M. Jurek, J.. Hedrick, G.. Wilkes, J.. McGrath, Chemical modification of matrix resin networks with engineering thermoplastics: 1. Synthesis, morphology, physical behaviour and toughening mechanisms of poly(arylene ether sulphone) modified epoxy networks, Polymer. 32 (1991) 2020–2032.

[46] B. Francis, S. Thomas, G.V. Asari, R. Ramaswamy, S. Jose, V.L. Rao, Synthesis of hydroxyl-terminated poly(ether ether ketone) with pendenttert-butyl groups and its use as a toughener for epoxy resins, J. Polym. Sci. Part B Polym. Phys. 44 (2006) 541–556.

[47] W. Xie, H. Ju, G.M. Geise, B.D. Freeman, J.I. Mardel, A.J. Hill, J.E. McGrath, Effect of free volume on water and salt transport properties in directly copolymerized disulfonated poly(arylene ether sulfone) random copolymers, Macromolecules. 44 (2011) 4428–4438.

[48] G.M. Geise, D.R. Paul, B.D. Freeman, Fundamental water and salt transport properties of polymeric materials, Prog. Polym. Sci. 39 (2014) 1–24.

Supplementary information

Synthesis and characterization of post-sulfonated poly(arylene ether sulfone) membranes for water desalination

Shreya Roy Choudhury,[a] Ozma Lane,[a] Dana Kazerooni,[a,b] Gurtej S. Narang,[a] Eui Soung Jang,[c] Benny D. Freeman,[c] John J. Lesko,[b] J. S. Riffle[a*]

[a]Macromolecules Innovation Institute, Virginia Tech, Blacksburg, VA 24061, United States.
[b]College of Engineering, Virginia Tech, Blacksburg, VA-24061, United States.
[c]Department of Chemical Engineering and the Center for Energy and Environmental Resources, University of Texas at Austin, Austin, TX 78758, United States.

Supplementary section 1: Determination of the estimated M_n of the oligomers before and after sulfonation by ^{1}H-NMR

- % HQ containing repeat units in the polymer backbone

$$= \frac{\frac{[(A+A_1)-(B+B_1+G)]}{4}}{\frac{[(A+A_1)-2(A+A_1)]}{8}+\frac{[(A+A_1)-(B+B_1+G)]}{4}} * 100 \qquad \text{(S-Equation-1)}$$

- Estimation of M_n by ^{1}H-NMR before sulfonation

$$= [\left(\frac{[(A+A_1)-(B+B_1+G)]}{4} \times 324.26\right) + \left(\frac{[(A+A_1)-2(A+A_1)]}{8} \times 464.43\right)] \times 2 \qquad \text{(S-Equation-2)}$$

- Estimation of M_n by ^{1}H-NMR after sulfonation

$$= \left[\left(\frac{[(A+A_1)-(B+B_1+G)]}{4} \times 405.42\right) + \left(\frac{[(A+A_1)-2(A+A_1)]}{8} \times 464.43\right)\right] \times 2 \qquad \text{(S-Equation-3)}$$

Sample calculation using integral from Fig 6a

% HQ containing repeat units: $\frac{4.88}{4.88+2.53} * 100 = 65.8\%$

Calculated M_n before sulfonation

$[(4.88 \times 324.26) + (2.53 \times 464.43)] \times 2 = 5513$ Da

Calculated M_n after sulfonation

$[[(4.88 \times 405.42) + (2.53 \times 464.43)] \times 2 = 6306$ Da

Membrane	Average IEC by ^{1}H NMR	Average Water Uptake %	Average fixed charge concentration (mol of ions per L of sorbed water)
50-SHQS-5k	0.90	14 ± 0.8	6.42
65-SHQS-5k	1.21	24 ± 2.5	5.05
80-SHQS-5k	1.51	37 ± 1.2	4.08
40-SHQS-10k	0.76	15 ± 0.9	5.06
50-SHQS-10k	0.95	18 ± 0.7	5.27
65-SHQS-10k	1.26	24 ± 0.5	5.25
40-SHQS	0.88	17 ±1.7	5.18
50-SHQS	1.14	25±1.7	4.60
60-SHQS	1.30	33±3.1	3.94

Table S1: Properties of hydroquinone based monosulfonated networks cured from 5000 and 10,000g/mol M_n oligomers and linear membranes cast from high M_n polymers

Chapter 3 : Structure-property relationships of post-sulfonated poly(arylene ether sulfone) membranes for water desalination

Shreya Roy Choudhury[a], Eui Soung Jang[b], Dana Kazerooni[a], Benny D. Freeman[b], J. S. Riffle[a]

[a]Macromolecules Innovation Institute, Virginia Tech, Blacksburg, VA 24061, United States.

[b]Department of Chemical Engineering and the Center for Energy and Environmental Resources, University of Texas at Austin, Austin, TX 78758, United States.

Abstract

Transport properties of the linear and crosslinked post sulfonated poly(arylene ether sulfone) membranes were studied to determine their suitability in reverse osmosis. The post sulfonated membranes had sulfonate ions on isolated rings of hydroquinone moiety and a kinked backbone as compared to previously studied sulfonated polysulfone membranes that were synthesized with pre-disulfonated monomer. This chapter focuses on the effect of polymer structure- placement of sulfonate ions and kinked backbone- on transport properties of the membranes. At similar values of water uptake, the post sulfonated membranes had higher water permeabilities and water/salt permeability selectivities than the previously studied membranes. These membranes also did not show an appreciable decrease in salt rejection with increase in water permeabilities. Most importantly, the post sulfonated membranes did not show a compromise in the rejection of monovalent ions in the presence of divalent ions in mixed feed water. The superior properties of the post-sulfonated membranes can potentially be attributed to the presence of a high number of kinked sulfone groups in the backbone structure that probably increased the free volume in the membranes, and the sulfonated ions were spaced apart to potentially reduce chelation of calcium by the sulfonate ions.

3.1 Introduction

Desalination of water has emerged as the key to tackle the global water crisis. Sea water reverse osmosis is the major method for desalination. However, desalinating brackish groundwater that comprises around 55% of the groundwater is also important [1]. Brackish water is low salinity water with ~1000-10,000 mg/L of total dissolved solids [2]. Apart from reverse osmosis (RO), electrodialysis (ED) is another commonly used technique to produce potable water from brackish water [3].

RO processes apply pressure greater than and opposite to the osmotic pressure on the upstream feed water (brine) side of the membrane to force water downstream through the membrane, while the salts are rejected on the upstream side of the membrane [4–7]. Composite membranes can have advantages over single material asymmetric membranes because the top barrier layer and the bottom porous substrate can be independently modified to optimize the membrane permeability and selectivity with excellent mechanical strength [7–11]. The current state-of-the-art aromatic polyamide thin-film composite (PA-TFC) RO membranes are made by interfacial polymerization of an aromatic amine such as *m*-phenylene diamine, with one or more aromatic acyl halides such as trimesoyl chloride [8,13–15]. These membranes have the right combination of flux and salt rejection, but fouling and poor chlorine resistance limit their lifetime and performance properties [16]. The amide linkages are susceptible to oxidative degradation by chlorine-based disinfectants that are used to prevent biofouling in water purification systems. Consequently, de-chlorination and re-chlorination steps are necessary to prolong membrane performance. Additionally, PA-TFCs have a rough surface which makes them more susceptible to biofouling [17,18]. Sulfonated polysulfone membranes are promising candidates for water desalination because of their chlorine resistance compared to PA-TFCs, as a result of the absence

of amide linkages in the polymer backbone [19,20]. Sulfonated polysulfone membranes also have smoother surfaces than PA-TFCs, thus reducing susceptibility to biofouling [18].

Part 1 of this paper describes the synthesis and characterization of poly(arylene ether sulfone) membranes synthesized by post-polymerization. They contain hydroquinone moieties that are the locus of sulfonation. These membranes have sulfonate groups only on isolated rings of the polymer backbone as opposed to having at least some sulfonate groups on adjacent rings. Early work on post-sulfonated polysulfones for water desalination included microstructures without precise control of the sulfonate placement. Later, McGrath et al. introduced a pre-disulfonated monomer, 3,3'-disulfonated-4,4'-dichlorodiphenyl sulfone, to prepare sulfonated polysulfone membranes with the sulfonate ions precisely in pairs on adjacent rings, with the pairs randomly distributed along the polymer backbone [16,21].

One way of determining the influence of polymer chemistry and structure on the transport properties is to study their impact on parameters including water/salt permeability and the diffusivity trade-off relationship. The recently established water/salt permeability selectivity trade-off relationship serves as a benchmark to compare the membranes for desalination applications [22]. At a given applied pressure, as the IEC of the sulfonated polysulfone membranes is increased, the water permeability increases, since increasing the IEC of a membrane is generally accompanied by an increase in membrane water content. However, increases in membrane water content typically reduces salt rejection, mainly due to weakening of Donnan exclusion [23].

ED requires ion exchange membranes that allow counter ions to pass through while rejecting the co-ions. Ion transport through such membranes is strongly influenced by interactions of the fixed charge groups and the mobile ions (i.e. Donnan exclusion). Hence, one way to characterize ion exchange membranes is in terms of their fixed charge concentration (moles of ions per liter of

absorbed water) [24,25]. ED membranes require high fixed charge concentrations to repel co-ions. However, with an increase in fixed charge concentration, there is an increase in water uptake, leading to poorly hydrated mechanical properties. Thus, the membranes are crosslinked to obtain better mechanical integrity. One current class of cation exchange membranes are crosslinked sulfonated styrene-divinylbenzene systems that are extremely brittle [26,27]. To counteract this problem, a thick layer of resin is crosslinked on a support layer. Due to the increased thickness of the membranes, they offer higher resistance to the current path, and the efficiency of the process is reduced. Hence, our goal is to develop membranes for ED with high fixed charge concentration, optimum water uptake and good mechanical properties in hydrated conditions, with primary focus on cation exchange membranes.

For RO applications, in addition to high permeate flux, high salt rejection, and good chemical and fouling resistance, membranes also require good mechanical stability and durability. Mechanical properties are important because the membrane should be able to withstand the high transmembrane pressure required in the RO process. Hydrated mechanical properties of sulfonated polysulfone membranes have been reported for applications in ED, RO [26] and electrolysis [28]. However, overall very few papers have reported the mechanical properties of the membranes under immersion conditions.

In the 1970-1980s, salt and water transport properties of post-sulfonated polysulfone membranes synthesized from bisphenol A and 4,4’-dichlorodiphenylsulfone were studied [19,29,30] The degree of sulfonation and the placement of sulfonate groups along the chains were not controllable with this method of synthesis. Also, the salt rejection values were approximately 95%, significantly lower than current polyamide TFC membranes. In the 2000s McGrath and Freeman et al. introduced a pre-sulfonated monomer, 3,3’-disulfonated-4,4’-

dichlorodiphenylsulfone [31] that was directly polymerized to produce copolymers with controlled levels of sulfonation and microstructures that contained the sulfonate groups in sets of two on adjacent rings [16,32–35]. Rose et al. disclosed post-sulfonated linear polysulfones containing hydroquinone moieties wherein only the hydroquinone rings were sulfonated because all of the other rings were deactivated against the electrophilic aromatic sulfonation reaction [36–41]. The advantage of this method was that the degree of sulfonation could be controlled without the need to synthesize a pre-sulfonated monomer. This paper describes the transport and hydrated mechanical properties of post-sulfonated polysulfone linear and crosslinked membranes with a series of controlled degrees of sulfonation. The crosslinked membranes were synthesized from a series of controlled molecular weight, amine terminated oligomers with M_n ~5000 and 10,000 g/mol by reaction of the amine end groups with a tetraepoxide. Part I of this series describes the synthesis and characterization of the oligomers and the high molecular weight linear polymers.

3.2 Experimental

Film casting and characterization

Epoxy-amine crosslinking of the oligomers

The crosslinked films were prepared by adding the oligomer and TGBAM in the molar ratio of 1:2.5 respectively. Triphenylphosphine (TPP) was used in a 3.0 % by weight ratio relative to the weight of TGBAM. The following steps were completed to prepare a crosslinked film containing 50-SHQS-10k. A mixture of 50-SHQS-10k (0.046 mmol, 0.63 g), TGBAM (0.114 mmol, 0.048 g) and TPP (1.44 mg) were dissolved in 8 mL of DMAc in a vial, and stirred until a homogeneous solution was obtained. The solution was syringe-filtered through a 0.45 μm PTFE filter into a new vial. The original vial was washed with 7 mL of DMAc and filtered into the new vial to transfer

any residual oligomers. The solution was sonicated for 15 min and was cast on a circular Teflon mold with flat edges and a diameter 10 cm. The mold was placed on a level surface in an oven at 70 °C. The temperature of the oven was ramped up from 70 to 175 °C gradually over 6 h and the film was cured at a steady temperature of 175 °C for 12 h. The temperature of the oven was gradually ramped down to 120 °C and the film was dried under vacuum for 12 h. The oven was turned off and the film was allowed to cool in the oven to room temperature. The epoxy-cured network was detached from the Teflon mold by immersion in deionized water. The thickness of the film was approximately 70 μm.

Film casting of the high molecular weight linear polymers

A copolymer (1.2 g) was dissolved in 10 mL of DMAc in a glass vial. The solution was filtered through a 0.45 μm PTFE filter and the vial was washed with 2 mL of DMAc to form a 10 wt/v% polymer solution. The solution was sonicated for 10 min and cast on a level 4" x 4" clean glass plate. The plate was cleaned in a base bath, washed and dried prior to film casting. The films were heated under an IR lamp with a starting temperature of ~45 °C. The temperature of the IR lamp was ramped up by 20 °C every 2 h until the temperature reached ~75 °C. The plate with the film was kept at that temperature for 8-10 h. The film was then dried under vacuum at 110 °C for 24 h. The film was delaminated from the glass plate by immersion in deionized water. The film, in the acidic form, was stirred in 0.1 N aqueous NaCl for 3 days to convert it into the salt form. The thickness of the film was ~100 μm.

Gel fraction measurements on the crosslinked films

Crosslinked films were dried at 120 °C under vacuum overnight. After drying, 0.1−0.2 g of the sample was placed in a 20-mL scintillation vial filled with DMAc and stirred at 100 °C for ~12

h. The remaining solid was filtered, transferred to a weighed vial, dried to a constant weight at 160 °C under vacuum for ~12 h, and then weighed. Three measurements were taken for each film and gel fractions were calculated by equation 1.

$$Gel\ Fraction\ (\%) = \frac{Final\ mass\ of\ extracted\ film}{initial\ mass\ of\ dried\ film} \times 100 \qquad \text{(Equation 1)}$$

Water uptake

The water uptakes of the crosslinked and high molecular weight linear membranes were determined gravimetrically. The membranes in their sodium salt form were dried at 120 °C under vacuum for 24 h and weighed. The membranes were soaked in water at room temperature for 24 h. Wet membranes were removed from the water, blotted dry to remove surface droplets, and quickly weighed. The water uptake of the membranes was calculated according to equation 2, where $mass_{dry}$ and $mass_{wet}$ refer to the masses of the dry and the wet membranes, respectively.

$$\text{Water Uptake}\ (\%) = \frac{Mass_{wet} - Mass_{dry}}{Mass_{dry}} \times 100 \qquad \text{(Equation 2)}$$

Salt permeability measurements made with a direct permeation cell

Salt permeability was measured using direct permeation cells (Side-bi-Side Cells, PermeGear, Hellertown, PA, USA). A polymer film was clamped between two cells equipped with a water jacket of circulating water from an isothermal bath to maintain constant temperature at 25 °C. The driving force for salt transport through the polymer membrane in this experiment is the concentration difference between donor and receiver cells. Thus, the donor cell was filled with 0.1 M aqueous NaCl solution and the receiver cell was filled with DI water. The increase in salt concentration in the receiver cell was monitored and recorded with a conductivity meter (WTW LR 325/01 conductivity probe, Weilheim, Germany) as a function of time. A calibration curve for NaCl

was established before the salt permeability measurements and used for converting conductivity to salt concentration. The steady-state salt permeability, P_s, was calculated using equation (3)

$$\ln\left[1 - \frac{2C_{sl}^{s}[t]}{C_{s0}^{s}[0]}\right] = -\left(\frac{2AP_s}{VL}\right)t \quad (3)$$

where $C_{sl}^{s}[t]$ is the receptor salt concentration at time t, $C_{s0}^{s}[0]$ is the initial donor concentration of salt (0.1 M NaCl in this study), V is the donor or receptor volume (35 mL), A is the effective film area (1.77 cm^2), and L is the membrane thickness.

Salt permeability tests conducted in a cross flow filtration cell

Water purification properties of the dense cross-linked oligomers were determined at 25 °C in a previously described cross-flow filtration system using stainless steel cross-flow cells machined at the University of Texas at Austin [42,43]. Permeate solutions were collected and analyzed for their mass and conductivity, which were measured to calculate water permeability (L μmm^{-2} h^{-1} bar^{-1} or cm^2 s^{-1}), salt permeability (cm^2 s^{-1}), salt rejection (%), and water/NaCl selectivity. The pressure difference across the membrane was 400 psi (27.6 bar). The aqueous feed contained 2000 ppm NaCl, and the feed solution was circulated past the samples at a continuous flow rate of 3.8 L min^{-1}. The feed pH was adjusted to 6.5−7.5 using a 10 g L^{-1} sodium bicarbonate solution. NaCl concentrations in the feedwater and permeate were measured as conductivities with an Oakton 100 digital conductivity meter.

3.3 Results and Discussion

Transport properties of the membranes

Transport properties of the crosslinked membranes by direct permeation

Ion transport property in polymer membranes is typically quantified by the salt permeability coefficients. This section describes the salt permeability coefficients of the crosslinked membranes and they are compared with that of commercial membranes from GE Power & Water measured under similar conditions. The salt permeability coefficients were measured by direct permeation cells and the upstream NaCl concentration was fixed at 0.1 M. The following structures were studied

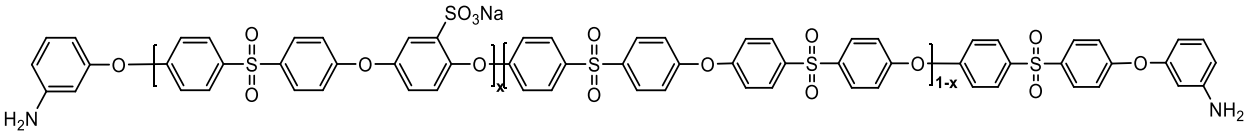

I - Amine terminated SHQS oligomers of 5000 g/mol and 10,000 g/mol that were epoxy cured to form crosslinked SHQS membranes

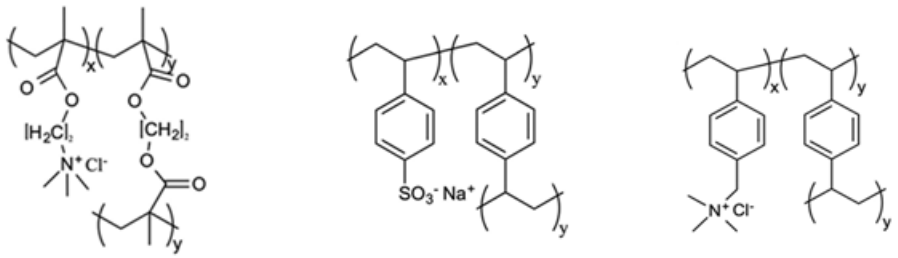

II- Commercial membranes by GE power and water

Figure 3.1 represents the salt permeability, $<P_s>$, of the crosslinked SHQS membranes as a function of water uptake where 50, 65 and 80 represent the degree of monosulfonation of the membranes with target molecular weight 5000 and 10,000 g/mol. The salt permeabilities of the crosslinked SHQS membranes decreased with decrease in the water uptake. Moreover, crosslinked membranes of disulfonated polysulfone and commercial membranes, including polystyrene-divinylbenzene and acrylic structures synthesized by free radical polymerization , show a similar trend [26]. This observation indicates that water uptake influences salt permeability of these crosslinked ion exchange membranes significantly regardless of their chemistry or block length of

the copolymer [46]. The membranes considered in this study are dense, nonporous, and ion transport in these materials can be described by the solution-diffusion model. According to this model, salt permeability coefficients are related to mobile salt sorption (i.e., partition) coefficients and mobile salt diffusion coefficient [44]. Salt diffusion occurs in free volume taken by sorbed water in hydrated polymer [34,35]. Thus, membrane water content (i.e. mass or volume fraction of water in a hydrated membrane) is correlated with salt diffusion and, in turn, salt permeability coefficients, as observed in this study.

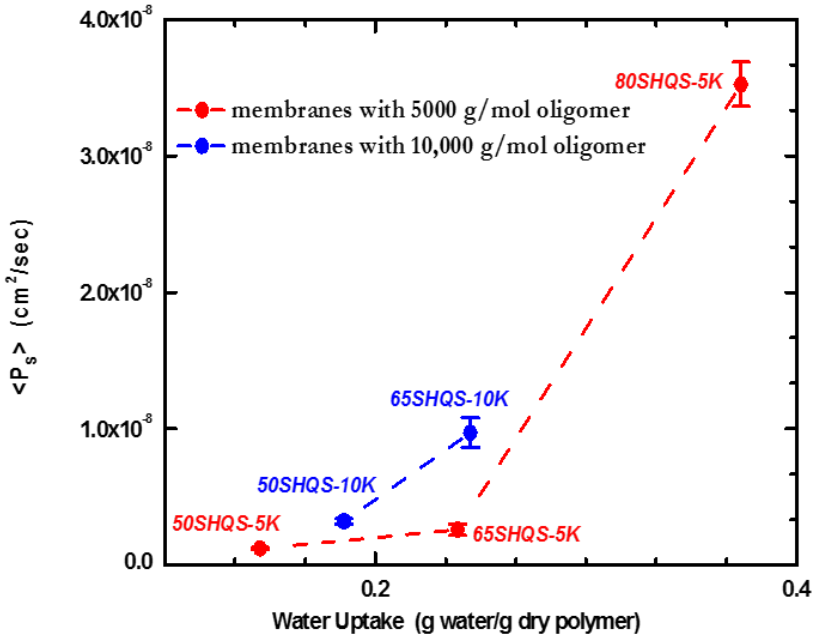

Figure 3.1 The salt permeability increases with an increase in water uptake for crosslinked SHQS-5k and 10k membranes

Salt permeability coefficients depend strongly on mobile salt sorption in ion exchange membranes. The extent to which mobile ions can be excluded from the charged membranes depends on the strength of the Donnan potential [24]. Increasing the membrane fixed charge concentration increases the Donnan potential in the membrane, thus resulting in decrease in salt permeability

coefficients. To illustrate this point, salt permeability is presented as function of fixed charge concentration in Figure 3.2 [45]. As shown in Figure 3.2, the salt permeability decreased with an increase in the fixed charge concentration in the membranes. High co-ion exclusion increases the membrane selectivity in electrodialysis and decreases salt permeability in reverse osmosis [46]. The extent to which co-ions can be excluded from the charged membranes depends on the strength of the Donnan potential [24]. Increasing the membrane fixed charge concentration increases the counter ions in the membrane, thus resulting in an effective increase in the Donnan potential as seen in the figure below. The membranes with 50-60% degree of mono sulfonation are ideal for applications in water desalination.

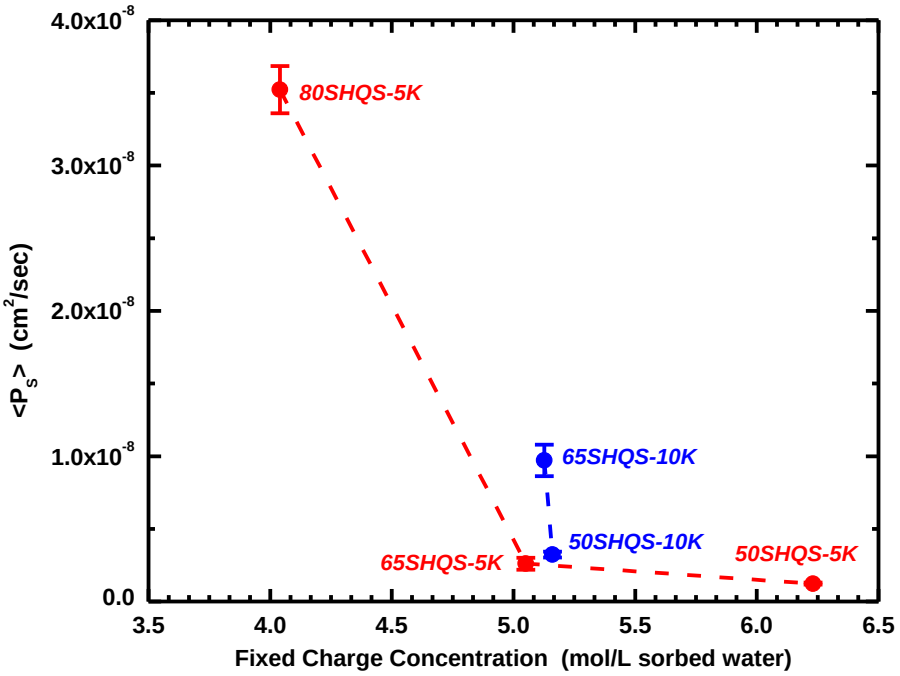

Figure 3.2: The salt permeability increases with a decrease in fixed charge concentration for crosslinked SHQS 5k and SHQS 10k membranes

It is necessary to know the benchmark for the commercial membranes to understand the potential of the SHQS membranes for application in electrodialysis. The transport properties of the

crosslinked membranes can be compared to the commercially available GE electrodialysis membranes as shown in Figure 3.3. as both sets of the samples were analyzed by a direct permeation cell.

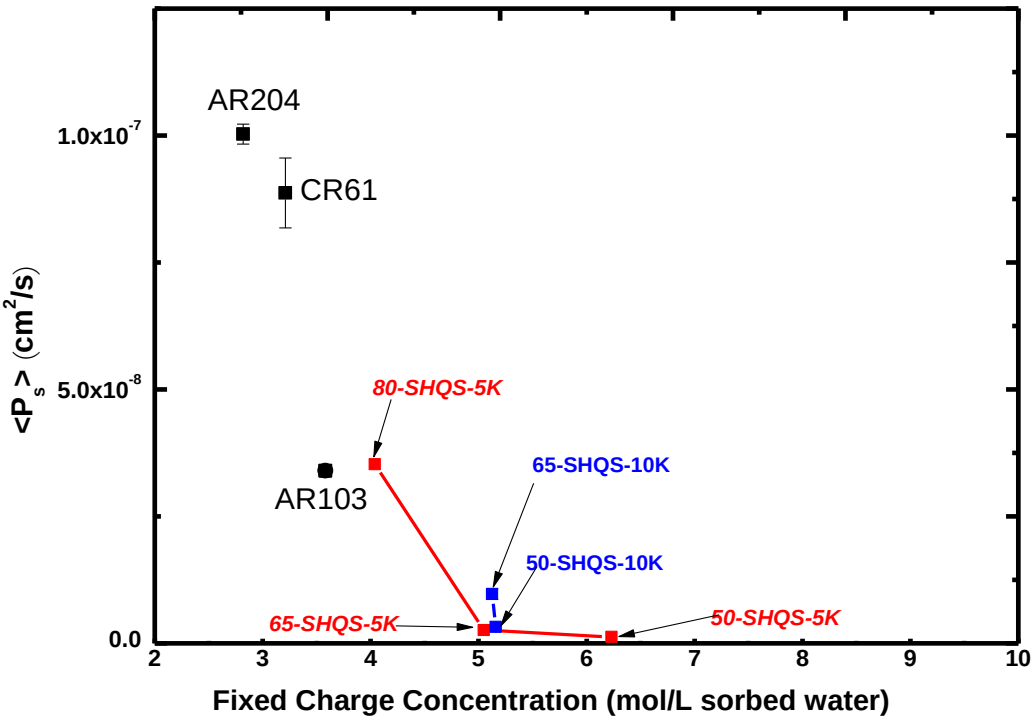

Figure 3.3: The salt permeability increases with a decrease in fixed charge concentration for commercial electrodialysis membranes

CR61 is a styrenic cation exchange membrane, AR103 is a styrenic anion exchange membrane, and AR204 is an acrylic anion exchange membrane as shown in Figure 3.3 [45]. The trend of decreasing salt permeability with an increase in fixed charge concentration was also followed by the commercial membranes.

All SHQS linear membranes (Structure I) and, 40-SHQS-10k and 50-SHQS-10k crosslinked membranes were analyzed by cross flow filtration with 2000 ppm NaCl at a pressure of 400 psi and pH 7. In this section the transport properties of the SHQS membranes were compared

to the BPS membranes (Structure II). Table 1 tabulates the various transport properties of the SHQS membranes including salt rejection and hydraulic water permeability. The table also lists the transport properties of BPS membranes that were synthesized by pre-disulfonated monomers.

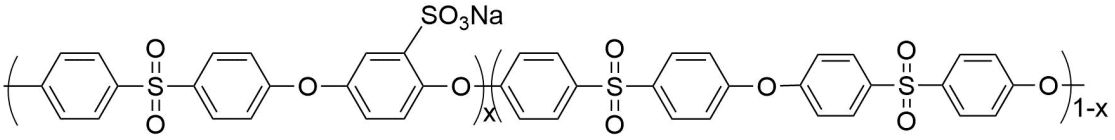

Structure I- monosulfonated SHQS membranes synthesized by post polymerization sulfonation

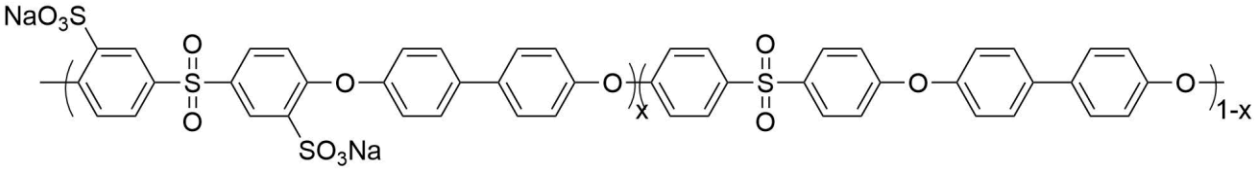

Structure II- disulfonated BPS membranes synthesized by pre-sulfonated monomer

Membranes	IEC	Water uptake (weight fraction)	Salt rejection (%)	Hydraulic water permeability (L μm/(m^2 h bar))
40-SHQS	0.88	0.17	97.97 ± 0.49	0.18
50-SHQS	1.14	0.25	97.85 ± 0.30	0.42
60-SHQS	1.30	0.33	97.05 ± 0.69	0.84
50-SHQS-10k	0.95	0.18	98.20 ± 0.25	0.30
40-SHQS-10k	0.76	0.15	96.7	0.19
BPS 20	0.92	0.19	99.2	0.04
BPS 30	1.34	0.33	96.2	0.22
BPS 35	1.48	0.40	94.3	0.39
BPS 40	1.66	0.55	92.5	0.65

Table 3.1: Water desalination properties of the linear SHQS membranes measured by cross flow filtration, and the BPS membranes synthesized from the disulfonated monomer obtained from the literature [21].

Water transport

Generally, equilibrium water content exhibits a strong influence on water permeability. Figure 3.4 represents the hydraulic water permeabilities of the SHQS membranes as a function of water uptake and compares them with the BPS membranes synthesized from the disulfonated monomer. The numbers adjacent to the data points represent IEC values of the membranes. The SHQS membranes showed an increase in hydraulic water permeabilities with increase in water uptake. This observation is consistent with the results in other membranes.

The backbone of the SHQS membranes are chemically different from the BPS membranes. The SHQS membranes have more sulfone units and ether linkages than the BPS membranes. The sulfone groups are kinked and rigid and more of those will open the structure. The ether linkages would increase the flexibility of the SHQS membranes. Thus, these factors will potentially increase the free volume in the membranes, thereby increasing the water permeability.

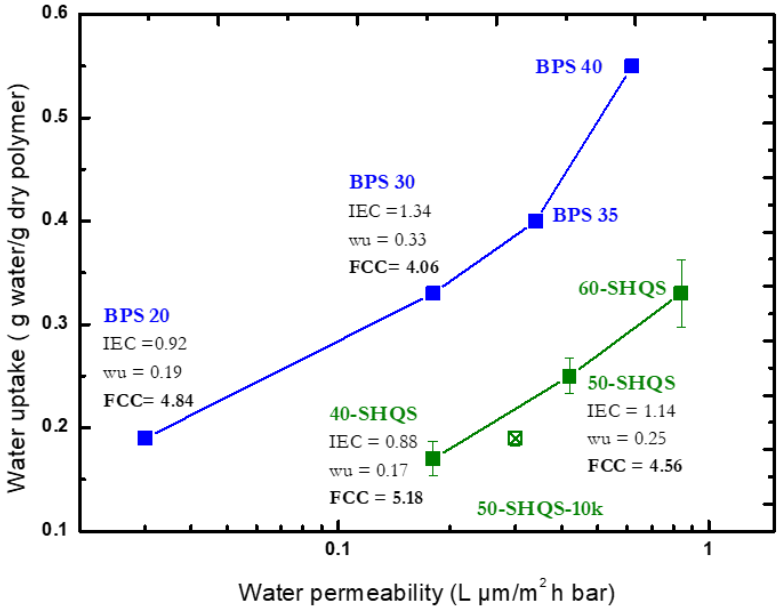

Figure 3.4: Hydraulic water permeabilities and water uptake of the SHQS and BPS membranes

Salt transport

As shown in Figure 3.5. the linear SHQS series showed no compromise in salt rejection with increase in water permeability. The salt rejection was high, ~97-98%, despite an increase in the water permeabilities. For example, the 40-SHQS had a salt rejection of ~98% at an IEC of 0.88 and hydraulic water permeability of 0.18 L μm/(m^2 h bar) and the 60-SHQS had a salt rejection of ~97% at an IEC of 1.33 with hydraulic water permeability of 0.84 L μm/(m^2 h bar). We can hypothesize that increasing the polarity of the backbone increased the water permeability in the SHQS membranes without increasing the IEC. This led to high water permeability and high salt rejection at low IECs.

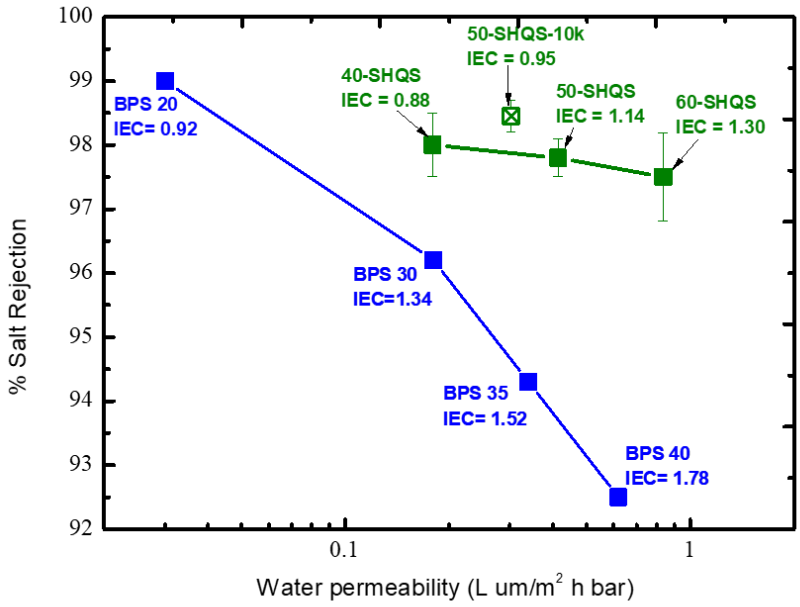

Figure 3.5: Salt rejection of SHQS membranes compared to the linear and crosslinked BPS membranes.

In the linear BPS series, the salt rejection was compromised with an increase in water permeability as shown in Figure 3.5. However, the linear SHQS membranes showed a high salt rejection even at high water permeabilities. The crosslinked 50-SHQS-10k sample also showed a similar trend as the linear series.

At similar values of water permeabilities the SHQS membranes had a higher salt rejection because the SHQS membrane had a higher fixed charge concentration at that water permeability. For example 50-SHQS showed water permeability of 0.42 L μm/(m^2 h bar) and BPS 35 had a comparable water permeability of 0.39 L μm/(m^2 h bar) but 50-SHQS had a salt rejection of 97.85% with a fixed charge concentration of 4.56 meq/mL and the BPS 35 had a salt rejection of 94.3% with a fixed charge concentration of 3.70 meq/mL. Since the SHQS membranes had higher water permeabilities than the BPS membranes at comparable water uptakes, it is hypothesized that the water may be more uniformly distributed throughout the SHQS membranes with the more polar backbone.

Water /Salt Permeability Selectivity

Membranes	IEC	Water uptake (weight fraction)	Fixed charge concentration	Diffusive Water permeability (10^{-7} cm^2/s)	Salt permeability (10^{-10} cm^2/s)	permeability selectivity (P_w/P_s) × 10^3
40-SHQS	0.88	0.17	5.2	6.84	2.92	2.34
50-SHQS	1.14	0.25	4.6	15.9	6.58	2.42
60-SHQS	1.30	0.33	3.9	24.9	12.5	1.99

Table 3.2: Water desalination properties of the linear SHQS membranes measured by cross flow filtration

Table 3.2 shows the diffusive water permeability, salt permeability and selectivity of the membranes. Salt rejection, permeance and water flux depend on the operating conditions including thickness, feed pressure and salt concentration. On the other hand, selectivity and diffusive water permeability are intrinsic membrane properties. Selectivity is the ratio of diffusive water

permeability and salt permeability constants. The permeability and selectivity trade-off in water desalination membranes suggests the existence of upper-bound relations similar to gas separation membranes [22]. The upper bound is an empirically formulated line representing the best transport results obtainable for a given combination of selectivity and water permeability as represented in Figure 3.6. The membranes with the best desalination properties are the ones on or close to the upper-bound line on the plot.

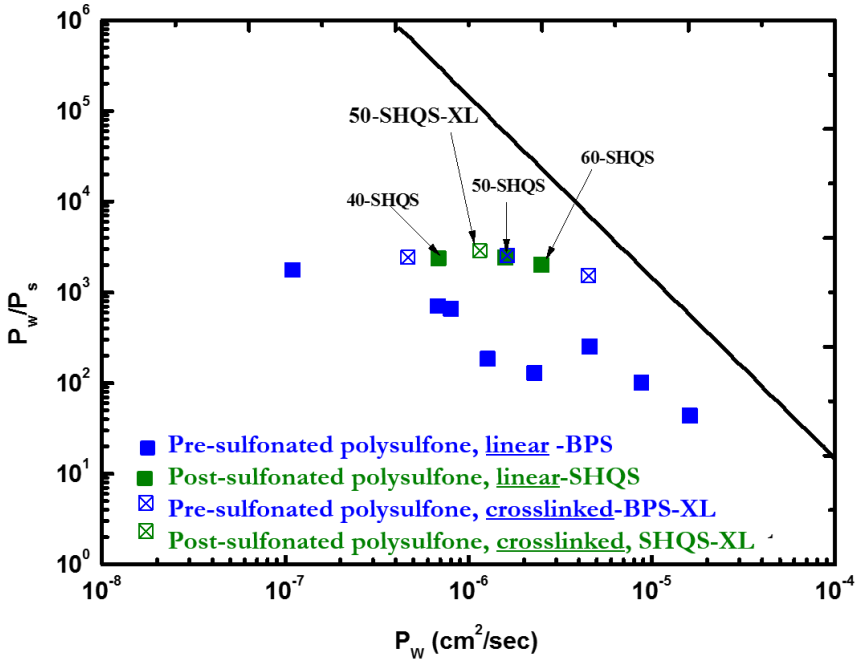

Figure 3.6 : Fundamental transport properties of water/NaCl permeability selectivity, P_w/P_s, and permeability coefficients, P_w: comparison between linear SHQS.

As seen in Figure 3.6 the BPS membranes prominently depict the trade-off in the water/salt permeability selectivity and the water permeability. They are scattered all over the plot with a vast difference in selectivity with changing water permeabilities. On the other hand, the SHQS membranes show higher selectivity with nearly constant values as water permeabilities increase. It is also observed that the performance of the SHQS membranes was identical to the crosslinked BPS

membranes but at lower IECs. This trait may be due to the linear SHQS membranes having lower water uptakes than the BPS membranes [32].

Calcium ion rejection

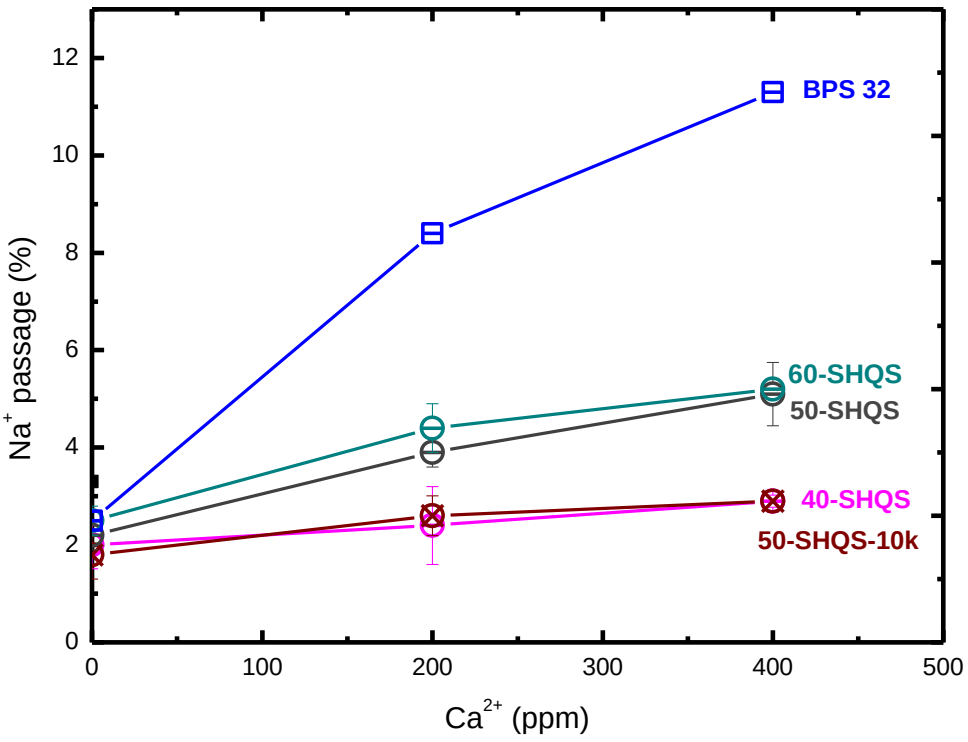

Figure 3.7: Rejection of salts by SHQS membranes and the BPS-32 membrane in mixed feed water containing both Na^+ and Ca^{2+} ions

The mixed feed data for the linear SHQS membranes and the crosslinked 50-SHQS-10k membrane showed constant salt rejections with up to 400 ppm of calcium ions (Figure 3.7). On the other hand, the BPS-32 membrane showed a compromised rejection of monovalent ions in the presence of calcium ions. In the BPS membranes the sulfonate ions are present on the adjacent rings of the bisphenol moieties whereas in the SHQS membranes the sulfonate ions are present on the isolated rings of the hydroquinone moieties. It might be possible that the sulfonate ions on the

adjacent rings in the BPS membranes can chelate Ca^{2+} ions. This would likely not be possible in the SHQS membranes because the sulfonate ions are too far apart in the backbone.

3.4 Conclusion

The work herein reports the transport properties of the post-sulfonated polysulfone membranes with sulfonate ions placed strategically apart on the polymer backbone. The membranes showed no compromise in the rejection of monovalent ions in the presence of divalent ions. The polymer backbones are also likely more flexible due to more ether linkages in the backbone, but yet more open due to the kinked but rigid sulfone structure in the backbones as compared to the previously studied membranes. These structural differences may have led to increased water permeabilities and salt rejection with better water/salt selectivities.

References

[1] J.R. Werber, A. Deshmukh, M. Elimelech, The Critical Need for Increased Selectivity, Not Increased Water Permeability, for Desalination Membranes, Environ. Sci. Technol. Lett. 3 (2016) 112-120

[2] L.F. Greenlee, D.F. Lawler, B.D. Freeman, B. Marrot, P. Moulin, Reverse osmosis desalination: Water sources, technology, and today's challenges, Water Res. 43 (2009) 2317–2348.

[3] H. Strathmann, Electrodialysis, a mature technology with a multitude of new applications, Desalination. 264 (2010) 268–288.

[4] K.P. Lee, T.C. Arnot, D. Mattia, A review of reverse osmosis membrane materials for desalination—Development to date and future potential, J. Memb. Sci. 370 (2011) 1–22.

[5] C. Fritzmann, J. Löwenberg, T. Wintgens, T. Melin, State-of-the-art of reverse osmosis desalination, Desalination. 216 (2007) 1–76.

[6] A. Pérez-González, A.M. Urtiaga, R. Ibáñez, I. Ortiz, State of the art and review on the treatment technologies of water reverse osmosis concentrates, Water Res. 46 (2012) 267–283. doi:10.1016/J.WATRES.2011.10.046.

[7] H.J. Kim, K. Choi, Y. Baek, D.-G. Kim, J. Shim, J. Yoon, J.-C. Lee, High-Performance Reverse Osmosis CNT/Polyamide Nanocomposite Membrane by Controlled Interfacial Interactions, ACS Appl. Mater. Interfaces. 6 (2014) 2819–2829.

[8] J.E. Cadotte, R.J. Petersen, R.E. Larson, E.E. Erickson, A new thin-film composite seawater reverse osmosis membrane, Desalination. 32 (1980) 25–31.

[9] R.J. Petersen, Composite reverse osmosis and nanofiltration membranes, J. Memb. Sci. 83 (1993) 81–150.

[10] A. Prakash Rao, N.V. Desai, R. Rangarajan, Interfacially synthesized thin film composite RO membranes for seawater desalination, J. Memb. Sci. 124 (1997) 263–272.

[11] M. Kurihara, Y. Fusaoka, T. Sasaki, R. Bairinji, T. Uemura, Development of crosslinked fully aromatic polyamide ultra-thin composite membranes for seawater desalination, Desalination. 96 (1994) 133–143

[12] W.G. Light, J.L. Perlman, A.B. Riedinger, D.F. Needham, Desalination of non-chlorinated surface seawater using TFCR membrane elements, Desalination. 70 (1988) 47–64.

[13] Y. Song, P. Sun, L.L. Henry, B. Sun, Mechanisms of structure and performance controlled thin film composite membrane formation via interfacial polymerization process, J. Memb. Sci. 251 (2005) 67–79.

[14] G.-Y.Y. Chai, W.B. Krantz, Formation and characterization of polyamide membranes via interfacial polymerization, J. Memb. Sci. 93 (1994) 175–192.

[15] W. Xie, G.M. Geise, B.D. Freeman, H.-S. Lee, G. Byun, J.E. McGrath, Polyamide interfacial composite membranes prepared from m-phenylene diamine, trimesoyl chloride and a new disulfonated diamine, J. Memb. Sci. 403–404 (2012) 152–161.

[16] B.D. McGrath, J. E.; Park, H. B.; Freeman, J. McGrath, Chlorine resistant desalination membranes based on directly sulfonated poly(Arylene Ether Sulfone) copolymers, in: 2011.

[17] A. Nebipasagil, B.J. Sundell, O.R. Lane, S.J. Mecham, J.S. Riffle, J.E. McGrath, Synthesis and photocrosslinking of disulfonated poly(arylene ether sulfone) copolymers for potential reverse osmosis membrane materials, Polymer. 93 (2016) 14–22.

[18] C.H. Lee, B.D. McCloskey, J. Cook, O. Lane, W. Xie, B.D. Freeman, Y.M. Lee, J.E. McGrath, Disulfonated poly(arylene ether sulfone) random copolymer thin film composite membrane fabricated using a benign solvent for reverse osmosis applications, J. Memb. Sci. 389 (2012) 363–371.

[19] A.E. Allegrezza, B.S. Parekh, P.L. Parise, E.J. Swiniarski, J.L. White, Chlorine resistant polysulfone reverse osmosis modules, Desalination. 64 (1987) 285–304.

[20] A. Noshay, L.M. Robeson, Sulfonated polysulfone, J. Appl. Polym. Sci. 20 (1976) 1885–1903.

[21] W. Xie, J. Cook, H.B. Park, B.D. Freeman, C.H. Lee, J.E. McGrath, Fundamental salt and water transport properties in directly copolymerized disulfonated poly(arylene ether sulfone) random copolymers, Polymer. 52 (2011) 2032–2043.

[22] G.M. Geise, H.B. Park, A.C. Sagle, B.D. Freeman, J.E. Mcgrath, Water permeability and water/salt selectivity tradeoff in polymers for desalination, J. Memb. Sci. 369 (2010) 130–138.

[23] Helferrich Friedrich, Ion Exchange, General Publishing Company, 1962.

[24] J. Kamcev, B.D. Freeman, Charged Polymer Membranes for Environmental/Energy Applications, Annu. Rev. Chem. Biomol. Eng. 7 (2016) 111–133.

[25] J. Kamcev, D.R. Paul, B.D. Freeman, M. Elimelech, C. Gavach, M.G. Mclin, J.J. Fontanella, Effect of fixed charge group concentration on equilibrium ion sorption in ion exchange membranes, J. Mater. Chem. A. 5 (2017) 4638–4650.

[26] A. Daryaei, E.S. Jang, S. Roy Choudhury, D. Kazerooni, J.J. Lesko, B.D. Freeman, J.S. Riffle, J.E. McGrath, Structure-property relationships of crosslinked disulfonated poly(arylene ether sulfone) membranes for desalination of water, Polymer. 132 (2017) 286–293.

[27] J. Kamcev, D.R. Paul, B.D. Freeman, Ion Activity Coefficients in Ion Exchange Polymers: Applicability of Manning's Counterion Condensation Theory, Macromolecules. 48 (2015) 8011–8024.

[28] A. Daryaei, G.C. Miller, J. Willey, S. Roy Choudhury, B. Vondrasek, D. Kazerooni, M.R. Burtner, C. Mittelsteadt, J.J. Lesko, J.S. Riffle, J.E. McGrath, Synthesis and Membrane Properties of Sulfonated Poly(arylene ether sulfone) Statistical Copolymers for Electrolysis of Water: Influence of Meta- and Para-Substituted Comonomers, ACS Appl. Mater. Interfaces. 9 (2017) 20067–20075.

[29] C. Brousse, R. Chapurlat, J.P. Quentin, New membranes for reverse osmosis I. Characteristics of the base polymer: sulphonated polysulphones, Desalination. 18 (1976) 137–153.

[30] J. Quentin, Sulfonated polyarylethersulfones, US3709841A, 1970.

[31] W.L. Harrison, F. Wang, J.B. Mecham, V.A. Bhanu, M. Hill, Y.S. Kim, J.E. McGrath, Influence of the bisphenol structure on the direct synthesis of sulfonated poly(arylene ether) copolymers. I, J. Polym. Sci. Part A Polym. Chem. 41 (2003) 2264–2276.

[32] G.M. Geise, D.R. Paul, B.D. Freeman, Fundamental water and salt transport properties of polymeric materials, Prog. Polym. Sci. 39 (2014) 1–24.

[33] G.M. Geise, H.-S. Lee, D.J. Miller, B.D. Freeman, J.E. McGrath, D.R. Paul, Water purification by membranes: The role of polymer science, J. Polym. Sci. Part B Polym. Phys. 48 (2010) 1685–1718.

[34] H.B. Park, B.D. Freeman, Z.-B. Zhang, M. Sankir, J.E. McGrath, Highly Chlorine-Tolerant Polymers for Desalination, Angew. Chemie. 120 (2008) 6108–6113.

[35] B.D. McGrath, J. E.; Park, H. B.; Freeman, J. McGrath, H.B. Park, B.D. Freeman, Chlorine resistant desalination membranes based on directly sulfonated poly(Arylene Ether Sulfone) copolymers, US 8,028,842 B2, 2007.

[36] J. Rose, Sulphonated polyaryletherketones and process for the manufacture thereof, EP0008895A1, 1978.

[37] J. Rose, Sulphonated polyaryletherketones, EP0041780A1, 1981.

[38] J.B. Rose, Sulphonated polyarylethersulphone copolymers, US4273903, 1978.

[39] A. Bunn, Rose John B, Sulphonation of poly(phenylene ether sulphone)s containing hydroquinone residues, Polymer. 34 (1993) 1992–1994.

[40] A. Al-Omran, J.B. Rose, Synthesis and sulfonation of poly(phenylene ether ether sulfone)s containing methylated hydroquinone residues, Polymer. 37 (1996) 1735–1743.

[41] J.B. Rose, Sulphonated polyarylethersulphone copolymers and process for the manufacture thereof, EP0008894A1, 1983.

[42] B.J. Sundell, E.-S.S. Jang, J.R. Cook, B.D. Freeman, J.S. Riffle, J.E. McGrath, Cross-Linked Disulfonated Poly(arylene ether sulfone) Telechelic Oligomers. 2. Elevated Transport Performance with Increasing Hydrophilicity, Ind. Eng. Chem. Res. 55 (2016) 1419–1426.

[43] E.M. Van Wagner, A.C. Sagle, M.M. Sharma, B.D. Freeman, Effect of crossflow testing conditions, including feed pH and continuous feed filtration, on commercial reverse osmosis membrane performance, J. Memb. Sci. 345 (2009) 97–109.

[44] J.G. Wijmans, R.W. Baker, The solution-diffusion model: a review, J. Memb. Sci. 107 (1995) 1–21.

[45] J. Kamcev, M. Galizia, F.M. Benedetti, E.-S. Jang, D.R. Paul, B.D. Freeman, G.S. Manning, Partitioning of mobile ions between ion exchange polymers and aqueous salt solutions: importance of counter-ion condensation, Phyical Chem. Chem. Phys. 18 (2016) 6021–6031.

[46] H. Strathmann, A. Grabowski, G. Eigenberger, Ion-Exchange Membranes in the Chemical Process Industry, Ind. Eng. Chem. Res, 52 (2013) 10364-10379.

Chapter 4 : Synthesis, characterization, and reaction kinetics of post-sulfonated poly(arylene ether sulfone) membranes containing biphenol for water desalination

Shreya Roy Choudhury, [a] Dana Kazerooni,[a,b] Eui Soung Jang,[c] Benny D. Freeman,[c] John J. Lesko,[b] J. S. Riffle[a*]

[a]Macromolecules Innovation Institute, Virginia Tech, Blacksburg, VA 24061, United States

[b]College of Engineering, Virginia Tech, Blacksburg, VA 24061, United States

[c]Department of Chemical Engineering and the Center for Energy and Environmental Resources, University of Texas at Austin, Austin, TX 78758, United States

Abstract

This study focuses on post-sulfonated poly(arylene ether sulfone) membranes that have sulfonate ions on adjacent rings of a biphenol moiety. High molecular weight sulfonated polysulfone membrane, of ion exchange capacity of 1.00 meq/g, was synthesized by post-sulfonation of pre-formed polymers. Research on the kinetics of the sulfonation reaction proved that the polymer was sulfonated on dissolving in sulfuric acid. The sulfonated polymer showed bimodal chromatogram, and possible aggregation, when analyzed by SEC in DMac/LiCl. At water uptake of 18% the fully hydrated membrane had an elastic modulus of 1082.7 MPa and yiled strength of 31.95 MPa. It had an ultimate strain of ~80% . Interestingly, the membrane, like it's hydroquinone based counterparts, did not show a compromise in the rejection of monovalent ions in presence of divalent calcium ions in mixed feed.

4.1 Introduction

According to the World Economic Forum, the water supply crisis has remained one of the top five global risks in terms of societal impact since 2012 [1]. The global population tripled in the

twentieth century and is projected to reach 8.6 billion by 2030, leading to a rise in water demand [2]. The water crisis has been further worsened by industrialization and climate change. In today's economies, food, energy and water are inherently linked (food-energy-water nexus) [3,4]. Thus, a water crisis can have a cascading effect on availability of food and energy. Saltwater desalination has emerged as the key to tackle the water crisis. Reverse osmosis is the most widely used process for water desalination. It is a membrane-based process and does not rely on a phase change like thermal methods of desalination. Hence it is more economical and efficient than thermal methods. Sulfonated polysulfone membranes are a potential alternative to the state-of-the-art polyamide reverse osmosis membranes because they are resistant to chlorinated disinfectants in the feed water [5].

McGrath et al. developed a sulfonated monomer [6,7] by disulfonation of the commercial activated aromatic dihalide monomer, 4,4'-dichlorodiphenyl sulfone (DCDPS). Random copolymers were synthesized by a direct aromatic nucleophilic substitution step polymerization of the pre-sulfonated monomer, 3,3'-disulfonated, 4,4'dichlorodiphenyl sulfone (SDCDPS) [8–13]. The hydrophilicity of the membranes was tailored by changing the concentration of the sulfonated comonomer. It was found that altering the hydrophilicity of these materials had a pronounced effect on the transport properties [11,14]. The sulfonate ions are placed on the adjacent rings of the disulfonated dihalide moiety. Apart from the need to synthesize the sulfonated comonomer the membranes cast from these polymers have compromised monovalent salt rejection in water with mixed salt feeds that contain divalent ions [15]. A substantial decrease in the monovalent salt rejection with added calcium chloride to the feed water results along with an increase in water permeabilities. It is important to study the positions of the sulfonate ions along the polymer

backbone because the divalent ions can potentially chelate closely spaced sulfonate groups, thus allowing the monovalent ions to pass through the membrane.

Post polymerization sulfonation is an alternative approach to synthesize sulfonated polysulfones. Historically, the method of employing the post-sulfonation route led to uncontrolled sequences of sulfonic acid groups along the chains unless special compositions were utilized. Most previous work on post-sulfonation of polysulfones utilized rather harsh conditions because the rings to be sulfonated included both activated and deactivated rings toward the electrophilic aromatic sulfonation reaction. Allegrezza and co-workers found that the sulfonated poly(arylene ether sulfone) membranes were resistant to chlorine (100 ppm free chlorine) and exhibited >95% salt rejection at 400 psi pressure [5]. However, these membranes showed decreased NaCl rejection with an increase in Ca^{2+} concentration in mixed feeds. Alternatively, Rose and coworkers reported controlled post-sulfonation of poly(arylene ether sulfone)s that contained hydroquinone units [16]. The sulfonation reaction proceeded only at the hydroquinone because all of the other rings were deactivated toward electrophilic aromatic sulfonation by the electron withdrawing sulfone groups [16–20]. The advantage of this method was that the degree of sulfonation could be controlled without the need to synthesize a pre-sulfonated monomer. This modification can be utilized to place the sulfonate ions strategically along the polysulfone backbone and may provide a novel alternative material for reverse osmosis. Research in our group has shown that post-sulfonated polysulfones with sulfonate ions placed strategically only on the isolated hydroquinone rings had little to no compromise on the rejection of Na^{+} ions in the presence of Ca^{2+} ions. The current work focuses on the synthesis and characterization of post-sulfonated polysulfones synthesized with biphenol instead of hydroquinone, such that disulfonation was obtained only on the biphenol moieties. This

polymer can provide a direct comparison of the effect of placing the sulfonate ions on adjacent rings versus on isolated rings.

Post-sulfonation of commercial poly(phenylsulfone), Radel R™, have been carried out in sulfuric acid, to sulfonate the biphenol rings, for proton exchange membranes in fuel cell applications [21–23]. However no information has been provided on the molecular weights of the sulfonated poly(phenylsulfone)s. In the current work, the post-sulfonation reaction kinetics and measurements of molecular weight of a polysulfone containing biphenol were studied to optimize the sulfonation process with a minimal level of chain scission.

4.2 Experimental

Materials

4,4'-Dichlorodiphenylsulfone (DCDPS) was kindly donated by Solvay Advanced Polymers and was recrystallized in toluene. It was dried under vacuum at 110 ºC for 12 h prior to use. Bisphenol sulfone (Bis-S) also provided by Solvay Advanced Polymers was recrystallized in methanol and dried under vacuum at 110 ºC for 12 h. 4,4'-biphenol (BP) provided by Eastman Chemical Company was recrystallized in ethanol and dried under vacuum at 110 ºC for 12 h. Potassium carbonate was purchased from Sigma-Aldrich and was dried under vacuum at 160 ºC for 72 h. Concentrated sulfuric acid was obtained from VWR and used as received. Sulfolane, *N*,*N*-dimethylacetamide (DMAc) and toluene were purchased from Sigma-Aldrich.

Synthesis and reaction kinetics of post-sulfonated poly(arylene ether sulfone)s with sulfonate ions on adjacent rings

Synthesis of high molecular weight biphenol sulfone (xx-BiPS) polymers (where xx = degree of disulfonation)

Aromatic nucleophilic substitution step copolymerization was used to synthesize a series of biphenol-based, high molecular weight poly(arylene ether sulfone) copolymers (xx-BiPS). The reaction for the synthesis of a polymer with 28 mol % of the bisphenol moieties being biphenol (28-BiPS) is provided. BP (4.34 g , 23.3 mmol), Bis-S (15 g, 59.9 mmol), were dissolved in 123 mL of sulfolane in a 3-neck round bottom flask equipped with a nitrogen inlet, overhead stirrer, and condenser with a Dean Stark trap. The reaction temperature was controlled with a temperature controller connected to a thermocouple in a salt bath. Toluene (34 mL) and K_2CO_3 (13.80 g, 100 mmol) were added and the reaction was refluxed at 180-185 ºC to azeotropically remove any water. After 4 h, the toluene was removed from the Dean Stark trap. DCDPS (23.90 g, 83.2 mmol) was added into the reaction flask and the reaction temperature was raised to 200-210 ºC. After 36 h of reaction, the mixture was allowed to cool to ~150 ℃ and then diluted with 40 mL of DMAc. The mixture was kept above the melting point of sulfolane (27.5 ℃) and precipitated in hot water to remove traces of sulfolane and DMAc. The precipitation was carried out in a blender to reduce the size of the particles, that aids in the post-sulfonation reaction step. The polymer was boiled with 3 changes of water to remove trace amounts of sulfolane and then dried at 50 ºC for 4 h, followed by 12 h under vacuum at 110 ºC. The reaction had a yield of 97 %.

Kinetics of post-sulfonation of biphenol sulfone polymers (xx-SBiPS)

Kinetics of the post sulfonation reaction was performed with 28 BiPS. The polymer was powdered in a blender to provide a high surface area powder. This facilitated rapid dissolution during the sulfonation reaction. For the sulfonation reaction, a four-neck flask equipped with an overhead stirrer, nitrogen inlet, condenser and a thermometer were assembled. An oil bath with a thermocouple and temperature controller was used to control the reaction temperature. Sulfuric acid

(30 mL) was heated in the flask to 60 ºC. Once the acid attained the desired temperature the polymer was added in small increments. The reaction was stirred vigorously to promote rapid dissolution and to break up any clumps of acid-swollen polymer. Reactions were performed at 60, 70, and 75 ºC. Time zero was designated when the polymer was first added to the acid (~15 mins). Aliquots of 5-10 mL were removed at 0, 15, 30, 60, 90 and 120 min. The aliquots were quenched by precipitation in deionized water, followed by washing with copious amounts of deionized water until the pH reached at least 5.

Characterization

Nuclear magnetic resonance spectroscopy (NMR)

Quantitative ^{1}H NMR and COSY NMR analyses were performed on the oligomeric copolymers and high molecular weight polymers on a Varian Unity Plus spectrometer operating at 400 MHz at a pulse angle of 30º with a pulse delay of 5 s. The spectra of the copolymers were obtained from a 10 % (w/v) solution in DMSO-d_6 with 64 scans.

Titration

A measured amount (~ 0.1-0.2 g) of the polymer was stirred in 1.0 M NaCl solution for a day. This facilitated exchange of the H^+ ions of the sulfonic acid groups in the polymer backbone with the Na^+ ions of the NaCl solution. The resulting HCl solution was titrated against 0.0967 M NaOH solution that was standardized with KHP.

Size Exclusion Chromatography

Size exclusion chromatography (SEC) was conducted on the polymers to measure molecular weights and molecular weight distributions. The solvent was DMAc that was distilled from CaH_2 and that contained dry LiCl (0.10 M). The column set consisted of 3 Agilent PLgel 10-μm Mixed B-LS columns 300x7.5 mm (polystyrene/divinylbenzene) connected in series with a

guard column having the same stationary phase. The column set was maintained at 50 °C. An isocratic pump (Agilent 1260 infinity, Agilent Technologies) with an online degasser (Agilent 1260), autosampler and column oven was used for mobile phase delivery and sample injection. A system of multiple detectors connected in series was used for the analyses. A multi-angle laser light scattering (MALLS) detector (DAWN-HELEOS II, Wyatt Technology Corp.), operating at a wavelength of 658 nm, and a refractive index detector operating at a wavelength of 658 nm (Optilab T-rEX, Wyatt Technology Corp.) provided online results. The system was corrected for interdetector delay and band broadening. Data acquisition and analysis were conducted using Astra 6 software from Wyatt Technology Corp. Validation of the system was performed by monitoring the molar mass of a known molecular weight polystyrene sample by light scattering. The accepted variance of the 21,000 g/mole polystyrene standard was defined as 2 standard deviations (11.5% for M_n and 9% for M_w) derived from a set of 34 runs.

Film casting

A copolymer (1.2 g) was dissolved in 10 mL of DMAc in a glass vial. The solution was filtered through a 0.45 μm PTFE filter and the vial was washed with 2 mL of DMAc to form a 10 wt/v% polymer solution. The solution was sonicated for 10 min and cast on a level 4" x 4" clean glass plate. The plate was cleaned in a base bath, washed and dried prior to film casting. The films were heated under an IR lamp with a starting temperature of ~45 °C. The temperature of the IR lamp was ramped up by 20 ºC every 2 h until the temperature reached ~75 °C. The plate with the film was kept at that temperature for 8-10 h. The film was dried under vacuum at 110 °C for 24 h. The film was delaminated from the glass plate by immersion in deionized water. The film, in acidic form, was stirred in 0.1 N NaCl for 3 days to convert it into salt form. The film was stirred in deionized

water overnight to remove the excess salt and dried under vacuum at 110 °C overnight. The thickness of the film was found to be ~100 μm.

Water Uptake

Water uptake was measured gravimetrically. Polymer films (100 mg) were cast from a 10% (w/v) solution in DMAc onto a clean glass plate and placed under an IR lamp for 6-12 h. Films were removed via immersion in deionized water. The samples were dried overnight at 110 °C under vacuum. Films were then equilibrated in deionized water overnight, converted from the acid to their salt form by heating in 1.0 M NaCl at 80 °C for 2 h and subsequently were kept at room temperature in the water overnight. They were blotted and weighed to obtain the wet weight (W_{wet}). Films were dried under vacuum at 110 °C for 12 h to obtain dry weights (W_{dry}). The water uptake in the sodium salt form was determined as follows:

$$Water\ Uptake = \frac{W_{wet} - W_{dry}}{W_{dry}} * 100\%$$

Tensile tests of hydrated membranes

The crosslinked membranes were cut into dogbone samples with a gauge width of 3.18 mm and gauge length of 25 mm, Type V according to ASTM D638-14, using a Cricut Explore One™ cutting machine. Seven samples with uniform thickness of 60-70 μm from each membrane were tested. The thickness of the dogbones were measured at five points along the gauge length using a Mitutoyo digimatic micrometer model MDC-1"SXF. A hydrated testing cell was secured onto the Instron to test samples under fully hydrated conditions. The wet samples were loaded into the hydrated cell of the Instron and the cell was filled with DI water. The samples were immersed in DI water for at least 24 h prior to testing and allowed to equilibrate in the Instron in the water for 3 min. Uniaxial load tests were performed using an Instron ElectroPuls E1000 testing machine

equipped with a 250-N Dynacell load cell. The crosshead displacement rate was 10 mm/min and the initial grip separation was 25 mm.

4.3 Results and Discussion

The placement of the sulfonate ions on the polysulfone backbone plays a crucial role in the transport properties of the membranes. Sulfonated polysulfone membranes with sulfonate ions on the adjacent rings have been studied extensively. In structure (I) the sulfonate ions are on the rings separated by a sulfone group. These polymers were synthesized by a polycondensation reaction that contained a pre-sulfonated monomer.

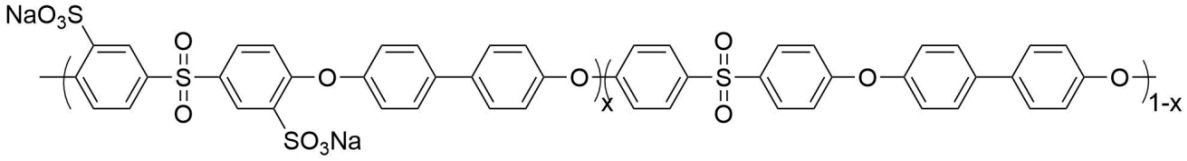

(I) BPS

Sulfonated polysulfone membranes with sulfonate ions on isolated rings were also synthesized. In structure (II) the sulfonate ions are strategically placed only on the hydroquinone rings as all other rings are deactivated against electrophilic aromatic sulfonation. It should be noted that the sulfonate ions were only on the rings that were not connected to the sulfone group. These polymers were synthesized by post polymerization sulfonation of the non-sulfonated polymer containing hydroquinone units. The membranes of structure (II) showed superior transport properties - no compromise on the rejection of monovalent ions in mixed feed water containing divalent ions. The salt rejection did not decrease drastically with increase in water permeability, and at comparable values of water permeabilities the SHQS membranes had a higher water/salt selectivity than BPS membranes.

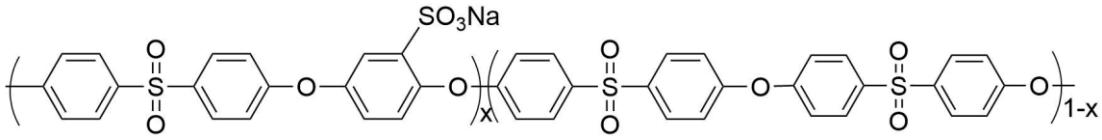

(II) SHQS

The polymer backbones of the SHQS membranes were different from the BPS membranes. In this research, polymers with structure (III), sulfonated biphenol sulfone (SBiPS), have been studied. In these polymers the non-sulfonated repeat units are identical to the SHQS series but the sulfonate ions are placed on adjacent rings to obtain a direct comparison of properties relative to the SHQS membranes.

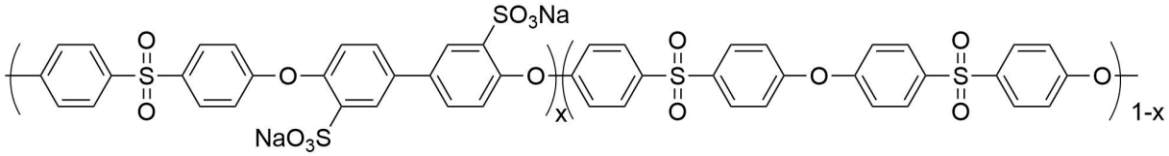

(III) SBiPS

Synthesis of high molecular weight biphenol sulfone (xx- BiPS) polymers

Biphenol containing polysulfones were synthesized via nucleophilic aromatic substitution step growth polymerization with a weak base in a dipolar aprotic solvent (Figure 4.1). The weak base abstracts a proton from the phenols and generates a phenolate nucleophile. The phenolate nucleophile attacks the activated halide forming the Meisenheimer complex in the rate limiting step. In the second step of the reaction, the Meisenheimer complex decomposes to generate the product. The reaction was azeotropically dehydrated with toluene to remove water generated from the reaction of the base with the phenol, which might compete with the phenolate nucleophile and hydrolyze the dihalide. Due to the presence of the electron withdrawing sulfone group between the

rings, the phenoxide ions of Bis-S are poorly nucleophilic. Hence, the reaction was carried out at a high temperature of 200 °C for 36 h in a high boiling solvent, sulfolane. After completion of the reaction, the product was diluted with DMAc to reduce the viscosity of the solution and precipitated in water. The yield of the reaction was `98%

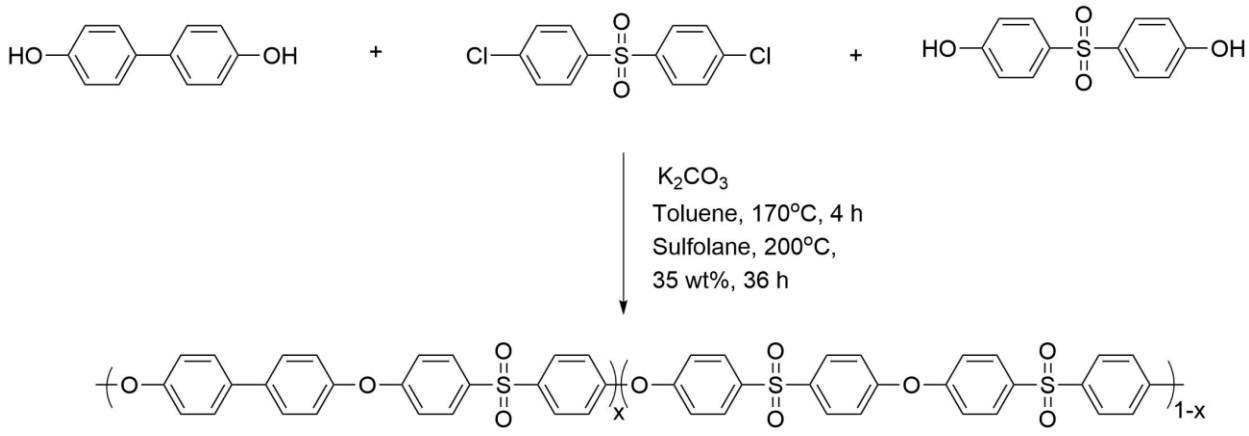

Figure 4.1: Synthesis of high molecular weight random polymers by nucleophilic aromatic substitution. x= 0.28

Kinetics of post-sulfonation of biphenol sulfone polymers (xx-SBiPS)- structure (III)

A detailed discussion on the results observed at 60 °C are given in the following sections. The sulfuric acid was heated to a stable temperature of 60 °C. The polymer was crushed with a mortar and pestle before adding it to the stirring acid to increase the solid/liquid interface. 28 BiPs was added into the acid in small increments over ~30 minutes to dissolve fully in the acid. It was observed that a large amount of added polymer formed a swollen clump in the acid. Moreover, it was difficult to dissolve the polymer in the acid because it would stick to the glass walls of the flask. It could be also attributed to the weakening of the reactivity of sulfuric acid due to the production of water during the reaction [24]. It is important to use H_2SO_4 with a minimum amount

of water because even a small amount of water can decrease the reactivity significantly [24]. The reaction scheme for the post sulfonation reaction at 60 ºC for 30 min is shown in Figure 4.2. Only the aromatic rings of the biphenol units were sulfonated because all of the other rings were

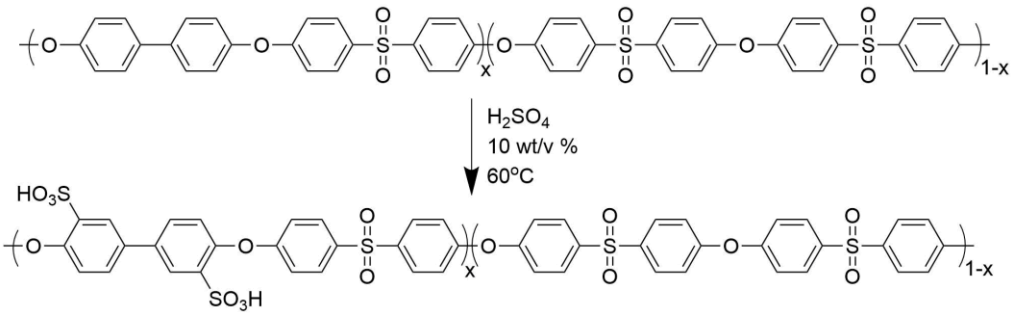

deactivated for electrophilic aromatic sulfonation by the electron withdrawing sulfone groups.

Figure 4.2: Post sulfonation of xx-BiPS at 60 °C for 60 mins by electrophilic sulfonation

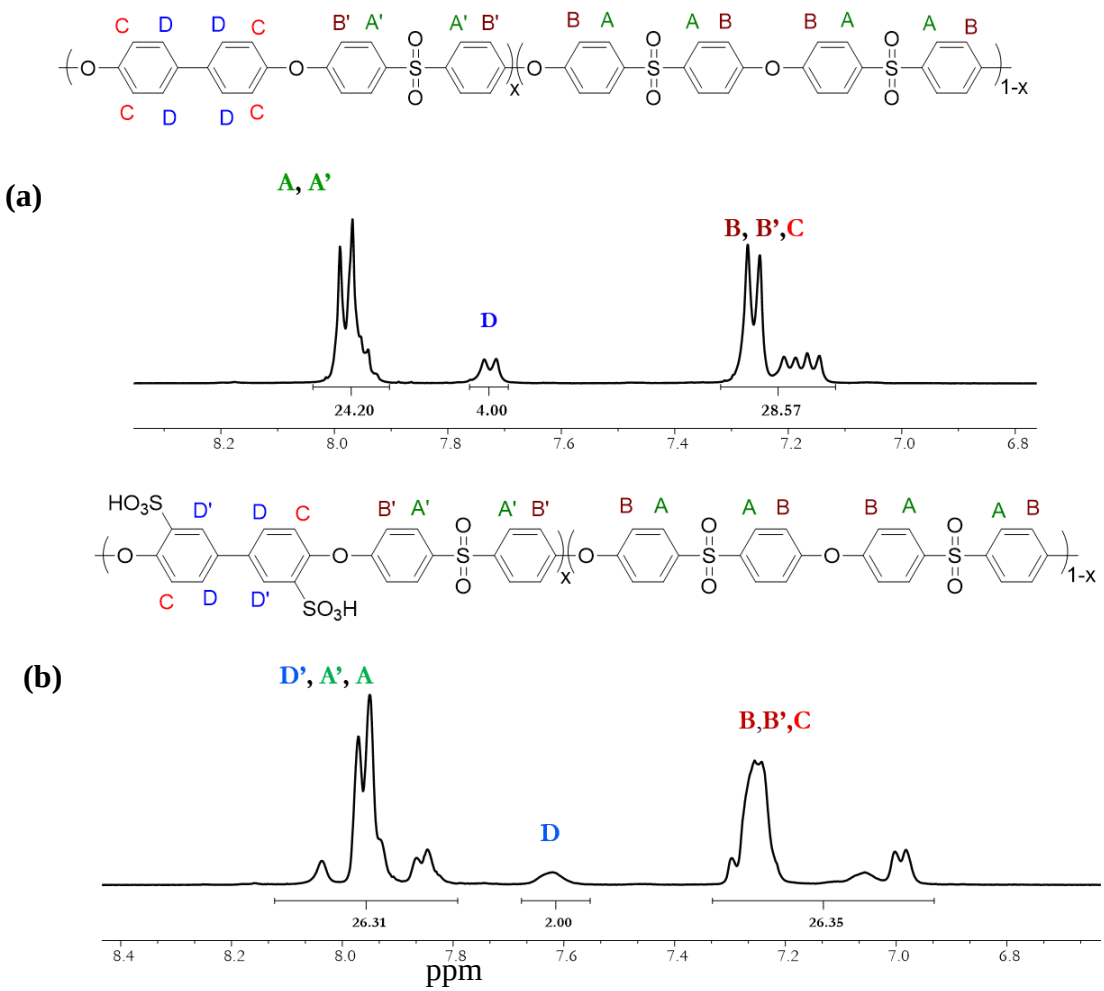

Figure 4.3: ^{1}H NMR of 28BiPS (a) before sulfonation (b) after sulfonation at 60 ºC for 180 min

The ^{1}H NMR study used a 30º pulse angle and 5 s pulse delay for relaxation of the protons and to ensure that all of them had relaxed completely before each subsequent pulse. The ^{1}H NMR of a non-sulfonated polymer with 28 mol% of biphenol (28-BiPs) is shown in Figure 4.3(a). The A protons are on the rings next to a sulfone group and ortho to the sulfone group in the hydrophobic repeat units that contain the Bis S moiety. The A' protons are present on the ring next to the sulfone group and ortho to the sulfone group in the biphenol containing repeat units. The B protons are present on the bisphenol ring and ortho to the ether linkage in the Bis S containing repeat unit. B_1 protons are present on the sulfone ring but connected by 3 bonds to the ether linkage in the biphenol

containing repeat unit. The C and D protons are on the biphenol unit. The C protons are connected to the ether linkage whereas the D protons are away from the ether linkage. The A and A' protons resonate downfield at ~8 ppm due to the deshielding effect by the sulfone groups. The B, B_1 and C protons peaks overlap with each other and resonate upfield at ~7.1-7.4 ppm due to the shielding experienced by the electron cloud of the oxygen of the ether linkage. The D peaks resonate at ~7.75 ppm. The spectra were integrated by normalizing the D peaks to 4.00. The amount of biphenol containing repeat units was calculated to be 29.60% (relative to 28% targeted) based on the integrals of C and A.

In the spectrum of the post-sulfonated polymer, 28-SBiPS (Figure 4.3b), the position of the A', A', B and B' resonances remain unchanged. The protons on the carbon atom adjacent to the sulfonic acid is labelled as D'. D' protons resonate downfield and overlap with the A and A' protons. The spectrum was normalized using the non-sulfonated D peaks. It was observed that the integration of A, A' increased by 2 with the appearance of the peak D' that overlapped with the A'A' peaks. The integration of B, C, B' decreased by two indicating that two protons of C were lost during the post-sulfonation reaction. The degree of disulfonation was found to be 28.26%, very near the targeted value.

Figure 4.4 represents the ^{1}H NMR spectra of aliquots taken at different time intervals. All of the fractions achieved an ~28% disulfonation irrespective of the time interval the aliquot was removed. Thus, the reaction had proceeded to completion as soon as the polymer dissolved in the acid.

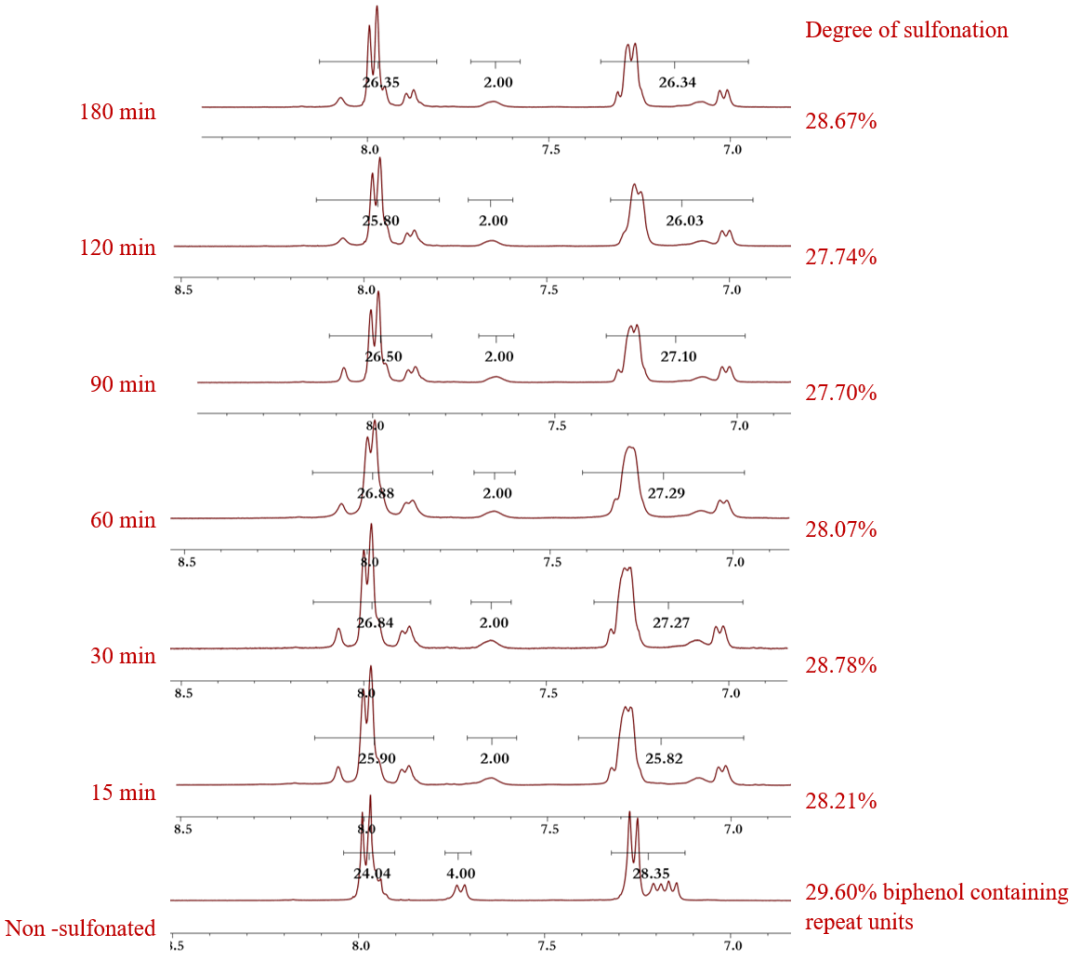

Figure 4.4: ^{1}H NMR spectra of post-sulfonation reaction at 60 ºC. Aliquots were analyzed at 15, 30, 60, 90,120 and 180 minutes from the first addition of the polymer to the acid.

The degree of sulfonation was calculated from the spectra of the sulfonated polymers, and the ion exchange capacities were calculated using the degrees of sulfonation (Equation 1). In equation 1, DS is the degree of sulfonation, MW_{SRU} is the molecular weight of the sulfonated repeat unit in the Na^{+} form, and MW_{NSRU} is the molecular weight of the non-sulfonated repeat unit.

$$IEC_{oligomer} = \frac{1000*DS}{(DS*MW_{SRU})+[(1-DS)*MW_{NSRU}]} \quad \text{(Equation 1)}$$

2-D homonuclear correlational spectroscopy experiments were conducted to investigate correlations between neighboring protons in 28-SBiPS. Figure 4.5 shows the COSY NMR spectrum of an aliquot from the reaction mixture removed at 180 minutes. The D' protons correlated only to themselves and did not show a three-bond correlation to any other protons. Moreover, there were no other uncorrelated protons. This confirmed that there were no secondary sites of sulfonation and all the biphenol moieties were strategically disulfonated even at 180 minutes of the reaction.

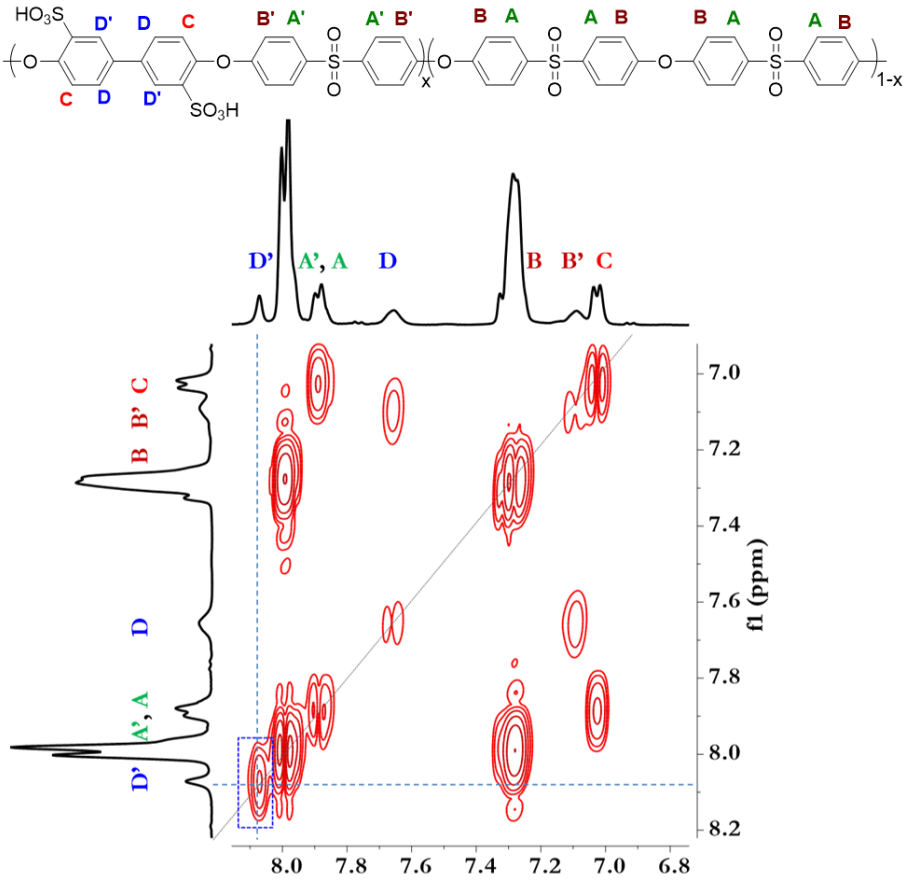

Figure 4.5: COSY NMR of post-sulfonated 28-SBiPS at 60 ºC and 180 mins.

The peaks obtained by ^{1}H NMR were broad and added to the uncertainty of the measurement. Hence, the ion exchange capacities of the sulfonated polymers were measured by

titration. The sulfonated polymer fractions obtained at longer time points (60 minutes and above) were analyzed further. Fractions at 70 °C- 60 minutes and 75 °C- 60 minutes were also titrated. Table 1 shows the IEC values obtained by titration and by ^{1}H NMR. The values obtained by both methods matched with each other and were also close to the target IEC of 1.1. Furthermore, there was no increase in the IECs of the membranes with increase in temperature.

Sample	% Degree of sulfonation	IEC by ^{1}H NMR	IEC by titration
60 °C - 60 mins	28.07	1.11	1.10
60 °C - 120 mins	27.74	1.10	0.97
60 °C - 180 mins	28.67	1.13	1.08
70 °C - 60 mins	28.52	1.13	0.97
75 °C - 60 mins	28.32	1.12	1.05

Table 4.1: IECs of 28-SBiPS synthesized in different reaction conditions

It was confirmed that the post-sulfonation reaction carried out in the temperature range of 60-75 ºC 28-SBiPs had 100% disulfonation of the biphenol moieties. It could also be possible that the fractions of sulfonated polymers with higher degrees of sulfonation were soluble in water (the non-solvent used for precipitation) and could be separated from the fractions that had the desired level of sulfonation [24].

Molecular weight degradation due to chain scission is a common disadvantage reported in the literature during post polymerization sulfonation [25]. The SEC chromatograms on the 28-SBiPS indicate that the sulfonation process does not produce degradation within the sulfonation conditions studied. The molecular weights provide good evidence that the reaction conditions utilized herein can avoid the molecular weight degradation that has previously caused concern in

other post-sulfonated polysulfones. However, the light scattering chromatograms showed bimodal peaks with high polydispersities (Figure 4.6). The refractive index detector detected unimodal peaks for all samples but high molecular weight shoulders were observed (Figure 4.7). A similar trend was observed for aliquots from reactions at other temperatures (Figure 4.8). The bimodality might be due to the inter and intra chain interactions in the column, but the reason remains unknown It was confirmed that the post-sulfonation reaction carried out in temperature range of 60-75 °C 28-SBiPs had 100% disulfonation of the biphenol moieties in the temperature range of 60-75 °C. It could also be possible that the fractions of sulfonated polymers with higher degrees of sulfonation were soluble in water (non-solvent used for precipitation) and could be separated from the fractions that had the desired level of sulfonation [47].

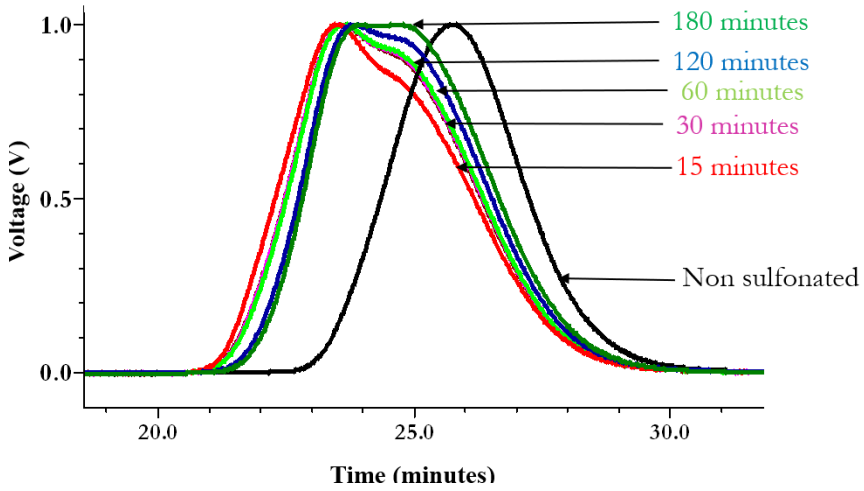

Figure 4.6: SEC light scattering chromatogram of 28-BiPS and 28-SBiPS at various time points at 60 °C

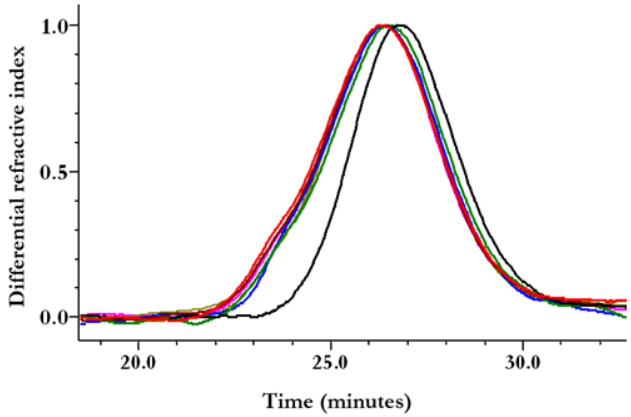

Figure 4.7: SEC refractive index chromatograms of 28-BiPS and 28-SBiPS at various time points at 60 °C

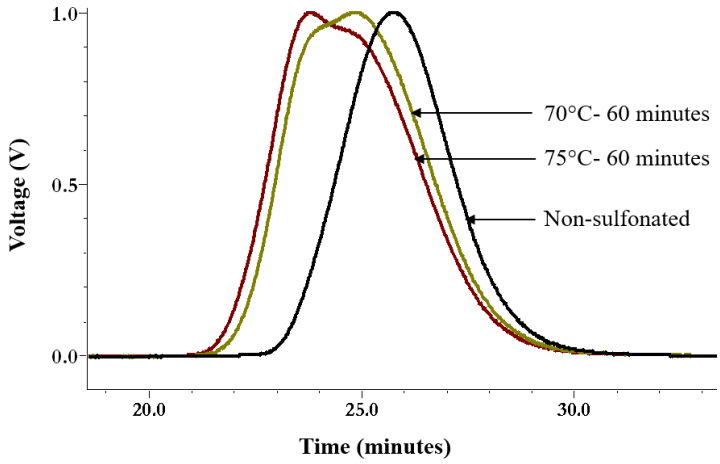

Figure 4.8: SEC light scattering of 28-SBiPS at 70 °C and 75 °C

The M_W's that were obtained were much higher than expected (Table 2) The exaggeration of M_w in sulfonated polyphenylene sulfones have been previously reported [24]. Although LiCl was added into the mobile phase of the SEC solvent, solutions of such anionic polysulfones in dipolar aprotic solvents, even with added salt, can be complicated. This phenomenon was observed in previous studies. Nunes at al. reported a similar issue in the SEC chromatograms of poly(phenyl sulfone)s that were post sulfonated on the biphenol ring with SO_3 and $(CH_3)SiSO_3Cl$ [24].

Exaggeration in molecular weight was reported in polymers with a degree of monosulfonation between 70-100%.

Sample	Mn (kDa)	Mw (kDa)	dn/dc (mL/g)
28% Non-sulfonated (28-BiPS)	39.9	76.7	0.1764
Sulfonated polymers- 28-SBiPS			
60 °C - 15 mins	42.4	145.9	0.1748
60 °C - 30 mins	51.0	136.9	0.1800
60 °C - 60 mins	54.0	138.6	0.1748
60 °C - 120 mins	48.1	122.6	0.1744
60 °C - 180 mins	56.6	136.0	0.1781
70 °C - 60 mins	56.0	145.4	0.1726
75 °C - 60 mins	40.7	104.3	0.1789

Table 4.2: Molecular weights of 28-BiPS and 28-SBiPS synthesized in various reaction conditions

It was established that increasing the reaction temperature and time did not cause any significant change in the degree of sulfonation or in the molecular weights of 28-SBiPS. Although increases in temperature decreased the dissolution times for the BiPS in sulfuric acid there is always a possibility of chain scission at high temperatures. Hence to maintain mild reaction conditions, 28-BiPS was post-sulfonated at 60 °C for 60 minutes.

Hydrated mechanical properties

It is important for reverse osmosis membranes to have good mechanical properties to withstand high hydrostatic pressures. The 28-SBiPS membrane remained glassy in fully hydrated

conditions. One of the objectives of this work is to develop membranes that have superior mechanical properties in fully hydrated conditions to withstand high applied pressure in reverse osmosis. The stress-strain plot for the membrane is shown in Figure 4.9. At a maximum water uptake of 18%, 28-SBiPS exhibited an elastic modulus of 1082.68 MPa and yield strength of 31.95 MPa. These membranes break at higher strains as compared to the hydroquinone based SHQS series. The biphenol comonomers and lower number of flexible ether linkages increased the stiffness of the chains as compared to the SHQS membranes that had hydroquinone comonomers and higher number of ether linkages. The SHQS membranes are densely packed because the flexible backbone. It can be speculated that once a small defect formed in SHQS membranes, it propagated quickly because the chains did not have room to relax back to their original conformation. In SBiPS membranes, the polymer chains were less densely packed because of comparatively lower number of ether linkages. As a result, the defects form could not propagate quickly and the membrane broke at higher strains.

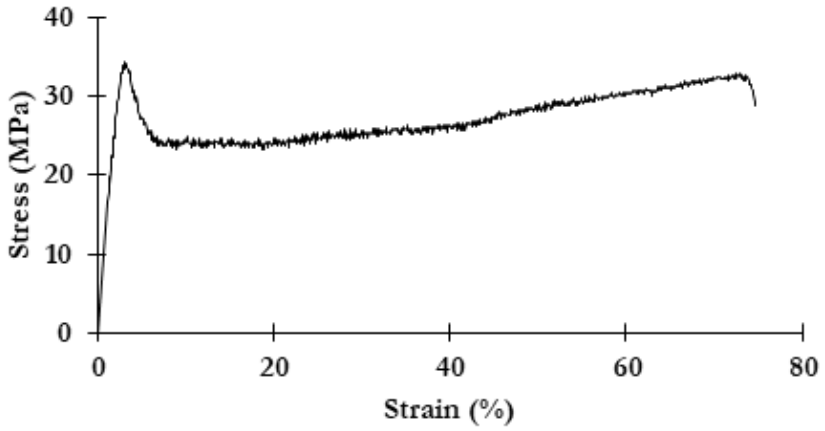

Figure 4.9: Stress-strain plot of fully hydrated 28-SBiPS

Transport properties

Polymer Membrane	IEC	Water uptake	Fixed charge concentration (meq/g)	% Salt rejection	Hydraulic water permeability (L μm/(m^2h bar)
28-SBiPS	1.10	0.18	6.11	97.7 ± 0.7	0.15
BPS 20	0.92	0.19	4.84	99.2	0.04
BPS 30	1.34	0.33	4.06	96.2	0.22
SHQS 50	1.14	0.25	4.56	97.8	0.18

Table 4.3*:* Transport properties of 28-SBiPS

Table 4.3 shows the transport properties of the 28-SBiPS membrane. At a comparable IEC, the SBiPS membrane had a higher fixed charge concentration but slightly lower salt rejection than the BPS 20 membrane (Structure I and 20% degree of disulfonation). At comparable degrees of water uptake, the SBiPS 28 membrane also had a higher water permeability than the BPS 20 membrane. High water permeability in the SBiPS can be attributed to the relatively polar backbone and probably due to the distribution of water in the membrane. The trends in the transport properties of the SBiPS might be similar to the SHQS membranes that showed a low but constant salt rejection and higher water permeabilities than the BPS membranes. Membranes of SBiPS with varying degrees of sulfonation have to be analyzed to determine whether a similar trend exists.

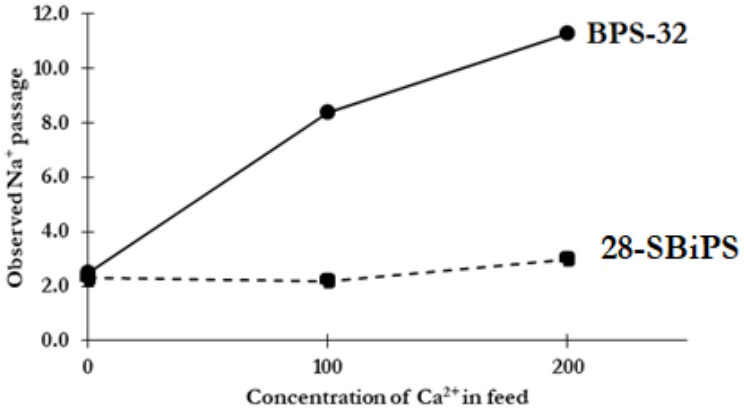

Figure 4.10: Rejection of salts by 28-SBiPS and BPS-32 membranes in mixed feed containing Ca^{2+} ions

The mixed feed data for the 28-SBiPS membrane showed a constant salt rejection in the presence of up to 200 ppm calcium ions (Figure 4.10). On the other hand, the BPS 32 membrane showed a compromised rejection of monovalent ions in the presence of calcium ions. There was a drastic improvement in the membrane properties from structure I to structure III. In the BPS membranes the sulfonate ions are present on adjacent rings of the bisphenol moieties whereas in the SBiPS membranes, the sulfonate ions are on adjacent rings of the biphenol moieties. The SBiPS membranes had good transport properties even though the sulfonate ions were present on adjacent rings. It might be possible that the kinked and rigid structure of the disulfonated sulfone moiety positions the sulfonates sufficiently close to chelate hydrated calcium ions, whereas the disulfonated biphenol with its non-planar rings keeps the sulfonates too far apart to efficiently chelate the calcium. However, further studies need to be carried out to understand the transport properties of these membranes.

4.4 Conclusion

Post sulfonation is an efficient method to synthesize sulfonated poly(arylene ether sulfone)s with sufonate ions strategically placed along the polymer backbone. The work herein reports the synthesis of post sulfonated polysulfones with sulfonate ions on adjacent rings of the biphenol comonomer. Studies on the kinetics of the post-sulfonation reaction showed that the reaction can be carried out under mild conditions and without degradation of the polymer molecular weight. Most importantly, these membranes showed no compromise in the rejection of monovalent ions in the presence of divalent

References

[1] World Economic Forum, The Global Risks Report 2018-13th Edition, 2018.

[2] H.K. Lonsdale, H. Podall, Reverse Osmosis Membrane Research, Plenum press, New York, 1972.

[3] N.R. Armstrong, R.C. Shallcross, K. Ogden, S. Snyder, A. Achilli, E.L. Armstrong, Challenges and opportunities at the nexus of energy, water, and food: A perspective from the southwest United States, MRS Energy Sustain. 5 (2018) 1–18.

[4] Healy RW, Alley WM, Engle MA, McMahon PB, Bales JD, The Water-Energy Nexus: An Earth Science Perspective, (2015).

[5] A.E. Allegrezza, B.S. Parekh, P.L. Parise, E.J. Swiniarski, J.L. White, Chlorine resistant polysulfone reverse osmosis modules, Desalination. 64 (1987) 285–304.

[6] W.L. Harrison, F. Wang, J.B. Mecham, V.A. Bhanu, M. Hill, Y.S. Kim, J.E. McGrath, Influence of the bisphenol structure on the direct synthesis of sulfonated poly(arylene ether) copolymers. I, J. Polym. Sci. Part A Polym. Chem. 41 (2003) 2264–2276.

[7] M. Sankir, V.A. Bhanu, W.L. Harrison, H. Ghassemi, K.B. Wiles, T.E. Glass, A.E. Brink, M.H. Brink, J.E. McGrath, Synthesis and characterization of 3,3′-disulfonated-4,4′-dichlorodiphenyl sulfone (SDCDPS) monomer for proton exchange membranes (PEM) in fuel cell applications, J. Appl. Polym. Sci. 100 (2006) 4595–4602.

[8] F. Wang, M. Hickner, Y.S. Kim, T.A. Zawodzinski, J.E. McGrath, J.E. Direct polymerization of sulfonated poly(arylene ether sulfone) random (statistical) copolymers: candidates for new proton exchange membranes, J. Memb. Sci. 197 (2002) 231–242.

[9] B.C. Johnson, İ. Yilgör, C. Tran, M. Iqbal, J.P. Wightman, D.R. Lloyd, J.E. McGrath, Synthesis and characterization of sulfonated poly(acrylene ether sulfones), J. Polym. Sci. Polym. Chem. Ed. 22 (1984) 721–737.

[10] Y.S. Kim, M.A. Hickner, L. Dong, B.S. Pivovar, J.E. McGrath, Sulfonated poly(arylene ether sulfone) copolymer proton exchange membranes: composition and morphology effects on the methanol permeability, J. Memb. Sci. 243 (2004) 317–326.

[11] W. Xie, J. Cook, H.B. Park, B.D. Freeman, C.H. Lee, J.E. McGrath, Fundamental salt and water transport properties in directly copolymerized disulfonated poly(arylene ether sulfone) random copolymers, Polymer. 52 (2011) 2032–2043.

[12] H.B. Park, B.D. Freeman, Z.-B. Zhang, M. Sankir, J.E. McGrath, Highly Chlorine-Tolerant Polymers for Desalination, Angew. Chemie. 120 (2008) 6108–6113.

[13] D.R. Lloyd, L.E. Gerlowski, C.D. Sunderland, J.P. Wightman, J.E. Mcgrath, M. Igbal, Y.

Kang, Poly(aryl ether) Membranes for Reverse Osmosis, in: Synth. Membr., American Chemical Society, 1981: pp. 327–350.

[14] W. Xie, H.-B. Park, J. Cook, C.H. Lee, G. Byun, B.D. Freeman, J.E. McGrath, Advances in membrane materials: desalination membranes based on directly copolymerized disulfonated poly(arylene ether sulfone) random copolymers, Water Sci. Technol. 61 (2010) 619–624.

[15] D.M. Stevens, B. Mickols, C. V. Funk, Asymmetric reverse osmosis sulfonated poly(arylene ether sulfone) copolymer membranes, J. Memb. Sci. 452 (2014) 193–202.

[16] J. Rose, Sulphonated polyaryletherketones and process for the manufacture thereof, EP0008895A1, 1978.

[17] J. Rose, Sulphonated polyaryletherketones, EP0041780A1, 1981.

[18] J.B. Rose, Sulphonated polyarylethersulphone copolymers, US4273903, 1978.

[19] A. Bunn, Rose John B, Sulphonation of poly(phenylene ether sulphone)s containing hydroquinone residues, Polymer. 34 (1993) 1992–1994.

[20] A. Al-Omran, J.B. Rose, Synthesis and sulfonation of poly(phenylene ether ether sulfone)s containing methylated hydroquinone residues, Polymer. 37 (1996) 1735–1743.

[21] J.-D. Kim, A. Donnadio, M.-S. Jun, M.L. Di Vona, Crosslinked SPES-SPPSU membranes for high temperature PEMFCs, Int. J. Hydrogen Energy. 38 (2013) 1517–1523.

[22] M.L. Di Vona, E. Sgreccia, M. Tamilvanan, M. Khadhraoui, C. Chassigneux, P. Knauth, High ionic exchange capacity polyphenylsulfone (SPPSU) and polyethersulfone (SPES) cross-linked by annealing treatment: Thermal stability, hydration level and mechanical properties, J. Memb. Sci. 354 (2010) 134–141.

[23] D. Xing, J. Kerres, Improved performance of sulfonated polyarylene ethers for proton exchange membrane fuel cells, Polym. Adv. Technol. 17 (2006) 591–597.

[24] A. Dyck, D. Fritsch, S.P. Nunes, Proton-Conductive Membranes of Sulfonated Polyphenylsulfone, J. Appl. Polym. Sci. 86 (2002) 2820–2827.

[25] W.L. Harrison, Synthesis and Characterization of Sulfonated Poly(arylene ether sulfone) copolymers via direct copolymerization: Candidates for Proton Exchange Membrane Fuel Cells., Ph.D. Dissertation, Virginia Polytechnic and State University, 2002

Chapter 5 : Challenges and recommendations for future work

In chapter 2, the post-sulfonated polymers and oligomers were synthesized, characterized, and cast into linear and crosslinked films respectively. The challenges involved were determination of molecular weights of the oligomers and crosslinking of the oligomers.

The molecular weights were calculated by ^{1}H NMR and by measured by SEC. It was found that the molecular weights obtained by SEC appeared higher than that calculated by ^{1}H NMR. The increase in apparent molecular weights (Mn) were prominent for oligomers with 5000g/mol and also increased with increasing degrees of sulfonation across all oligomers of both 5000 and 10,000g/mol.

Concentration of salt and presence of water in the DMAc/LiCl can affect the hydrodynamic radius of a polymer chain. DMAc was distilled under CaH_2 and LiCl was vacuum dried before use to ensure that water is removed from the system. Yet, it has established that water will be present in the DMAc/LiCl system because LiCl is highly hygroscopic. So, the SEC analyses were performed on ternary system - DMAc/LiCl/water. Water has a pronounced influence on the solvent polarity. Due to the salting effect, the inorganic ions modify the configuration of the polymers in water by affecting the solvent water at the polymer interface and also in the bulk [1]. Presence of water induces polyelectrolyte type interactions in cellulose pulp [2]. Furthermore, the polysulfone backbone in the non-sulfonated and post-sulfonated oligomers is polar and its conformation can be affected in the presence of water. Thus, presence of LiCl and water complicates the system. It is necessary to conduct studies on the SHQS oligomers with increasing degrees of sulfonation to determine the amount of salt required to reduce the electrostatic effects. In the sulfonated oligomers it might be possible that the presence of water decreased the screening effect of the LiCl

on the sulfonate ions 0.1M LiCl was optimum to screen the electrostatic effects but the presence of water affected the efficiency of the system in various ways like decreasing the viscosity, increasing the polarity of DMAc, associating with LiCl. Hence, although cumbersome it is useful to determine the water content in the DMAc/LiCl system to understand the reasons for an increased hydrodynamic radius.

In determining offline dn/dc (specific refractive index) it is important to ascertain if the polymer is at Donnan equilibrium when dealing with binary systems (DMAc/LiCl). The measurements conducted here did not take into account the presence of lithium salts which have a strong tendency to bind to the polymer. This can disrupt the chemical potential and the refractive index of the solvent that is present in half of the refractometer cell and the sample which is in the other. For future studies, dialysis can be performed on the using a dialysis cassette to enable a constant chemical potential. This procedure is frequently used for the offline determination of dn/dc of polyelectrolyte oligomers [3]. The dn/dc values were used for determination of absolute molecular weights by light scattering detector.

Another challenge was epoxy-amine curing of the oligomers to form defect free networks. Epoxy-amine thermal crosslinking reaction might not be the most efficient way to chemically crosslink the SHQS oligomers because it is a time-consuming process. It was difficult to remove the oligomer films from the silanized glass plate and many membranes obtained had defects that limited it's use in highly pressurized reverse osmosis systems. Sundell et al.[4] determined that a molar ratio of epoxy : amine functional groups of 2.5:1 gave membranes with highest gel fractions and this result was used to cast membranes in this dissertation. Although amine terminated, the oligomers studied were chemically different than the SHQS oligomers. The crosslinked

membranes studied in this dissertation were also cast from dilute solutions with amine : epoxy molar ratio being 1:2.5. Systematic study is required to determine the concentration and molar ratio that gives the highest gel fraction. It is also necessary to study the epoxy-amine crosslinking reaction by DSC and FTIR to study the curing reaction.

An alternative approach to epoxy-amine crosslinking is to react the amine end groups with

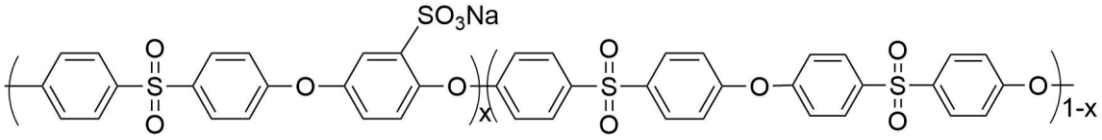

acetyl chloride followed by photo crosslinking in the presence of a photoinitiator [5]. The photo crosslinking reaction takes place quicker than the epoxy-amine curing reactions. Modifying the amine end group is a better option than changing the end groups altogether because it has been established that the ring of m-aminophenol is not sulfonated under the mild reaction conditions that we are using.

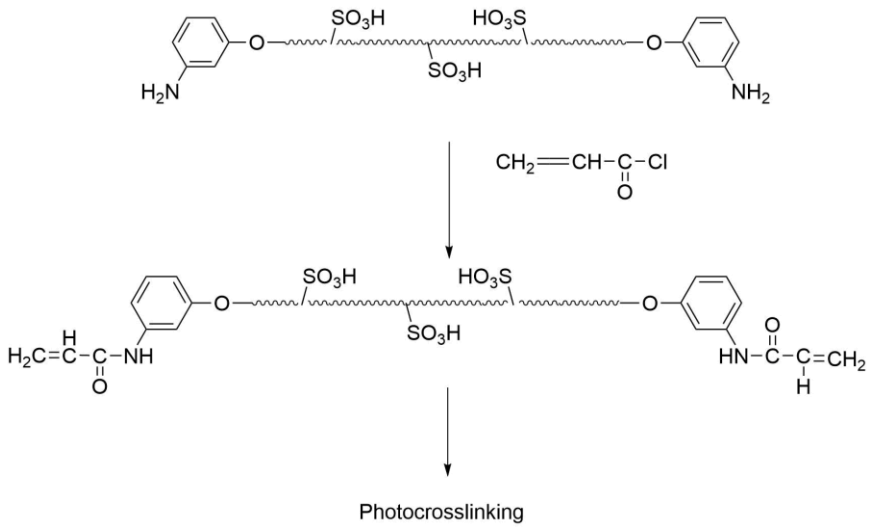

Figure 5.1: Alternative procedure for crosslinking of amine terminated oligomers

In chapters 3 and 4 it was shown that the rejection of sodium ions by the SHQS and 28-SBiPS membranes were studied. The following chemical structure did not show any compromise

in the monovalent salt rejection is not compromised in the presence of calcium ions in the feed water.

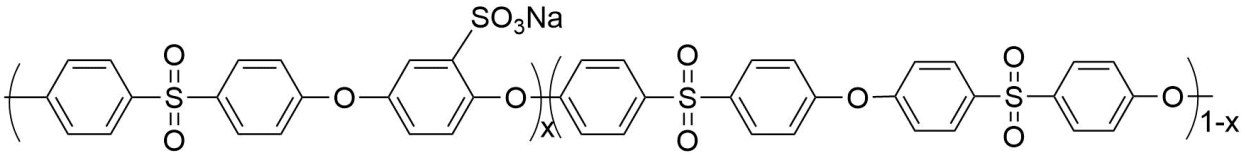

SHQS (I)

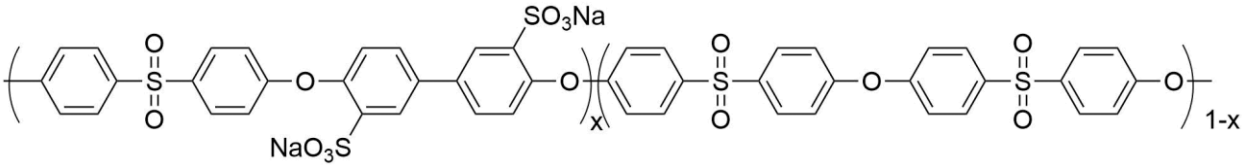

SBiPS (II)

It is hypothesized that in SHQS membranes, the calcium ion cannot chelate with the sulfonate ions because the ionic groups are spaced far apart from each other. In 28-SBiPS the sulfonate ions were on the adjacent rings but it was hypothesized the disulfonated biphenol with its non-planar rings keeps the sulfonates too far apart to efficiently chelate the calcium.

The following structure of the BPS membranes showed a compromise of monovalent salt rejection in the presence of calcium ions. It might be possible that the kinked and rigid structure of the disulfonated sulfone moiety positions the sulfonates sufficiently close to chelate hydrated calcium ions.

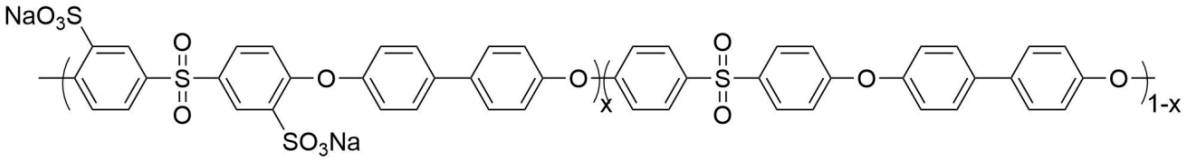

BPS (III)

In order to assess the effect of the kinked sulfone groups it might be useful to synthesize a polymer with structure (IV) at a low ion exchange. Structure (IV) has the sulfonate ions on the kinked bisphenol moieties like the BPS (III) membranes but the backbone is identical to that of the SHQS (I) and SBiPS (II) membranes. So, a compromise on sodium ion rejection in the presence of calcium ion would prove that the kinked sulfone group facilitates calcium chelation. This polymer will have a high polarity and might not be suitable for applications in water desalintion. Hoever, it can give an idea on the calcium ion rejection.

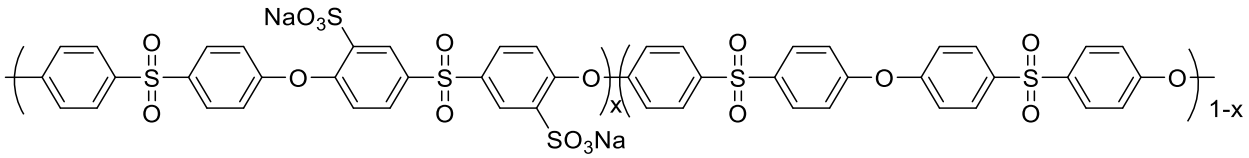

(IV)

Study of coordination number and geometry of calcium coordination complex

Coordination number is an important parameter that governs the transport of water and salt across a membrane. It characterizes the number of atoms in a spherical volume around the reference atom by taking into account different interacting sites including ion-ion, ion-water, and water-water interactions [3]. The strength and stability of the bond between calcium ions and the fixed charge groups depends on many factors including the coordination number of Ca^{2+}, local dielectric constants of water and the calcium chelate structure. When Ca^{2+} ions interact with large molecules such as chelators, and in this case sulfonated polysulfone, the binding is less governed

by the ionic field strength and more by the flexibility of the polymer backbone and its ability to conform to a particular geometry [4]. Knowing the calcium coordination environment in BPS membrane is necessary to understand what atoms are contributing to the chelation. The sulfonate ions in the BPS membrane are placed next to the sulfone group, whereas in the SHQS and SBiPS membranes the sulfonate ions are placed away from the sulfone group. Oxygen atoms are present in the sulfone groups and also in water. It is important to know which of these oxygen atoms contribute to the formation of the coordinate complex with calcium in the BPS membranes. Hence, a detailed study of the calcium coordination complex on BPS membranes is required.

Furthermore, Ca^{2+} can have a variable range of coordination numbers (6,7,8,9). So, these cations have significant flexibility in selecting a stereo-chemically fitting binding site, usually oxygen atoms. Picock et al. [6] studied Ca^{2+} binding sites in proteins and found that helices and sheets contributed relatively few of the ligands to Ca^{2+} whereas the loop/turn structure of proteins could readily supply ligands for calcium binding. Thus, the folding of the polymer backbone plays a crucial role in determining the calcium binding sites. The SHQS (I) and SBiPS (II) membranes are more flexible due to many ether linkages. It might be possible that the way the SHQS and SBiPS backbone orients is not conducive to the formation of the calcium complex whereas the folding of the BPS (III) backbone favors formation of calcium coordination complex at similar ionic content. Transport studies on structure (IV) can help determine if the folding of the polymer backbone influences the formation of calcium coordination complex.

Geise et al determined the coordination number of aluminum in sulfonated styrenic pentablock copolymer films using ^{27}Al magic angle spinning NMR spectroscopy [7]. It was

observed that aluminum atoms were octahedrally coordinated with 6 oxygen atoms. Three Al-O bonds were formed between aluminum and oxygen atoms of the polymer. The additional three coordination were likely attributed to either the sulfonate group's double-bonded oxygen atoms or absorbed water. It is useful to study the coordination number and geometry of the calcium coordination complex in BPS membranes (III) to know the number of oxygen atoms that are binding with the calcium atom. ^{43}Ca NMR spectroscopy can be used but it is challenging due to various reasons- time required to record a ^{43}Ca NMR spectrum with a usable signal to noise ratio is very long compared to NMR studies routinely used by synthetic chemists and most importantly due to the low natural abundance of ^{43}Ca [8]. Hence, some other techniques can be used to find the coordination number and geometry of the calcium coordination complex.

Alternatively, X-ray absorption near edge structure (XANES) at a calcium K-edge can be used to obtain qualitative information on the calcium coordination environment. X-ray absorption spectroscopy is well suited for structural investigations of non- or poorly crystalline materials like the polymers studied in this research. X ray absorption near edge structure is usually defined as the region extending from just below the absorption edge to 30-50 eV past the edge and takes into account the local environment of the absorbing atom. XANES spectra of a wide range of well characterized calcium minerals and compounds were correlated to the known calcium/oxygen coordination environment. Calcium K-edge XANES spectra from novel compounds of unknown structure can be interpreted to elucidate the calcium environment [9]. Hence, XANES at calcium K-edge is a suitable technique that can be applied to determine the calcium coordination environment.

Several researchers have used FTIR to study the coordination structure of Ca^{2+} chelation complexes in various compounds including lignin [10], proteins [11] and polyelectrolyte brushes [12]. It is recommended that FTIR study should be performed on BPS membranes before and after saturation with calcium ions. When Ca^{2+} chelates the sulfonate ions in sulfonated polysulfones it is expected that the O=S=O bond stretches will shift, and new absorption peaks will appear due to the formation of Ca-O bonds. It is helpful to know the various oxygen atoms that calcium can bind with in the BPS membranes. It is obvious that the singly bonded oxygen atom of S-O of sulfonate ions contribute to the ligand. It is not clear of there are other oxygen atoms in the vicinity of calcium that will help formation of coordination complex in BPS membranes.

Calcium chelation can be quantified with calcium ion selective electrodes [13]. Transport studies on the sulfonated polysulfone membranes cannot quantify the amount of chelation. A calcium calibration curve is constructed with known concentrations of $CaCl_2$. The sulfonated polysulfone membrane could be soaked in $CaCl_2$ solution to enable chelation of the binding sites with the Ca^{2+} ions. This will lead to a decrease in the free Ca^{2+} ions in the solution. The difference in the free ions before and after the membrane functional groups are chelated can then be used to quantify the amount of chelation. This process can also be repeated with the polymers (before casting the membrane) to understand how the membrane properties affect the Ca^{2+} ion chelation. However, a disadvantage of this process is that the electrodes are expensive.

References:

[1] S. Saito, Salt Effect on Polymer Solutions, 1969.

[2] T. Bikova, A. Treimanis, Problems of the MMD analysis of cellulose by SEC using

DMA/LiCl: A review, Carbohydr. Polym. 48 (2002) 23–28.

[3] S. Podzimek, Light scattering, in: Light Scatt. Size Exclusion Chromatogr. Asymmetric Flow F. Flow Fractionation, John Wiley and Sons, 2010: pp. 37–98.

[4] B.J. Sundell, E.-S.S. Jang, J.R. Cook, B.D. Freeman, J.S. Riffle, J.E. McGrath, Cross-Linked Disulfonated Poly(arylene ether sulfone) Telechelic Oligomers. 2. Elevated Transport Performance with Increasing Hydrophilicity, Ind. Eng. Chem. Res. 55 (2016) 1419–1426.

[5] A. Nebipasagil, B.J. Sundell, O.R. Lane, S.J. Mecham, J.S. Riffle, J.E. McGrath, Synthesis and photocrosslinking of disulfonated poly(arylene ether sulfone) copolymers for potential reverse osmosis membrane materials, Polymer 93 (2016) 14–22.

[6] E. Pidcock, R. Moore, Structural characteristics of protein binding sites for calcium and lanthanide ions, J Biol Inorg Chem. 6 (2001) 479–489.

[7] G.M. Geise, C.L. Willis, C.M. Doherty, A.J. Hill, T.J. Bastow, J. Ford, K.I. Winey, B.D. Freeman, D.R. Paul, Characterization of aluminum-neutralized sulfonated styrenic pentablock copolymer films, Ind. Eng. Chem. Res. 52 (2013) 1056–1068.

[8] D.L. Bryce, Calcium binding environments probed by 43Ca NMR spectroscopy, Dalt. Trans. 39 (2010) 8593.

[9] F.E. Sowrey, L.J. Skipper, D.M. Pickup, K.O. Drake, Z. Lin, M.E. Smith, R.J. Newport, Systematic empirical analysis of calcium–oxygen coordination environment by calcium K-edge XANES, Phys. Chem. Chem. Phys. 6 (2004) 188–192.

[10] H.A. Shnawa, Evaluation of Lignin-Calcium Complex as Thermal Stabilizer for Poly Vinyl Chloride, Mater. Sci. Appl. 02 (2011) 692–699.

[11] M. Nara, H. Morii, M. Tanokura, Coordination to divalent cations by calcium-binding proteins studied by FTIR spectroscopy, Biochim. Biophys. Acta - Biomembr. 1828 (2013) 2319–2327.

[12] M.J. Roman, E.A. Decker, J.M. Goddard, Fourier Transform Infrared Studies on the Dissociation Behavior of Metal-Chelating Polyelectrolyte Brushes, ACS Appl. Mater.

Interfaces. 6 (2014) 5383–5387. doi:10.1021/am501212g.

[13] J.R. Blinks, W.G. Wier, P. Hess, F.G. Prendergast, Measurement of Ca^{2+} concentrations in living cells, Prog. Biophys. Mol. Biol. 40 (1982) 1–114.